

REPORT DOCUMENTATION PAGE

AFRL-SR-BL-TR-98

Public reporting burden for this collection of information is estimated to average 1 hour per response, including reviewing the data needed, and completing and reviewing the collection of information. Send comments and suggestions for reducing this burden, to Washington Headquarters Services, Directorate for Information Operations and Reports, 1204, Arlington, VA 22202-4302, and to the Office of Management and Budget, Paperwork Reduction Project (0704-0188), Washington, DC 20503.

1. AGENCY USE ONLY (Leave Blank)

2. REPORT DATE
May 19933. REPORT TYPE
Final

0412

4. TITLE AND SUBTITLE

A Bifurcation Approach Modeling Cavitation in Anisotropic Nonlinearly Elastic Solids

5. FUNDING NUMBERS

6. AUTHORS

Debra Ann Polignone

7. PERFORMING ORGANIZATION NAME(S) AND ADDRESS(ES)

University of Virginia

8. PERFORMING ORGANIZATION
REPORT NUMBER

9. SPONSORING/MONITORING AGENCY NAME(S) AND ADDRESS(ES)

AFOSR/NI

110 Duncan Avenue, Room B-115
Bolling Air Force Base, DC 20332-808010. SPONSORING/MONITORING
AGENCY REPORT NUMBER

11. SUPPLEMENTARY NOTES

12a. DISTRIBUTION AVAILABILITY STATEMENT

Approved for Public Release

12b. DISTRIBUTION CODE

13. ABSTRACT (Maximum 200 words)

See attached.

19980504 150

DTIC QUALITY INSPECTED 4

14. SUBJECT TERMS

15. NUMBER OF PAGES

16. PRICE CODE

17. SECURITY CLASSIFICATION
OF REPORT
Unclassified18. SECURITY CLASSIFICATION
OF THIS PAGE
Unclassified19. SECURITY CLASSIFICATION
OF ABSTRACT
Unclassified20. LIMITATION OF ABSTRACT
UL

**A BIFURCATION APPROACH MODELING CAVITATION
IN ANISOTROPIC NONLINEARLY ELASTIC SOLIDS**

ARMY FORCE OF SCIENTIFIC RESEARCH (AFSC)
OFFICE OF TRANSMITTAL TO DTIC

This technical report has been reviewed and is
approved for release under E.O. 12958-2
and is hereby released.

by
Program Manager

A Dissertation
Presented to
the Faculty of the School of Engineering and Applied Science
University of Virginia

Approved for publication as
distribution under E.O. 12958-2

In Partial Fulfillment
of the Requirements for the Ph.D. Degree
(Applied Mathematics)

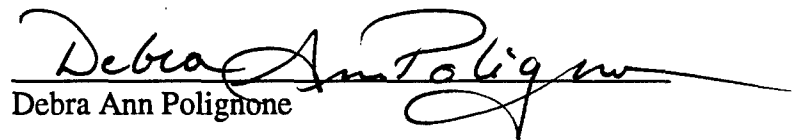
by

Debra Ann Polignone

May 1993

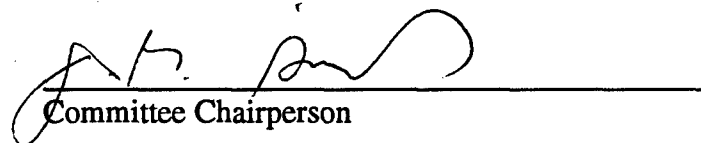
APPROVAL SHEET

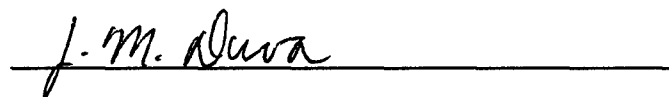
This thesis is submitted in partial fulfillment of the
requirements for the degree of
Ph. D. (Applied Mathematics)

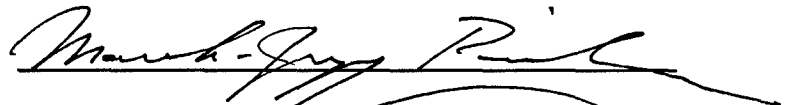

Debra Ann Polignone

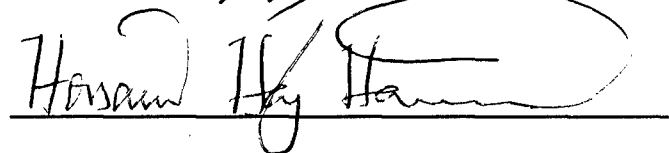
This thesis has been read and approved by the Examining
Committee:


Thesis Advisor


Committee Chairperson







Accepted for the School of Engineering and Applied Science:

Dean, School of Engineering
and Applied Science

May 1993

Abstract

In this thesis, material anisotropy and the phenomena of void formation and growth (cavitation) in nonlinearly elastic incompressible solids are considered. We first discuss materials which are transversely isotropic in the contexts of linear and nonlinear hyperelasticity, and derive important constitutive restrictions on the nonlinear stored-energy function, W , by relating W to the associated infinitesimal elastic moduli. We then propose a class of stored-energy functions satisfying these conditions to model incompressible transversely isotropic nonlinearly elastic materials. The effect of *material anisotropy* on void nucleation and growth in *incompressible* nonlinearly elastic solids is then examined. A bifurcation problem is considered for a solid sphere composed of an incompressible homogeneous nonlinearly elastic material that is transversely isotropic about the radial direction. Under a uniform radial tensile dead-load, a branch of radially symmetric configurations involving a traction-free internal cavity bifurcates from the undeformed configuration at sufficiently large loads. Closed form analytic solutions are obtained for a specific anisotropic material model. In contrast to the situation for an isotropic sphere, bifurcation here may occur locally either to the right (supercritical) or to the left (subcritical), depending on the degree of anisotropy. In the latter case, the cavity has finite radius on first appearance. Such dramatic cavitation instabilities were previously encountered by Antman and Negrón-Marrero [4] for anisotropic *compressible* solids and by Horgan and Pence [20] for *composite* incompressible spheres. Finally, the effects of *material anisotropy* and *inhomogeneity* on void nucleation and growth in incompressible anisotropic nonlinearly elastic solids are examined via a similar bifurcation problem for a composite sphere whose phases are each composed of an arbitrary homogeneous incompressible transversely isotropic material. Several types of bifurcation are found to occur. Explicit conditions determining the type of bifurcation are established for the general transversely isotropic composite sphere. In particular, if each phase is described by an explicit anisotropic material model (a generalization of the classic neo-Hookean model to anisotropic materials), phenomena which were not observed for the homogeneous anisotropic sphere nor for the composite neo-Hookean sphere may occur. The stress distribution is also examined.

Acknowledgements

Dedicated to my loving parents, Jean and Anthony Polignone,
as a very small token of my love and appreciation for two wonderful people
I am honored to call Mom and Dad.

I would also like to express my sincere appreciation and thanks to several others who have contributed to both the development of this thesis and my graduate experience, and who exemplify excellent role models as I aspire to my post-graduate career. I am grateful to the members of my Ph. D. committee, Mr. J. G. Simmonds (Chairman), Mr. C. O. Horgan, Mr. J. M. Duva, Mr. M-J Pindera, and Mr. H. Haj-Hariri, for their participation and helpful suggestions; each brings their own interesting perspectives, insight, and expertise to my overall appreciation of my dissertation topic. I would especially like to thank my advisor, C. O. Horgan, for the valuable guidance and insight he has provided throughout my graduate work, and for his genuine interest and willingness to devote time and effort to the development of my academic career. Two others without whom I would have incurred many more headaches along the way are Kay Holden and Beve Martin. I will surely miss their smiling faces, conversation, and helpfulness.

Finally, I cannot thank the U.S. Air Force enough for their support of my doctoral study in awarding me a National Defense Science and Engineering Graduate Fellowship (NDSEGF). The opportunities this support has provided me have been invaluable and far-reaching. The support of the U.S. National Science Foundation during the early stages of my graduate work is also gratefully acknowledged.

Table of Contents

Abstract	i
Acknowledgements	ii
Table of Contents	iii
List of Figures	v
List of Symbols	vii
Chapter 1 INTRODUCTION	1
Chapter 2 ANISOTROPY, TRANSVERSE ISOTROPY, AND ELASTIC PARAMETERS	6
Section 2.1 Introduction	6
Section 2.2 Isotropy, anisotropy, and transverse isotropy	7
Section 2.3 Elastic parameters: linear, compressible, transversely isotropic materials	10
Section 2.4 Elastic parameters: linear, incompressible, transversely isotropic materials	13
Section 2.5 Implications for the nonlinearly elastic stored-energy	15
Section 2.5.1 Generalized moduli and restrictions on $W(I_1, I_2, I_4, I_5)$	17
Section 2.5.2 Further considerations of $W(I_1, I_2, 1, 0, I_5)$	32
Section 2.5.3 Implications for a special class of nonlinearly elastic materials	36
Chapter 3 HOMOGENEOUS ANISOTROPIC SPHERE	40
Section 3.1 Introduction	40

Section 3.2 Problem formulation	41
Section 3.3 Solutions	46
Section 3.4 The critical load and bifurcation	49
Section 3.5 Illustrative example	51
Section 3.5.1 A class of anisotropic incompressible elastic materials	51
Section 3.5.2 Cavitation solutions	54
Section 3.6 Energy and stability of solutions	58
Section 3.7 Stress distribution	65
Chapter 4 COMPOSITE ANISOTROPIC SPHERE	77
Section 4.1 Introduction	77
Section 4.2 Problem formulation	79
Section 4.3 Solutions	84
Section 4.4 The critical load and bifurcation	88
Section 4.5 Energy and stability of solutions	94
Section 4.6 Illustrative example	101
Section 4.7 Stress distribution	112
Chapter 5 Conclusions	137
Appendix A	143
Appendix B	144
Appendix C	147
Appendix D	151
References	155

List of Figures

Figure 2.1	8
Figure 2.2	9
Figure 3.1	69
Figure 3.2	70
Figure 3.3	71
Figure 3.4	72
Figure 3.5	73
Figure 3.6	74
Figure 3.7	75
Figure 3.8	76
Figure 4.1	118
Figure 4.2	119
Figure 4.3	120
Figure 4.4	121
Figure 4.5(a)	122
Figure 4.5(b)	123
Figure 4.6(a)	124
Figure 4.6(b)	125
Figure 4.6(c)	126
Figure 4.6(d)	127

Figure 4.6(e)	128
Figure 4.7	129
Figure 4.8	130
Figure 4.9	131
Figure 4.10	132
Figure 4.11	133
Figure 4.12	134
Figure 4.13	135
Figure 4.14	136

List of Symbols

\mathbf{X}	undeformed coordinate vector
$X_i \ (i = 1, 2, 3)$	undeformed coordinates
\mathbf{x}	deformed coordinate vector
$x_i \ (i = 1, 2, 3)$	deformed coordinates
J	Jacobian determinant of \mathbf{F}
∇	gradient operator
\det	determinant
\mathbf{F}	deformation gradient tensor
\mathbf{Q}	proper orthogonal tensor
\mathbf{Q}^T	transpose of \mathbf{Q}
\mathbf{I}	identity tensor (3×3 matrix)
W	nonlinear stored-energy function
\mathcal{O}	origin
w	linear stored-energy function
$\hat{a}, \bar{a}, \mu, b, \bar{\mu}$	transversely isotropic linearly elastic parameters

\mathbf{E}	infinitesimal strain tensor
$E_{ij} \ (i, j = 1, 2, 3)$	components of \mathbf{E}
$E, \bar{E}, \nu, \bar{\nu}, \mu, \bar{\mu}$	transversely isotropic linearly elastic moduli
$\lambda, \mu_T, \hat{\alpha}, \mu_L, \gamma$	transversely isotropic linearly elastic parameters
\mathbf{a}	unit vector in direction of anisotropy
tr	trace
\bullet	usual dot product
$\sigma_{ij} \ (i, j = 1, 2, 3)$	components of stress tensor (linear)
\mathbf{C}	right Cauchy-Green deformation tensor
$I_k \ (k = 1, 2, 3, 4, 5)$	strain invariants in transverse isotropy
$C_{ij} \ (i, j = 1, 2, 3)$	components of \mathbf{C}
Λ	stretch in uniaxial tension
$T_{ij} \ (i, j = 1, 2, 3)$	components of Cauchy stress
W_k	$\partial W / \partial I_k$
$\bar{E}(\Lambda)$	generalized Young's modulus in direction of anisotropy
\bar{E}	Young's modulus in direction of anisotropy

κ	amount of (simple) shear
$\bar{\mu}(\kappa^2)$	generalized shear modulus involving direction of anisotropy
$\mu(\kappa^2)$	generalized shear modulus in direction not involving axis of anisotropy
Γ	stretch in equibiaxial stress/stretch
a	dimensionless measure of degree of anisotropy
p_0	prescribed dead-load
p_{cr}	critical load
c	cavity radius
D_0	undeformed sphere
(R, Θ, Φ)	undeformed coordinates
B	outer radius of undeformed sphere
(r, θ, ϕ)	deformed coordinates
$r(R)$	radial deformation
\dot{r}	dr/dR
\mathbf{T}	Cauchy stress tensor

p	hydrostatic pressure
$\mathbf{1}$	unit tensor
\mathbf{B}	left Cauchy-Green deformation tensor
\mathbf{M}, \mathbf{N}	deformation tensors associated with anisotropy
$M_{ij}, N_{ij}, F_{ij} \ (i, j = 1, 2, 3)$	components of deformation tensors
T_{rr}	radial Cauchy stress component
$T_{\theta\theta}, T_{\phi\phi}$	hoop Cauchy stress components
div	divergence
v	stretch
ρ	dimensionless cavity radius
$\lambda_i \ (i = 1, 2, 3)$	principal stretches
$\lambda_r, \lambda_\theta, \lambda_\phi$	principal stretches
\mathbf{S}	Piola-Kirchoff stress tensor
P	dimensionless load
P_{cr}	dimensionless critical load
a_0	critical value of a

$E(c)$	total energy
$\Sigma(c)$	dimensionless energy
(P_t, ρ_t)	turning point
A	radius of composite sphere interface
α	B/A
f	volume fraction of core to total material
\hat{p}	dimensionless load
\hat{p}_{cr}	dimensionless critical load
ω	dimensionless parameter
\bar{E}_1	\bar{E} for core material
\bar{E}_2	\bar{E} for surrounding material
a_1	core material anisotropy parameter
a_2	surrounding material anisotropy parameter
$(p_{t1}, \rho_{t1}), (p_{t2}, \rho_{t2})$	turning points
T_d	threshold value of interfacial normal stress

Chapter 1

INTRODUCTION

Void nucleation and growth in solids play a fundamental role in fracture and other failure mechanisms. (See e.g. Tvergaard [42] for a recent review of void growth in metals.) Sudden void formation ("cavitation") in vulcanized rubber has also been observed experimentally by Gent and Lindley [14]; see also Williams and Schapery [45]. A recent review on cavitation in rubber is that of Gent [13]. Nonlinear theories of solid mechanics have been extensively used recently to model such phenomena. The impetus for many of these developments has been supplied by the theoretical work of Ball [5] on a class of *bifurcation problems* for the equations of nonlinear elasticity that model the appearance of a cavity in the interior of a solid homogeneous isotropic elastic sphere or cylinder once a critical external load is attained. An alternative interpretation for such problems in terms of the sudden rapid growth of a *pre-existing* microvoid has been given by Horgan and Abeyaratne [19]; see also Sivaloganathan [32]. As pointed out for example, in [19], cavitation is an inherently *nonlinear* phenomenon and cannot be modeled using linearized solid mechanics theories.

In the comprehensive work of Ball [5] on radially symmetric solutions, bifurcation and stability analyses are carried out for displacement and traction boundary-value problems in n -dimensions for both incompressible and compressible isotropic materials. For incompressible materials the results are extensive, while those in the more difficult compressible case are comparatively limited and require several constitutive assumptions. Further studies in the *compressible* case were carried out in [39, 31, 19, 32,

33, 10, 28, 18, 40]. *Anisotropic* compressible materials were considered by Antman and Negron-Marrero [4]. Other contexts in which cavitation for compressible materials was investigated include consideration of non-radially symmetric solutions [26], elastodynamics [30], and elastic membrane theory [17, 37]; (see also [16] for a membrane made of an incompressible material). For *incompressible* materials, finite strain plasticity models were investigated in [9] while the effects of rate dependence were examined in [1]. Further studies for incompressible materials were carried out in [6, 24] for elastostatics and in [7] for elastodynamics. The effects of material inhomogeneity on cavitation in incompressible materials were investigated by Horgan and Pence [20-22]. Void collapse for both incompressible and compressible materials has been examined in [2]. Further work in plasticity was carried out in [23, 25, 43].

The purpose of this dissertation is to examine the effects of *material anisotropy* on cavitation for *incompressible* nonlinearly elastic solids. Two previous investigations [4, 20] provided particular motivation for this work. For classes of *compressible* transversely isotropic nonlinearly elastic cylinders and spheres, Antman and Negron-Marrero [4] found dramatic material instabilities. In particular they showed that solutions describing cavitation differ significantly from those obtained for *isotropic* materials. For example, for radially reinforced spheres (i.e. spheres transversely isotropic about the radial direction), it was shown in [4] that a jumping phenomenon can occur which is reminiscent of snap-through buckling in structural mechanics. A discontinuous change in stable equilibrium configurations was encountered which corresponds to the sudden appearance of a cavity of *finite* radius at a critical load. The same "snap cavitation" phenomenon was observed by Horgan and Pence [20, 21] in an investigation of cavitation for *composite incompressible* nonlinearly elastic materials

with isotropic phases.

The problems investigated in [4] and [20] required completely different analyses. For the classes of *compressible* materials considered in [4], giving rise to singular ordinary differential equations, phase-plane methods were employed to yield qualitative information on solution behavior. On the other hand, for *incompressible* materials, the zero volume change constraint allows for immediate determination of the functional form of the radial deformation field and the hydrostatic pressure is readily obtained by direct integration of the equilibrium equations (see e.g. [20]). Thus results on cavitation for incompressible materials are generally obtained in much more explicit form than is possible for compressible materials. In fact, for the illustrative example of a composite sphere composed of two neo-Hookean materials perfectly bonded across a spherical interface, closed form analytic results were obtained in [20], [21].

The present study was motivated by [4], [20], and [21] in several ways. First, it is clearly of interest to take advantage of the constraint of incompressibility to obtain more explicit information on the effect of *anisotropy* on cavitation. Secondly, as was remarked at the end of [20], the "homogenization" approach to composite material mechanics suggests it worthwhile to examine an "equivalent" anisotropic sphere as a model for a composite sphere isotropic phases. Finally, since consideration of a *composite isotropic* sphere [20, 21] provided interesting results on cavitation and material instabilities, it is worth investigating the combined effects of *anisotropy and material inhomogeneity*.

It is worth noting here, as was also observed in [4], that the radial anisotropy considered in [4] and in this dissertation does indeed arise in technological applications.

A striking example occurs in casting of metals where the temperature gradient in the freezing process induces molecular structure resulting in transverse isotropy about the radial direction (see e.g. Fig. p. 321 of [44]).

Chapter 2 is concerned with material properties, and focuses mainly on the type of anisotropy of concern in this dissertation. We consider the stored-energy functions corresponding to transversely isotropic materials in the contexts of both the linear and nonlinear theories of elasticity, and relate the infinitesimal elastic moduli to the nonlinear stored-energy function. We then obtain restrictions (inequalities) on the nonlinear stored-energy consistent with those known for the linearly elastic moduli. Finally, we obtain further results involving the nonlinearly elastic transversely isotropic incompressible stored-energy function and then apply the considerations of this Chapter to a special class of such materials. Chapter 3 is concerned with the cavitation problem for a homogeneous sphere composed of material which is incompressible and transversely isotropic about the radial direction, while Chapter 4 considers this problem for such a sphere which is inhomogeneous. For simplicity and illustration, the stability analysis in Chapter 3 is carried out for a specific material model. In Chapter 4, cavitation is analyzed for a nonlinear elastic composite sphere whose phases are composed of two (different) completely *general* transversely isotropic materials, and a subsequent illustrative example is then considered. The general results of Chapter 4 reduce to the corresponding general results for the homogeneous sphere with the proper choice of parameters.¹ Finally, in Chapter 5 we summarize some of the important and interesting results of Chapters 2 - 4, discuss some additional aspects of the cavitation problem, and

¹ Let the Chapter 4 parameters α , f of (4.4.2)₂, (4.4.9), respectively, be such that $f = \alpha = 1$, and/or set W^2 of (4.4.1) identically zero to recover the general results for the homogeneous sphere from those of Chapter 4.

indicate some areas for future research.

Chapter 2

ANISOTROPY, TRANSVERSE ISOTROPY, AND ELASTIC PARAMETERS

2.1. Introduction

Material properties are a basic aspect of continuum mechanical modeling. Characterization of the types of materials being considered is necessary to properly formulate the mathematical problem as well as describe its applicability to real materials. The purpose of this Chapter is to give a mathematical as well as physical interpretation for the types of elastic materials of concern in this dissertation. In Section 2.2 we describe what is meant by *isotropic*, *anisotropic*, and *transversely isotropic* materials, within the context of nonlinear hyperelasticity. These concepts have, of course, been formulated in the literature, and are presented here as an aid to the reader. In Section 2.3 we consider the elastic parameters associated with infinitesimal deformations of a *compressible* transversely isotropic material, and relate the five independent physical moduli to parameters appearing in two different but equivalent representations for the stored-energy function. In Section 2.4 we use the results of Section 2.3 to recover the elastic moduli for an *incompressible* transversely isotropic linearly elastic material, and then relate these to the nonlinearly elastic stored-energy function in Section 2.5. Finally in that Section, we examine the implications of these results for a specific material model proposed in Chapter 3, Section 5, and motivated by the considerations given in that Chapter.

2.2. Isotropy, anisotropy, and transverse isotropy

We refer to Figure 2.1 and consider a body B composed of elastic material which in its undeformed or reference configuration has associated with any point of B , the coordinate vector $\mathbf{X} = (X_1, X_2, X_3)$. A deformation of this body is then defined as

$$\mathbf{x} = \mathbf{x}(\mathbf{X}) \quad (2.2.1)$$

such that

$$J \equiv \det \nabla \mathbf{x} > 0, \quad (2.2.2)$$

where $\mathbf{x} = (x_1, x_2, x_3)$ refers to the position vector of a point in the deformed configuration, and the quantity J defined in (2.2.2) is physically significant in that it represents (locally) the deformed to reference volume ratio of a material volume element. The restriction $J > 0$ in (2.2.2) arises due to considerations of physically reasonable deformations, i.e., that material cannot be annihilated ($J \neq 0$), and that volume elements are positive. Associated with any hyperelastic material is a strain energy density (per unit undeformed volume) or stored-energy function, W , which is a measure of the elastic potential energy stored in the body due to deformation. This scalar function W depends on the *deformation gradient tensor*, \mathbf{F} , defined as

$$\mathbf{F} = \frac{\partial \mathbf{x}}{\partial \mathbf{X}} \quad (2.2.3)$$

with

$$J = \det \mathbf{F} > 0 \quad (2.2.4)$$

in view of (2.2.2), (2.2.3). As depicted in Fig. 2.1, if we now rotate the deformed body via \mathbf{Q} , an arbitrary proper orthogonal tensor, i.e.,

$$\mathbf{Q}\mathbf{Q}^T = \mathbf{Q}^T\mathbf{Q} = \mathbf{I} , \quad \det\mathbf{Q} = 1 , \quad (2.2.5)$$

where \mathbf{I} is the 3x3 identity tensor, then the resulting body whose particles have the position vector $\mathbf{Q}\mathbf{x}$ has associated with it a stored-energy $W(\mathbf{Q}\mathbf{F})$. Then the *principle of material frame-indifference*, which is also known by several other names, including the principle of *material objectivity*, (see e.g., [41]) states that

$$W(\mathbf{F}) = W(\mathbf{Q}\mathbf{F}) , \quad (2.2.6)$$

and thus a change of observer does not affect the elastic stored energy. Equation (2.2.6) is assumed to hold regardless of the type of material being considered, that is, regardless of whether the elastic material is isotropic or anisotropic (we define these two terms more precisely in what follows).

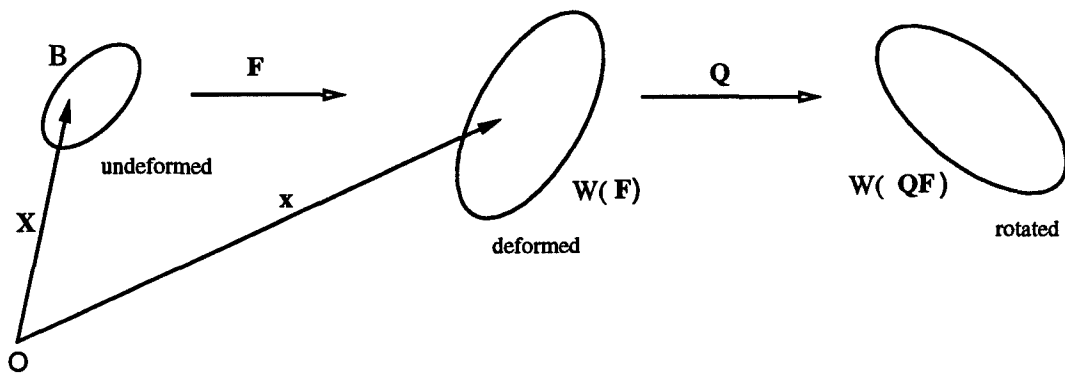


Figure 2.1. Principle of Material Frame Indifference: $W(\mathbf{F}) = W(\mathbf{Q}\mathbf{F})$

Consider now the situation depicted in Figure 2.2:

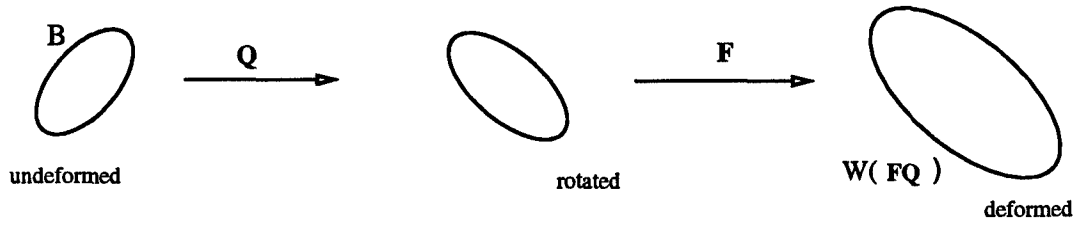


Figure 2.2. Isotropy: $W(F) = W(FQ)$

If the undeformed body is first rotated via Q satisfying (2.2.5) so that particles of the rotated body have the position vector QX , and is then deformed, the stored-energy associated with the final deformed configuration of the body is $W(FQ)$. The material is *isotropic* if it further holds that

$$W(F) = W(FQ), \quad (2.2.7)$$

so that the orientation of an isotropic material cannot be detected from experiments. The response of an isotropic material thus exhibits no preferred direction, and material properties are the same in all directions. If (2.2.7) does not hold for all Q satisfying (2.2.5), the material is said to be *anisotropic*, and the comments following (2.2.7) do not hold for such a material. For anisotropic materials, equation (2.2.7) is replaced by

$$W(F) = W(F\hat{Q}), \quad (2.2.8)$$

where \hat{Q} satisfies (2.2.5), and the set of all rotation tensors \hat{Q} which satisfy (2.2.8) is a proper subset of the set of all proper orthogonal tensors Q .

The type of anisotropy of concern in this dissertation is *transverse isotropy*. A transversely isotropic material is one which exhibits a single preferred direction at every point, so that material properties in the direction of transverse isotropy are different than

those in other directions. For a material which is transversely isotropic about an axis, the rotation tensors $\hat{\mathbf{Q}}$ satisfying (2.2.8) describe all rotations about that axis.

2.3. Elastic parameters: linear, compressible, transversely isotropic materials

The stored-energy function, w , for a compressible *linearly* elastic material which is transversely isotropic about an axis in a Cartesian coordinate system is given in [12]. We rewrite this quadratic form for a linearly elastic material that is transversely isotropic about the 1 direction in an orthonormal basis with associated indices (1,2,3) as

$$2w = \hat{a}(E_{22}^2 + E_{33}^2) + \bar{a}E_{11}^2 + 2(a - 2\mu)E_{22}E_{33} + 2b(E_{22} + E_{33})E_{11} + 4\bar{\mu}(E_{12}^2 + E_{13}^2) + 4\mu E_{23}^2, \quad (2.3.1)$$

where \mathbf{E} is the infinitesimal strain tensor defined as

$$\mathbf{E} = \frac{1}{2}(\mathbf{F} + \mathbf{F}^T) - \mathbf{I}, \quad (2.3.2)$$

the E_{ij} ($i, j = 1, 2, 3$) are the components of \mathbf{E} , and \hat{a} , \bar{a} , b , μ , and $\bar{\mu}$ are elastic parameters where μ is the shear modulus associated with the 2-3 direction, and $\bar{\mu}$ the shear modulus associated with the 1-2 and 1-3 directions.¹ In [12] the relationship between the parameters appearing in (2.3.1) and the elastic constants of physical significance is also given to be

$$\begin{aligned} E &= \frac{4\mu(\hat{a}\bar{a} - b^2 - \bar{a}\mu)}{\hat{a}\bar{a} - b^2}, \quad \bar{E} = \frac{\hat{a}\bar{a} - b^2 - \bar{a}\mu}{\hat{a} - \mu}, \\ v &= \frac{\hat{a}\bar{a} - b^2 - \bar{a}\mu}{\hat{a}\bar{a} - b^2}, \quad \bar{v} = \frac{b}{2(\hat{a} - \mu)}, \end{aligned} \quad (2.3.3)$$

¹ Here and in equation (2.3.3) we depart slightly from the notation employed in [12] so that the elastic moduli μ , $\bar{\mu}$ and E , \bar{E} , v , \bar{v} appearing in (2.3.1) and (2.3.3), respectively, are such that those with a superposed bar correspond to elastic moduli associated with material properties in the 1, 1-2, or 1-3 directions, while those without the superposed bar correspond to properties in the 2 and/or 3 directions only. In other words, $\bar{\mu}$, \bar{E} , \bar{v} indicate properties involving the direction of transverse isotropy.

where \bar{E} and E are the Young's moduli in the 1 direction and the 2 and 3 directions, respectively, while $\bar{\nu}$ and ν are Poisson's ratios associated with the 1-2 and 1-3 directions and the 2-3 direction, respectively. In addition, the relation

$$E = 2\mu(1 + \nu) \quad (2.3.4)$$

must hold, so that there exist five independent elastic moduli associated with a transversely isotropic linearly elastic material. That is, we have μ , $\bar{\mu}$, E , \bar{E} , ν , and $\bar{\nu}$ along with (2.3.4). We can invert the relations (2.3.3) to give

$$\left. \begin{aligned} \hat{a} &= \frac{E(1 - \bar{\nu}^2 E/\bar{E})}{(1 + \nu)(1 - \nu - 2\bar{\nu}^2 E/\bar{E})}, \\ \bar{a} &= \frac{\bar{E}(1 - \nu)}{(1 - \nu - 2\bar{\nu}^2 E/\bar{E})}, \\ b &= \frac{E\bar{\nu}}{(1 - \nu - 2\bar{\nu}^2 E/\bar{E})}, \end{aligned} \right\} \quad (2.3.5)$$

where (2.3.4) has been used.

A general representation for the strain energy function w for a linear elastic solid as a quadratic form in \mathbf{E} is given by [36] for a material transversely isotropic about the direction \mathbf{a} as

$$2w = \lambda(\text{tr}\mathbf{E})^2 + 2\mu_T \text{tr}\mathbf{E}^2 + 2\hat{\alpha}(\mathbf{a} \cdot \mathbf{E}\mathbf{a})\text{tr}\mathbf{E} + 4(\mu_L - \mu_T)\mathbf{a} \cdot \mathbf{E}^2 \mathbf{a} + \gamma(\mathbf{a} \cdot \mathbf{E}\mathbf{a})^2. \quad (2.3.6)$$

Here \mathbf{a} is a unit vector in the direction of transverse isotropy and λ , μ_T , μ_L , $\hat{\alpha}$, and γ are elastic parameters. Letting $\mathbf{a} = (1, 0, 0)$ in (2.3.6), so that the material is transversely isotropic about the 1 direction, on regrouping the E_{ij} as in (2.3.1) we obtain the following relationships among the parameters appearing in (2.3.1) and (2.3.6):

$$\begin{aligned}\hat{a} &= \lambda + 2\mu_T, \quad \bar{a} = \lambda - 2\mu_T + 2\hat{\alpha} + 4\mu_L + \gamma, \\ b &= \lambda + \hat{\alpha}, \quad \mu = \mu_T, \quad \bar{\mu} = \mu_L,\end{aligned}\tag{2.3.7}$$

or, on inverting,

$$\begin{aligned}\hat{\alpha} &= b - \hat{a} + 2\mu, \quad \gamma = \bar{a} + \hat{a} - 2b - 4\bar{\mu}, \\ \lambda &= \hat{a} - 2\mu, \quad \mu_T = \mu, \quad \mu_L = \bar{\mu}.\end{aligned}\tag{2.3.8}$$

Using (2.3.8), (2.3.5), and (2.3.4), we determine the parameters appearing in (2.3.6) in terms of the physical moduli to be

$$\left. \begin{aligned}\lambda &= \frac{E(v + \bar{v}^2 E/\bar{E})}{(1+v)(1-v-2\bar{v}^2 E/\bar{E})}, \\ \hat{\alpha} &= \frac{E(\bar{v} - v + v\bar{v} - \bar{v}^2 E/\bar{E})}{(1+v)(1-v-2\bar{v}^2 E/\bar{E})}, \\ \gamma &= \frac{\bar{E}(1-v^2) + E(1-2\bar{v} - 2v\bar{v} - \bar{v}^2 E/\bar{E})}{(1+v)(1-v-2\bar{v}^2 E/\bar{E})} - 4\bar{\mu},\end{aligned}\right\}\tag{2.3.9}$$

and trivially,

$$\mu_T = \mu, \quad \mu_L = \bar{\mu}.\tag{2.3.10}$$

Similarly, (2.3.3) and (2.3.7) give the physical elastic moduli associated with the parameters of (2.3.6) as

$$\left. \begin{aligned}E &= 4\mu_T \left[1 - \frac{\mu_T}{D} (\lambda - 2\mu_T + 2\hat{\alpha} + 4\mu_L + \gamma) \right], \\ \bar{E} &= [D - \mu_T (\lambda - 2\mu_T + 2\hat{\alpha} + 4\mu_L + \gamma)] / (\lambda + \mu_T), \\ v &= 1 - \frac{2\mu_T}{D} (\lambda - 2\mu_T + 2\hat{\alpha} + 4\mu_L + \gamma), \\ \bar{v} &= (\lambda + \hat{\alpha}) / 2(\lambda + \mu_T), \\ \bar{\mu} &= \mu_L,\end{aligned}\right\}\tag{2.3.11}$$

where D in (2.3.11) is defined as

$$D = (\lambda + 2\mu_T)(\lambda - 2\mu_T + 2\hat{\alpha} + 4\mu_L + \gamma) - (\lambda + \hat{\alpha})^2. \quad (2.3.12)$$

Finally, from [12] we also have the following necessary and sufficient conditions for positive definiteness of w :

$$\begin{aligned} E > 0, \quad \bar{E} > 0, \quad \mu > 0, \quad \bar{\mu} > 0, \\ -1 < \nu < 1, \quad 1 - \nu > 2 \frac{E}{\bar{E}} \nu^2. \end{aligned} \quad (2.3.13)$$

2.4. Elastic parameters: linear, incompressible, transversely isotropic materials

We first wish to show how the constitutive law for an *incompressible* linearly elastic transversely isotropic material can be recovered from that for a compressible material. From [35] we write down the latter for a material with preferred direction along the unit vector \mathbf{a} as

$$\begin{aligned} \sigma_{ij} = & \lambda E_{kk} \delta_{ij} + 2\mu_T E_{ij} + \hat{\alpha} (a_k a_m E_{km} \delta_{ij} + E_{kk} a_i a_j) \\ & + 2(\mu_L - \mu_T)(a_i a_k E_{kj} + a_j a_k E_{ki}) + \gamma a_k a_m E_{km} a_i a_j, \end{aligned} \quad (2.4.1)$$

where $i, j = 1, 2, 3$, σ_{ij} are components of the stress tensor in the linear theory, and summation of repeated indices is implied. As indicated in [35], the idealized incompressible material may be regarded as the limiting case of the material with constitutive equation (2.4.1) when

$$\lambda \rightarrow \infty \text{ and } E_{kk} \rightarrow 0 \text{ such that } \lambda E_{kk} \rightarrow -q, \quad (2.4.2)$$

where q is an arbitrary finite constant. Applying (2.4.2) to (2.4.1), we obtain the constitutive equation for an incompressible linearly elastic transversely isotropic material with preferred direction \mathbf{a} as

$$\sigma_{ij} = -(q - \alpha a_k a_m E_{km}) \delta_{ij} + 2\mu_T E_{ij} + 2(\mu_L - \mu_T)(a_i a_k E_{kj} + a_j a_k E_{ki}) + \gamma a_k a_m E_{km} a_i a_j . \quad (2.4.3)$$

As q is arbitrary, the term in (2.4.3) multiplying δ_{ij} is often written simply as $-p$, p arbitrary.

We now determine the corresponding stored-energy w from (2.4.3), (2.4.2), and

$$2w = \sigma_{ij} E_{ij} \quad (2.4.4)$$

to be

$$2w = 2\mu_T E_{ij} E_{ij} + 2(\mu_L - \mu_T)(a_i a_k E_{kj} + a_j a_k E_{ki}) E_{ij} + \gamma a_k a_m E_{km} a_i a_j E_{ij} , \quad (2.4.5)$$

or since \mathbf{E} is symmetric,

$$2w = 2\mu_T E_{ij} E_{ji} + 4(\mu_L - \mu_T) a_j a_k E_{ki} E_{ij} + \gamma (a_i a_j E_{ij})^2 . \quad (2.4.6)$$

In direct tensor notation, (2.4.6) is equivalent to

$$2w = 2\mu_T \text{tr} \mathbf{E}^2 + 4(\mu_L - \mu_T)(\mathbf{a} \bullet \mathbf{E}^2 \mathbf{a}) + \gamma (\mathbf{a} \bullet \mathbf{E} \mathbf{a})^2 . \quad (2.4.7)$$

Letting $\mathbf{a} = (1, 0, 0)$, the stored-energy for an incompressible linearly elastic material that is transversely isotropic about the 1 direction has the form

$$2w = 2\mu_T [2E_{12}^2 + 2E_{13}^2 + 2E_{23}^2 - (E_{11}^2 + E_{22}^2 + E_{33}^2)] + 4\mu_L (E_{11}^2 + E_{12}^2 + E_{13}^2) + \gamma E_{11}^2 . \quad (2.4.8)$$

We can determine the corresponding physical elastic moduli from the results of the previous section and (2.4.2). From (2.3.10), we again have

$$\mu = \mu_T , \quad \bar{\mu} = \mu_L \quad (2.4.9)$$

as the shear moduli, while the Young's moduli and Poisson's ratios can be determined from (2.3.11), (2.3.12) in the limit as $\lambda \rightarrow \infty$. Taking these limits and using l'Hopital's rule, the elastic parameters corresponding to incompressibility can be given as

$$\left. \begin{aligned}
 \lim_{\lambda \rightarrow \infty} E &= 4\mu_T \left[1 - \frac{\mu_T}{4\mu_L + \gamma} \right], \\
 \lim_{\lambda \rightarrow \infty} \bar{E} &= 4\mu_L + \gamma - \mu_T, \\
 \lim_{\lambda \rightarrow \infty} \nu &= 1 - \frac{2\mu_T}{4\mu_L + \gamma}, \\
 \lim_{\lambda \rightarrow \infty} \bar{\nu} &= 1/2,
 \end{aligned} \right\} \quad (2.4.10)$$

where again in (2.4.9), (2.4.10), the superposed bar refers to material properties involving the direction of transverse isotropy (e.g., the 1 direction) while parameters on the left hand sides of these equations without the superposed bar describe properties independent of this direction (e.g. the 2 and/or 3 directions only).

2.5. Implications for the nonlinearly elastic stored-energy

We return now to nonlinear hyperelasticity. As discussed in Section 2.2, there exists a stored-energy function

$$W = W(\mathbf{F}) \quad (2.5.1)$$

associated with any nonlinearly elastic material. For W to satisfy (2.2.6) for all proper orthogonal \mathbf{Q} , it can be shown further that W may be regarded as a function of $\mathbf{C} = \mathbf{F}^T \mathbf{F}$, i.e.,

$$W = W(\mathbf{C}). \quad (2.5.2)$$

Thus the strain energy W is independent of superposed rigid body motions (i.e., satisfies frame-indifference) when (2.5.2) holds instead of (2.5.1). (In the above and in what follows we only introduce new symbols for W depending on different arguments when there is a need to avoid confusion. The functions W on the right hand sides of (2.5.1) and

(2.5.2) are clearly not the same, but no new notation is employed in order to avoid an unnecessary proliferation of symbols.) In the case of a transversely isotropic material, equation (2.5.2) can be further simplified so that W depends on \mathbf{C} only through five invariants. Thus, (see e.g. [27]),

$$W = W(I_1, I_2, I_3, I_4, I_5), \quad (2.5.3)$$

where without loss of generality, taking the axis of symmetry (direction of transverse isotropy) to be the 1 direction, we can define the invariants in (2.5.3) to be

$$\left. \begin{aligned} I_1 &= \text{tr} \mathbf{C}, \\ I_2 &= \frac{1}{2} [(\text{tr} \mathbf{C})^2 - \text{tr} \mathbf{C}^2], \\ I_3 &= \det \mathbf{C}, \\ I_4 &= C_{12}^2 + C_{13}^2, \\ I_5 &= C_{11}. \end{aligned} \right\} \quad (2.5.4)$$

(We note that for an *isotropic* material, the stored-energy (2.5.3) depends only on the first three invariants defined exactly as in (2.5.4).) Recalling from Section 2.2 that $J = \det \mathbf{F}$ is a measure of volume change, the constraint

$$J = 1 \Rightarrow I_3 \equiv J^2 = 1 \quad (2.5.5)$$

must hold when the material is incompressible so that volume is preserved. Thus, for an incompressible material, (2.5.3) becomes

$$W = W(I_1, I_2, I_4, I_5) \quad (2.5.6)$$

and (2.5.5) must hold. With (2.5.6) as the general form for the stored-energy function of a transversely isotropic incompressible material, our next immediate goal is to determine a generalized Young's modulus in the direction of transverse isotropy in order to relate this nonlinear stored-energy to the quantity \bar{E} from the linear theory discussed in Section

2.4. The importance of such a relationship, aside from its intrinsic interest, will become evident in Chapters 3 and 4 of this dissertation.

2.5.1 Generalized moduli and restrictions on $W(I_1, I_2, I_4, I_5)$

(i) Uniaxial tension:

Consider first a uniaxial tension deformation in the x_1 direction for a nonlinearly elastic transversely isotropic material with stored-energy described by (2.5.4) - (2.5.6). This deformation is examined in [27, p.473]. As in [27], we write (2.2.1) for this deformation as

$$x_1 = \Lambda X_1, \quad x_2 = X_2 / \sqrt{\Lambda}, \quad x_3 = X_3 / \sqrt{\Lambda}, \quad (2.5.7)$$

so that corresponding to (2.5.7), the deformation gradient tensor \mathbf{F} defined in (2.2.3) is

$$\mathbf{F} = \begin{bmatrix} \Lambda & 0 & 0 \\ 0 & 1/\sqrt{\Lambda} & 0 \\ 0 & 0 & 1/\sqrt{\Lambda} \end{bmatrix}. \quad (2.5.8)$$

Then

$$\mathbf{C} = \mathbf{F}^T \mathbf{F} = \begin{bmatrix} \Lambda^2 & 0 & 0 \\ 0 & 1/\Lambda & 0 \\ 0 & 0 & 1/\Lambda \end{bmatrix} \quad (2.5.9)$$

and

$$I_3 = \det \mathbf{C} = 1, \quad (2.5.10)$$

so that the incompressibility constraint (2.5.5) holds. It is shown in [27] that the only non-zero stress T_{11} can be written as

$$T_{11} = 2\Lambda \left[\left(\Lambda - \frac{1}{\Lambda^2} \right) (W_1 + \frac{1}{\Lambda} W_2) + \Lambda W_5 \right], \quad (2.5.11)$$

where the $W_k \equiv \partial W / \partial I_k$ are evaluated at the following values of the invariants (defined by (2.5.4)) which correspond to this deformation:

$$\left. \begin{aligned} I_1 &= \Lambda^2 + 2/\Lambda, \\ I_2 &= 2\Lambda + \Lambda^{-2}, \\ I_4 &= 0, \\ I_5 &= \Lambda^2. \end{aligned} \right\} \quad (2.5.12)$$

We will return to (2.5.11), (2.5.12) after the following discussion of the uniaxial tension deformation for incompressible transversely isotropic *linearly* elastic materials.

Consider now uniaxial tension in the context of the linear theory of elasticity. From (2.3.2) and (2.5.8), the infinitesimal strain tensor \mathbf{E} has the form

$$\mathbf{E} = \begin{bmatrix} \Lambda - 1 & 0 & 0 \\ 0 & 1/\sqrt{\Lambda} - 1 & 0 \\ 0 & 0 & 1/\sqrt{\Lambda} - 1 \end{bmatrix}. \quad (2.5.13)$$

We write the linear stress-strain equations involving the physical moduli as (see e.g., [12])

$$\left. \begin{aligned} E_{11} &= \frac{1}{E} [\sigma_{11} - \bar{\nu}(\sigma_{22} + \sigma_{33})], \\ E_{22} &= \frac{1}{E} [\sigma_{22} - \bar{\nu}\sigma_{33} - \frac{E}{\bar{E}}\bar{\nu}\sigma_{11}], \\ E_{33} &= \frac{1}{E} [\sigma_{33} - \bar{\nu}\sigma_{22} - \frac{E}{\bar{E}}\bar{\nu}\sigma_{11}], \\ \sigma_{12} &= \sigma_{21} = 2\bar{\mu}E_{12}, \\ \sigma_{13} &= \sigma_{31} = 2\bar{\mu}E_{13}, \\ \sigma_{23} &= \sigma_{32} = 2\bar{\mu}E_{23}. \end{aligned} \right\} \quad (2.5.14)$$

The equation of interest in (2.5.14) involving Young's modulus in the 1 direction (the direction of transverse isotropy) is (2.5.14)₁. Now σ_{11} is the only non-zero stress component and so (2.5.13) and (2.5.14)₁ give

$$\sigma_{11} = \bar{E}(\Lambda - 1). \quad (2.5.15)$$

Thus, if we can write the nonlinear stress T_{11} of (2.5.11) in the same form as the linear stress σ_{11} of (2.5.15), i.e.,

$$T_{11} = \bar{E}(\Lambda)(\Lambda - 1), \quad (2.5.16)$$

then we call $\bar{E}(\Lambda)$ the generalized Young's modulus in the direction of transverse isotropy. This is analogous to the concept of the *generalized shear modulus* determined from comparisons of the linear and nonlinear (isotropic) simple shear problems (see e.g., [27], pp. 447-453 or [15], p.176).

To arrive at (2.5.16), we first multiply the right hand side of (2.5.11) by Λ^2/Λ^2 :

$$\begin{aligned} T_{11} &= \frac{2}{\Lambda} [(\Lambda^3 - 1)(W_1 + \frac{1}{\Lambda}W_2) + \Lambda^3W_5] \\ &= \frac{2}{\Lambda} [(\Lambda - 1)(\Lambda^2 + \Lambda + 1)(W_1 + \frac{1}{\Lambda}W_2) + \Lambda^3W_5], \end{aligned}$$

or

$$T_{11} = (\Lambda - 1) \left[\frac{2}{\Lambda} (\Lambda^2 + \Lambda + 1) (W_1 + \frac{1}{\Lambda}W_2) + \frac{2\Lambda^2}{(\Lambda - 1)} W_5 \right]. \quad (2.5.17)$$

Equation (2.5.17) is of the form (2.5.16) where

$$\bar{E}(\Lambda) = \frac{2}{\Lambda} (\Lambda^2 + \Lambda + 1) (W_1 + \frac{1}{\Lambda}W_2) + \frac{2\Lambda^2}{(\Lambda - 1)} W_5 \quad (2.5.18)$$

is the *generalized Young's modulus in the direction of transverse isotropy*. To be consistent with the classical linear theory (see e.g., [41] or [29], p.349), equation (2.5.18)

should be such that

$$\lim_{\Lambda \rightarrow 1} \bar{E}(\Lambda) = \bar{E}, \quad (2.5.19)$$

where \bar{E} on the right in (2.5.19) is the \bar{E} of Section 2.4, and the W_k of (2.5.18) are evaluated at the values of the invariants (2.5.12) consistent with $\Lambda \rightarrow 1$: $I_1 = I_2 = 3$, $I_4 = 0$, $I_5 = 1$. Applying (2.5.19) to (2.5.18) we obtain

$$\bar{E} = 6(W_1 + W_2)|_{I_1=I_2=3, I_4=0, I_5=1} + 2 \lim_{\Lambda \rightarrow 1} \frac{\Lambda^2 W_5}{\Lambda - 1}. \quad (2.5.20)$$

The remaining limit in (2.5.20) is an indeterminate form, since it will be seen in Chapter 3 that

$$W_5(3, 3, 1, 0, 1) = 0 \quad (2.5.21)$$

(see equation (3.2.10) and the sentence preceding it). On using l'Hopital's rule, we find that

$$\begin{aligned} \lim_{\Lambda \rightarrow 1} \frac{\Lambda^2 W_5}{\Lambda - 1} &= \lim_{\Lambda \rightarrow 1} \left(\Lambda^2 \frac{dW_5}{d\Lambda} + 2\Lambda W_5 \right) |_{I_1=I_2=3, I_4=0, I_5=1} \\ &= \lim_{\Lambda \rightarrow 1} \frac{dW_5}{d\Lambda} |_{I_1=I_2=3, I_4=0, I_5=1} \end{aligned} \quad (2.5.22)$$

on using (2.5.21). Now, since $I_3 \equiv 1$, $I_4 \equiv 0$, the chain rule gives

$$\frac{dW_5}{d\Lambda} = \frac{\partial W_5}{\partial I_1} \frac{dI_1}{d\Lambda} + \frac{\partial W_5}{\partial I_2} \frac{dI_2}{d\Lambda} + \frac{\partial W_5}{\partial I_5} \frac{dI_5}{d\Lambda}, \quad (2.5.23)$$

where, from (2.5.12),

$$\frac{dI_1}{d\Lambda} = 2\Lambda - 2\Lambda^{-2}, \quad \frac{dI_2}{d\Lambda} = 2 - 2\Lambda^{-3}, \quad \frac{dI_5}{d\Lambda} = 2\Lambda. \quad (2.5.24)$$

Substituting (2.5.24) into (2.5.23) and then taking the limit of (2.5.23) as $\Lambda \rightarrow 1$, we obtain

$$\lim_{\Lambda \rightarrow 1} \frac{\Lambda^2 W_5}{\Lambda - 1} = \lim_{\Lambda \rightarrow 1} \frac{dW_5}{d\Lambda} = 2W_{55} \Big|_{\substack{I_1 = I_2 = 3 \\ I_4 = 0, I_5 = 1}}, \quad (2.5.25)$$

where $W_{55} = \partial W_5 / \partial I_5 = \partial^2 W / \partial I_5^2$. Substituting (2.5.25) into (2.5.20), we determine the relation between the linear Young's modulus \bar{E} and the nonlinear strain energy W to be

$$\bar{E} = [6(W_1 + W_2) + 4W_{55}] \Big|_{\substack{I_1 = I_2 = 3 \\ I_4 = 0, I_5 = 1}}. \quad (2.5.26)$$

Then (2.5.26) and (2.3.13)₂ imply the following condition on the nonlinear stored-energy W :

$$[3(W_1 + W_2) + 2W_{55}] \Big|_{\substack{I_1 = I_2 = 3 \\ I_4 = 0, I_5 = 1}} > 0. \quad (2.5.27)$$

(ii) *Constitutive inequalities:*

The inequality (2.5.27) results from requiring consistency between the linear and nonlinear theories, and from one of the conditions for positive definiteness of the linear strain energy density. There are however six such conditions for positive definite w given in (2.3.13), which we restate here for convenience:

$$E > 0, \quad (2.5.28)$$

$$\bar{E} > 0, \quad (2.5.29)$$

$$\mu > 0, \quad (2.5.30)$$

$$\bar{\mu} > 0, \quad (2.5.31)$$

$$-1 < \nu < 1, \quad (2.5.32)$$

and

$$1 - \nu > 2 \frac{E - \bar{E}}{\bar{E}} \nu^2. \quad (2.5.33)$$

Constitutive inequalities are of great importance in elasticity to ensure physically

reasonable response. A thorough examination of such constitutive restrictions is carried out in [41] for compressible nonlinearly elastic materials. As remarked in [41], no comparable fundamental studies of inequalities had been undertaken for incompressible materials, which to this author's knowledge, remains the case today. It is therefore of interest to determine what restrictions are placed on the nonlinear stored-energy W from all of (2.5.28) - (2.5.33). We have thus far considered only (2.5.29). Toward this end, we first wish to show that in the case of incompressibility, it is not necessary to consider all of the conditions (2.5.28) - (2.5.33) from the linear theory. Since we have already determined the necessary restriction placed on the nonlinear strain energy W by (2.5.29), we assume in what follows that $\bar{E} > 0$ and show that the above conditions are not completely independent. We will show that it suffices to consider only (2.5.29) - (2.5.31), and thus we need only be concerned with two additional conditions analogous to (2.5.27). These two conditions on W associated with (2.5.30) and (2.5.31) will be determined later in this Section.

Proposition 1: Consider an incompressible linearly elastic transversely isotropic material.

Suppose $\bar{E} > 0$. Then $E > 0$ if $\mu > 0$.

Proof: From (2.4.10)₂, (2.4.9)₁,

$$\bar{E} > 0 \Rightarrow 4\mu_L + \gamma - \mu_T > 0 \quad (2.5.34)$$

$$\mu > 0 \Rightarrow \mu_T > 0 \quad (2.5.35)$$

Dividing (2.5.34) by μ_T , we have

$$\frac{4\mu_L + \gamma}{\mu_T} - 1 > 0$$

$$\begin{aligned}
&\Rightarrow \frac{4\mu_L + \gamma}{\mu_T} > 1 \Rightarrow \frac{\mu_T}{4\mu_L + \gamma} < 1 \\
&\Rightarrow 1 - \frac{\mu_T}{4\mu_L + \gamma} > 0.
\end{aligned} \tag{2.5.36}$$

Thus from (2.4.10)₁, (2.5.35), and (2.5.36),

$$E = 4\mu_T \left[1 - \frac{\mu_T}{4\mu_L + \gamma} \right] > 0, \tag{2.5.37}$$

and so (2.5.28) holds whenever (2.5.29) and (2.5.30) hold.

Proposition 2: Consider an incompressible linearly elastic transversely isotropic material.

Suppose $\bar{E} > 0$. Then $-1 < \nu < 1$ if $\mu > 0$.

Proof: We first show the left hand inequality, $-1 < \nu$. As in Proposition 1, (2.5.34), (2.5.35) lead to (2.5.36). Multiplying (2.5.36) by two, we have

$$2 - \frac{2\mu_T}{4\mu_L + \gamma} > 0 \tag{2.5.38}$$

or

$$1 - \frac{2\mu_T}{4\mu_L + \gamma} > -1. \tag{2.5.39}$$

Thus from (2.4.10)₃, we have the desired result $\nu > -1$.

We now show the right hand inequality of (2.5.32). From (2.5.34) and (2.5.35),

$$4\mu_L + \gamma > \mu_T > 0 \tag{2.5.40}$$

and so

$$0 < \frac{\mu_T}{4\mu_L + \gamma}. \tag{2.5.41}$$

Thus from (2.5.41) and (2.4.10)₃,

$$v = 1 - \frac{2\mu_T}{4\mu_L + \gamma} < 1, \quad (2.5.42)$$

and (2.5.32) therefore holds whenever (2.5.29), (2.5.30) hold. This completes the proof of Proposition 2.

Consider now the condition (2.5.33). From (2.4.10)₃, the left hand side of (2.5.33) is

$$1 - v = \frac{2\mu_T}{4\mu_L + \gamma}, \quad (2.5.43)$$

while the right hand side is, from (2.4.10),

$$\begin{aligned} 2 \frac{E}{\bar{v}} \bar{v}^2 &= 2 \frac{4\mu_T \left[\frac{4\mu_L + \gamma - \mu_T}{4\mu_L + \gamma} \right]}{4\mu_L + \gamma - \mu_T} \bar{v}^2 \\ &= \frac{8\mu_T}{4\mu_L + \gamma} \bar{v}^2. \end{aligned}$$

Therefore, since $\bar{v} \rightarrow 1/2$ according to (2.4.10)₄ in the incompressible case, we have

$$2 \frac{E}{\bar{v}} \bar{v}^2 \rightarrow \frac{2\mu_T}{4\mu_L + \gamma} \text{ as } \bar{v} \rightarrow 1/2. \quad (2.5.44)$$

While equations (2.5.43), (2.5.44) may at first seem to contradict (2.5.33), this situation is analogous however to that encountered in isotropic elasticity. It is well known in linear elasticity that the conditions which guarantee a positive definite isotropic stored-energy are $E > 0$, $-1 < v < 1/2$, but that $v = 1/2$ corresponds to incompressibility (see e.g., [15]). Similarly, for transverse isotropy we have in general (2.5.33) for positive definite w , but

$$1 - \nu = 2 \frac{E}{\bar{E}} \bar{\nu}^2 = \frac{E}{2\bar{E}} \quad (2.5.45)$$

corresponds to incompressibility, where (2.4.10)₄ has been employed to obtain the final equality in (2.5.45).

We thus have that in infinitesimal deformations of an incompressible transversely isotropic material, the condition (2.5.33) is replaced by (2.5.45), and the inequalities (2.5.28), (2.5.32) hold whenever (2.5.29), (2.5.30) hold. As stated earlier, the inequality (2.5.27) follows from (2.5.29). It therefore remains to determine what conditions are placed on the nonlinear stored-energy by (2.5.30), (2.5.31), and (2.5.45) only, to completely account for the conditions (2.5.28) - (2.5.33) from the linear theory of elasticity. We next address (2.5.30) and (2.5.31) in a manner similar to that undertaken in part (i) of Section 2.5.1. That is, we consider two simple shear deformations in order to determine *generalized shear moduli*, $\bar{\mu}(\kappa^2)$ and $\mu(\kappa^2)$, that can then be related to $\bar{\mu}$ and μ of the linear theory (see below). Finally in Section 2.5.1, we show that (2.5.45) puts no further restrictions on W .

(iii) *Simple shear:*

Consider a simple shear deformation of the form

$$x_1 = X_1 + \kappa X_2, \quad x_2 = X_2, \quad x_3 = X_3, \quad (2.5.46)$$

with corresponding deformation tensors

$$\mathbf{F} = \begin{bmatrix} 1 & \kappa & 0 \\ 0 & 1 & 0 \\ 0 & 0 & 1 \end{bmatrix}, \quad \mathbf{C} = \begin{bmatrix} 1 & \kappa & 0 \\ \kappa & 1 + \kappa^2 & 0 \\ 0 & 0 & 1 \end{bmatrix}, \quad (2.5.47)$$

and

$$I_3 = \det \mathbf{C} = 1 \quad (2.5.48)$$

so that the incompressibility constraint (2.5.5) holds. It can then be shown that the only non-zero shearing stress $T_{12} = T_{21}$ has the form

$$T_{12} = 2\kappa(W_1 + W_2 + W_4), \quad (2.5.49)$$

where the $W_k \equiv \partial W / \partial I_k$ are evaluated at the following values of the invariants (2.5.4) corresponding to this deformation:

$$\left. \begin{aligned} I_1 &= I_2 = 3 + \kappa^2, \\ I_4 &= \kappa^2, \\ I_5 &= 1. \end{aligned} \right\} \quad (2.5.50)$$

We now consider (2.5.46) in the context of linear theory. From (2.3.2) and (2.5.47)₁, the infinitesimal strain tensor has the form

$$\mathbf{E} = \begin{bmatrix} 0 & \kappa/2 & 0 \\ \kappa/2 & 0 & 0 \\ 0 & 0 & 0 \end{bmatrix}, \quad (2.5.51)$$

and σ_{12} , the only non-zero stress component, is thus given by (2.5.14)₄ and (2.5.51) as

$$\sigma_{12} = \bar{\mu}\kappa. \quad (2.5.52)$$

On comparing (2.5.52) and (2.5.49), we define the *generalized shear modulus* in the 1-2 direction as

$$\bar{\mu}(\kappa^2) = 2(W_1 + W_2 + W_4), \quad (2.5.53)$$

where $\bar{\mu}$ as a function of κ^2 results from the W_k being evaluated at the values of the invariants given by (2.5.50). Then in the limit as $\kappa^2 \rightarrow 0$, we recover the linear theory, so that the relationship between $\bar{\mu}$ and the nonlinear stored-energy W is

$$\bar{\mu} = \lim_{\kappa^2 \rightarrow 0} \bar{\mu}(\kappa^2) = 2(W_1 + W_2 + W_4) |_{I_1=I_2=3, I_4=0, I_5=1} \quad (2.5.54)$$

Therefore, the inequality (2.5.31) implies the condition

$$(W_1 + W_2 + W_4) |_{I_1=I_2=3, I_4=0, I_5=1} > 0. \quad (2.5.55)$$

We remark that (2.5.54), (2.5.55) could have also been obtained by considering simple shear in the 1-3 direction, so that starting with $x_1 = X_1 + \kappa X_3$, $x_2 = X_2$, $x_3 = X_3$, instead of (2.5.46) would have resulted in (2.5.54) on comparison of T_{13} and σ_{13} . Thus, (2.5.53) actually defines the generalized shear modulus involving the direction of transverse isotropy, i.e., in both the 1-2 and 1-3 directions.

We proceed now to determine the generalized shear modulus $\mu(\kappa^2)$ in the 2-3 direction, and thus the condition on the strain energy W implied by (2.5.30), by examining a second simple shear deformation defined by

$$x_1 = X_1, \quad x_2 = X_2 + \kappa X_3, \quad x_3 = X_3. \quad (2.5.56)$$

Then \mathbf{F} , \mathbf{C} corresponding to (2.5.56) are

$$\mathbf{F} = \begin{bmatrix} 1 & 0 & 0 \\ 0 & 1 & \kappa \\ 0 & 0 & 1 \end{bmatrix}, \quad \mathbf{C} = \begin{bmatrix} 1 & 0 & 0 \\ 0 & 1 & \kappa \\ 0 & \kappa & 1 + \kappa^2 \end{bmatrix}, \quad (2.5.57)$$

and again, incompressibility holds since $I_3 = 1$. We then have the only non-zero shearing stress $T_{23} = T_{32}$ as

$$T_{23} = 2\kappa(W_1 + W_2), \quad (2.5.58)$$

where the W_k are evaluated at the values of the invariants

$$\left. \begin{aligned} I_1 = I_2 = 3 + \kappa^2, \\ I_4 = 0, \\ I_5 = 1, \end{aligned} \right\} \quad (2.5.59)$$

associated with (2.5.57)₂.

In the linear theory, the only non-zero stress component σ_{23} is obtained from (2.5.14)₆ and

$$\mathbf{E} = \begin{bmatrix} 0 & 0 & 0 \\ 0 & 0 & \kappa/2 \\ 0 & \kappa/2 & 0 \end{bmatrix}, \quad (2.5.60)$$

as

$$\sigma_{23} = \mu \kappa. \quad (2.5.61)$$

Thus from (2.5.58) and (2.5.61), the *generalized shear modulus in the 2-3 direction* is

$$\mu(\kappa^2) = 2(W_1 + W_2) |_{I_1 = I_2 = 3 + \kappa^2, I_4 = 0, I_5 = 1}, \quad (2.5.62)$$

so that the relationship between μ and the nonlinear stored-energy W is

$$\mu = \lim_{\kappa^2 \rightarrow 0} \mu(\kappa^2) = 2(W_1 + W_2) |_{I_1 = I_2 = 3, I_4 = 0, I_5 = 1}. \quad (2.5.63)$$

Thus the inequality (2.5.30) implies the following condition on W :

$$(W_1 + W_2) |_{I_1 = I_2 = 3, I_4 = 0, I_5 = 1} > 0. \quad (2.5.64)$$

We remark that (2.5.62) - (2.5.64) reduce to the corresponding results for isotropic materials. That is, when the nonlinear stored-energy is viewed as a function of I_1 and I_2 only, and μ represents the shear modulus in infinitesimal deformations of an isotropic material, $\mu = 2(W_1 + W_2) |_{I_1 = I_2 = 3, (I_3 = 1)} > 0$, where the inequality is also a consequence of the

well-known Baker-Ericksen inequalities. The above is not surprising in that a material

that is transversely isotropic about the 1 direction may in some sense be viewed as "isotropic" when only the 2-3 direction is involved.

We have therefore determined three conditions, (2.5.27), (2.5.55), and (2.5.64) on the nonlinear stored-energy W , which result from (2.5.28) - (2.5.33). We claim that these three conditions are sufficient to guarantee that all of (2.5.28) - (2.5.32), and (2.5.45) are satisfied. For this claim to hold, it only remains to show that (2.5.45) puts no further restrictions on W . We do this in the upcoming final part of Section 2.5.1 by considering an equibiaxial stress/stretch deformation.

(iv) Equibiaxial stress/stretch:

We finally consider an equibiaxial stress/stretch deformation defined by

$$x_1 = \Gamma^{-2}X_1, \quad x_2 = \Gamma X_2, \quad x_3 = \Gamma X_3, \quad (2.5.65)$$

with corresponding deformation tensors

$$\mathbf{F} = \begin{bmatrix} \Gamma^{-2} & 0 & 0 \\ 0 & \Gamma & 0 \\ 0 & 0 & \Gamma \end{bmatrix}, \quad \mathbf{C} = \begin{bmatrix} \Gamma^{-4} & 0 & 0 \\ 0 & \Gamma^2 & 0 \\ 0 & 0 & \Gamma^2 \end{bmatrix}. \quad (2.5.66)$$

We again have $I_3 = 1$ so that the deformation is volume preserving. It can then be shown that on requiring $T_{11} = 0$, the only remaining non-zero stresses are

$$T \equiv T_{22} = T_{33} = 2[(\Gamma^2 - \Gamma^{-4})W_1 + (\Gamma^4 - \Gamma^{-2})W_2 - \Gamma^{-4}W_5], \quad (2.5.67)$$

where the W_k are evaluated at

$$\left. \begin{aligned} I_1 &= \Gamma^{-4} + 2\Gamma^2, \\ I_2 &= \Gamma^4 + 2\Gamma^{-2}, \\ I_4 &= 0, \\ I_5 &= \Gamma^{-4}. \end{aligned} \right\} \quad (2.5.68)$$

For reasons that will become clear in the next paragraph, we rewrite (2.5.67) as

$$\begin{aligned} T_{11} &= \frac{2}{\Gamma^4} [(\Gamma^6 - 1)W_1 + (\Gamma^8 - \Gamma^2)W_2 - W_5] \\ &= \frac{2}{\Gamma^4} [(\Gamma^3 - 1)(\Gamma^3 + 1)W_1 + \Gamma^2(\Gamma^3 - 1)(\Gamma^3 + 1)W_2 - W_5] \\ &= \frac{2}{\Gamma^4} [(\Gamma - 1)(\Gamma^2 + \Gamma + 1)(\Gamma^3 + 1)(W_1 + \Gamma^2 W_2) - W_5], \end{aligned}$$

or

$$T = 2[(\Gamma^2 + \Gamma + 1)(\Gamma^3 + 1)\left(\frac{W_1}{\Gamma^4} + \frac{W_2}{\Gamma^2}\right) - \frac{W_5}{\Gamma^4(\Gamma - 1)}](\Gamma - 1). \quad (2.5.69)$$

Consider now the equibiaxial stress/stretch deformation in the linear theory. Then \mathbf{E} corresponding to (2.5.66)₁ is

$$\mathbf{E} = \begin{bmatrix} \Gamma^{-2} - 1 & 0 & 0 \\ 0 & \Gamma - 1 & 0 \\ 0 & 0 & \Gamma - 1 \end{bmatrix}, \quad (2.5.70)$$

so that from (2.5.70), (2.5.14)₂, (2.5.14)₃, $\sigma_{11} = 0$, and $\sigma_{22} = \sigma_{33} \equiv \sigma$, we have

$$(\Gamma - 1) = \frac{1}{E} (1 - \nu) \sigma \quad (2.5.71)$$

or

$$\sigma = \frac{E}{(1 - \nu)} (\Gamma - 1). \quad (2.5.72)$$

On comparing (2.5.69) and (2.5.72), we define the following generalized parameter

$\frac{E}{1 - \nu}$ which is a function of Γ as

$$\frac{E}{(1-\nu)}(\Gamma) = 2[(\Gamma^2 + \Gamma + 1)(\Gamma^3 + 1)\left(\frac{W_1}{\Gamma^4} + \frac{W_2}{\Gamma^2}\right) - \frac{W_5}{\Gamma^4(\Gamma - 1)}], \quad (2.5.73)$$

where the W_k are evaluated at the values of the invariants given by (2.5.68). We now recall the condition (2.5.45), which we write here as

$$2\bar{E} = \frac{E}{(1-\nu)}. \quad (2.5.74)$$

Now our aim is to show that (2.5.45), or equivalently, (2.5.74), puts no additional restrictions on the nonlinear stored-energy W . This will be accomplished by showing that the generalized parameters (2.5.18) and (2.5.73) satisfy

$$2\bar{E}(1) = \frac{E}{(1-\nu)}(1), \quad (2.5.75)$$

where $\bar{E}(1)$ is given by (2.5.19), (2.5.26). Taking the limit of (2.5.73) as $\Gamma \rightarrow 1$, we obtain

$$\frac{E}{(1-\nu)}(1) = \lim_{\Gamma \rightarrow 1} \frac{E}{(1-\nu)}(\Gamma) = 2[6(W_1 + W_2) - \lim_{\Gamma \rightarrow 1} \frac{W_5}{\Gamma^4(\Gamma - 1)}] \Big|_{I_1=I_2=3, I_4=0, I_5=1}, \quad (2.5.76)$$

where, similarly to what occurred in part (i) of this Section, the remaining limit in (2.5.76) is as yet indeterminate by virtue of (2.5.21). On using l'Hopital's rule, we have that

$$\lim_{\Gamma \rightarrow 1} \frac{W_5}{\Gamma^4(\Gamma - 1)} = \lim_{\Gamma \rightarrow 1} \frac{dW_5/d\Gamma}{\Gamma^4 + 4\Gamma^3(\Gamma - 1)} = \frac{dW_5}{d\Gamma} \Big|_{I_1=I_2=3, I_4=0, I_5=1}. \quad (2.5.77)$$

By the chain rule

$$\frac{dW_5}{d\Gamma} = \frac{\partial W_5}{\partial I_k} \frac{dI_k}{d\Gamma} \quad (2.5.78)$$

where, since $I_3 \equiv 1$, $I_4 \equiv 0$, summation over the indices $k = 1, 2, 5$ is implied. From

(2.5.68),

$$\frac{dI_1}{d\Gamma} = -4\Gamma^{-5} + 4\Gamma, \quad \frac{dI_2}{d\Gamma} = 4\Gamma^3 - 4\Gamma^{-3}, \quad \frac{dI_5}{d\Gamma} = -4\Gamma^{-5}, \quad (2.5.79)$$

so that on substituting (2.5.79) into (2.5.78) and letting $\Gamma \rightarrow 1$, we obtain

$$\frac{dW_5}{d\Gamma} \Big|_{\substack{I_1=I_2=3 \\ I_4=0, I_5=1}} = -4W_{55} \Big|_{\substack{I_1=I_2=3 \\ I_4=0, I_5=1}}. \quad (2.5.80)$$

Then (2.5.80), (2.5.77), and (2.5.76) give

$$\frac{E}{(1-\nu)}(1) = 2[6(W_1 + W_2) + 4W_{55}] \Big|_{\substack{I_1=I_2=3 \\ I_4=0, I_5=1}}, \quad (2.5.81)$$

which is exactly $2\bar{E}(1)$ where $\bar{E}(1)$ is given by (2.5.26). *Thus the condition (2.5.75) holds identically for the nonlinear stored-energy, and so (2.5.74), or equivalently (2.5.45), puts no further restrictions on W.*

2.5.2 Further considerations of $W(I_1, I_2, 1, 0, I_5)$

We wish now to show the connection between the preceding and the cavitation problem of concern in this dissertation. We make no attempt at this point to elaborate on this problem or on the determination of the invariants or deformation tensors associated with it. This will be addressed in the next chapter. The results to come in this Section depend only on the assumptions of incompressibility and transverse isotropy, and on the ability to write the invariants associated with a particular deformation in the following form:

$$\left. \begin{aligned} I_1(v) &= v^{-4} + 2v^2, \\ I_2(v) &= v^4 + 2v^{-2}, \\ I_3 &= 1, \\ I_4 &= 0, \\ I_5(v) &= v^{-4}. \end{aligned} \right\} \quad (2.5.82)$$

Thus, Section 2.5.2 may be applicable to a broad array of problems which includes the cavitation problem. For example, the invariants (2.5.68) associated with equibiaxial stress/stretch are of this form, and on defining $\Lambda = v^{-2}$ in the uniaxial tension deformation of Section 2.5.1(i), the invariants (2.5.12) become (2.5.82). For this reason and because the goals of this Section are in the spirit of this Chapter, we present this material here rather than elsewhere.

We introduce the notation

$$W(I_1, I_2, 1, 0, I_5) \equiv \tilde{W}(I_1(v), I_2(v), I_5(v)) = \hat{W}(v), \quad (2.5.83)$$

and we first intend to show that

$$\frac{d^2 \hat{W}}{dv^2}(1) = 4\bar{E} (> 0). \quad (2.5.84)$$

With this goal in mind, we define

$$\hat{W}_1(v) \equiv \frac{d\hat{W}}{dv} = \frac{\partial \tilde{W}}{\partial I_k} \frac{dI_k}{dv} \quad (2.5.85)$$

where summation over the indices $k = 1, 2, 5$ is assumed. From (2.5.82),

$$\frac{dI_1}{dv} = -4v^{-5} + 4v, \quad \frac{dI_2}{dv} = 4v^3 - 4v^{-3}, \quad \frac{dI_5}{dv} = -4v^{-5}. \quad (2.5.86)$$

When evaluated at $v = 1$, $\frac{dI_1}{dv} = \frac{dI_2}{dv} = 0$, so that

$$\hat{W}_1(1) \equiv \frac{d\hat{W}}{dv}(1) = -4 \frac{\partial \tilde{W}}{\partial I_5} \Big|_{v=1} = -4W_5(3,3,1,0,1) = 0 \quad (2.5.87)$$

on using (2.5.21). Now, from (2.5.85)

$$\frac{d^2\hat{W}}{dv^2}(v) = \frac{\partial \tilde{W}}{\partial I_k} \frac{d^2 I_k}{dv^2} + \frac{d}{dv} \left[\frac{\partial \tilde{W}}{\partial I_k} \right] \frac{d I_k}{dv}, \quad (2.5.88)$$

so that, by the arguments leading to (2.5.87),

$$\frac{d^2\hat{W}}{dv^2}(1) = \left[\frac{\partial \tilde{W}}{\partial I_1} \frac{d^2 I_1}{dv^2} + \frac{\partial \tilde{W}}{\partial I_2} \frac{d^2 I_2}{dv^2} + \frac{d}{dv} \left[\frac{\partial \tilde{W}}{\partial I_5} \right] \frac{d I_5}{dv} \right] \Big|_{v=1}. \quad (2.5.89)$$

From (2.5.86),

$$\frac{d^2 I_1}{dv^2} = 20v^{-6} + 4, \quad \frac{d^2 I_2}{dv^2} = 12v^2 + 12v^{-4}. \quad (2.5.90)$$

On evaluating (2.5.90), (2.5.86)₃, and (2.5.82) at $v=1$ and using (2.5.83), equation (2.5.89) becomes

$$\frac{d^2\hat{W}}{dv^2}(1) = 24 [W_1(3, 3, 1, 0, 1) + W_2(3, 3, 1, 0, 1)] - 4 \frac{dW_5}{dv} \Big|_{v=1}, \quad (2.5.91)$$

where the last term in (2.5.91) is

$$-4 \frac{dW_5}{dv} \Big|_{v=1} = -4 \frac{\partial W_5}{\partial I_k} \frac{d I_k}{dv} \Big|_{v=1} = 16 W_{55}. \quad (2.5.92)$$

On substituting (2.5.92) into (2.5.91), we obtain

$$\frac{d^2\hat{W}}{dv^2}(1) = 4[6(W_1 + W_2) + 4W_{55}] \Big|_{\substack{I_1=I_2=3 \\ I_3=1, I_4=0, I_5=1}}. \quad (2.5.93)$$

Comparing (2.5.93) with (2.5.26) and noting (2.5.27), we obtain the result claimed in (2.5.84), i.e.,

$$\frac{d^2 \hat{W}}{dv^2}(1) = 4\bar{E} (> 0), \quad (2.5.94)$$

where \bar{E} is Young's modulus in the direction of anisotropy for infinitesimal deformations of an incompressible transversely isotropic material.

Consider now the stored-energy w for such a linearly elastic material given by (2.4.8). The deformation gradient tensor \mathbf{F} corresponding to the invariants (2.5.82) is written as

$$\mathbf{F} = \begin{bmatrix} v^{-2} & 0 & 0 \\ 0 & v & 0 \\ 0 & 0 & v \end{bmatrix}. \quad (2.5.95)$$

Thus the infinitesimal strain tensor \mathbf{E} whose components E_{ij} appear in (2.4.8) is determined for the types of deformation of concern from (2.5.95), (2.3.2) as

$$\mathbf{E} = \begin{bmatrix} v^{-2} - 1 & 0 & 0 \\ 0 & v - 1 & 0 \\ 0 & 0 & v - 1 \end{bmatrix}, \quad (2.5.96)$$

so that (2.4.8) takes the form

$$w = \hat{w}(v) = \mu_T [(v^{-2} - 1)^2 + 2(v - 1)^2] + 2(\mu_L - \mu_T) (v^{-2} - 1)^2 + \frac{1}{2} \gamma (v^{-2} - 1)^2. \quad (2.5.97)$$

A simple calculation gives

$$\begin{aligned} \frac{d\hat{w}}{dv}(v) &= \mu_T [-4v^{-3}(v^{-2} - 1) + 4(v - 1)] - 4[2(\mu_L - \mu_T) + \frac{1}{2} \gamma] v^{-3}(v^{-2} - 1) \\ &= 4\mu_T [-v^{-5} + v^{-3} + v - 1] - 4[2(\mu_L - \mu_T) + \frac{1}{2} \gamma] (v^{-5} - v^{-3}), \end{aligned} \quad (2.5.98)$$

so that

$$\frac{d^2 \hat{w}}{dv^2}(v) = 4\mu_T [5v^{-6} - 3v^{-4} + 1] - 4[2(\mu_L - \mu_T) + \frac{1}{2} \gamma] (-5v^{-6} + 3v^{-4}). \quad (2.5.99)$$

On letting $v = 1$ in (2.5.99), we obtain

$$\frac{d^2 \hat{w}}{dv^2}(1) = 4(3\mu_T) + 8[2(\mu_L - \mu_T) + \frac{1}{2} \gamma]$$

or

$$\frac{d^2 \hat{w}}{dv^2}(1) = 4(4\mu_L + \gamma - \mu_T). \quad (2.5.100)$$

On comparing (2.5.100) with (2.4.10)₂, we obtain

$$\frac{d^2 \hat{w}}{dv^2}(1) = 4\bar{E}, \quad (2.5.101)$$

so that consistency between the nonlinear result (2.5.94) and the linear (2.5.101) gives

$$\frac{d^2 \hat{W}}{dv^2}(1) = \frac{d^2 \hat{w}}{dv^2}(1), \quad (2.5.102)$$

or in terms of the generalized Young's modulus, (2.5.102) is the consistency requirement

$$\bar{E}(1) = \bar{E} \quad (2.5.103)$$

(see e.g., equation (2.5.19)). We remark that (2.5.102) would also follow from considering $v = 1 + \epsilon$, $0 < \epsilon \ll 1$, and equating the first non-zero coefficients in the expansions of $\hat{W}(v)$ and $\hat{w}(v)$ in powers of ϵ .

2.5.3 Implications for a special class of nonlinearly elastic materials

Consider an incompressible transversely isotropic nonlinearly elastic material with stored-energy

$$W = \frac{\bar{\mu}}{2} [(I_1 - 3) + g(I_2 - 3) + f(I_5)], \quad (2.5.104)$$

where $\bar{\mu}$ is a constant, and g and f are as yet arbitrary functions of their arguments. The

material model (2.5.104) is a generalization to transversely isotropic materials of the Rivlin-Saunders material for incompressible isotropic nonlinear elasticity

$$W = c_1 (I_1 - 3) + g(I_2 - 3), \quad c_1 \text{ constant.} \quad (2.5.105)$$

We note that the Rivlin-Saunders material reduces to the classic Mooney-Rivlin and neo-Hookean materials when $g = c_2(I_2 - 3)$, c_2 constant, and $g \equiv 0$, respectively. The proposed strain energy (2.5.104) has no dependence on I_3 by virtue of incompressibility, and no dependence on I_4 since, as stated earlier, our concern is with those deformations for which the invariants I_1, \dots, I_5 can be given by (2.5.82).

From (2.5.104), we see that we must have

$$g(0) + f(1) = 0 \quad (2.5.106)$$

for the stored-energy to be zero in the undeformed state

$$I_1 = I_2 = 3, \quad I_5 = 1. \quad (2.5.107)$$

In addition, the further normalization condition (2.5.21) implies

$$f'(1) = 0, \quad (2.5.108)$$

where the prime notation denotes differentiation with respect to argument. For the material (2.5.104), the conditions (2.5.26), (2.5.27) imply

$$\bar{E} = \bar{\mu} [3 + 3g'(0) + 2f''(1)] > 0, \quad (2.5.109)$$

or on employing (2.5.82) to write (2.5.104) in terms of v , the result (2.5.94) gives

$$\frac{d^2 \hat{W}}{dv^2}(1) = 4\bar{\mu} [3 + 3g'(0) + 2f''(1)] > 0. \quad (2.5.110)$$

In addition, the conditions (2.5.54), (2.5.55), and (2.5.63), (2.5.64) imply that for the

material (2.5.104),

$$\mu = \bar{\mu} = \tilde{\mu} [1 + g'(0)] > 0. \quad (2.5.111)$$

Therefore, the conditions on the material (2.5.104) for normalization and physical reasonability are (2.5.106), (2.5.108), (2.5.109), and (2.5.111). We note from (2.5.111) that if $g \equiv 0$, or if simply $g'(0) = 0$, then

$$\mu = \bar{\mu} = \tilde{\mu} \quad (2.5.112)$$

for the material (2.5.104).

A special case of the material model (2.5.104) with $g \equiv 0$ is employed in Chapters 3 and 4 of this dissertation. This is given by

$$W = \frac{\mu}{2} \left[(I_1 - 3) + a(I_5^2 - 2I_5 + 1) \right], \quad (2.5.113)$$

where we have $\mu > 0$ by virtue of (2.5.112) and the comment preceding it, and the choice

$$f(I_5) = a(I_5^2 - 2I_5 + 1) \quad (a: \text{constant}) \quad (2.5.114)$$

can easily be seen to satisfy the normalization conditions (2.5.106) and (2.5.108). Thus the only remaining condition that (2.5.113) must satisfy is (2.5.109), which implies

$$\bar{E} = \mu (3 + 4a) > 0. \quad (2.5.115)$$

By (2.5.109), (2.5.110), and (2.5.115), we also have

$$\frac{d^2 \hat{W}}{dv^2}(1) = 4\mu (3 + 4a) \quad (2.5.116)$$

for the material model (2.5.113). Finally, from (2.5.112), (2.5.115), we determine that we must have

$$a > -\frac{3}{4} . \quad (2.5.117)$$

We remark that when $a = 0$ in (2.5.113), we recover the neo-Hookean (isotropic) material.

Chapter 3

HOMOGENEOUS ANISOTROPIC SPHERE

3.1. Introduction

As stated in Chapter 1, our aim in this dissertation is to examine the effects of *anisotropy* on the problem of cavitation in nonlinearly elastic incompressible materials. This problem is examined for a homogeneous sphere in this Chapter. In Section 3.2, we formulate the basic boundary value problem of concern. We consider a sphere composed of an incompressible anisotropic nonlinearly elastic material, which is transversely isotropic about the radial direction. The sphere is subjected to a prescribed uniform radial tensile dead-load p_0 on its boundary. In Section 3.3, it is shown that one solution to this problem, for all values of p_0 , corresponds to a trivial homogeneous state in which the sphere remains undeformed but stressed. However, for sufficiently large values of p_0 , one has in addition other possible radially symmetric configurations involving an internal traction-free cavity. Such solutions bifurcate from the homogeneous solution at p_{cr} , a critical value of p_0 . The existence of these bifurcated solutions depends on the constitutive law of the material (Section 3.4). In Section 3.5, a specific anisotropic material model (which may be viewed as a generalization of the classic isotropic neo-Hookean model) is considered and explicit results are obtained for the relationship $p_0 = p_0(c)$ between the applied tensile load p_0 and the deformed cavity radius c . In contrast to the situation for a neo-Hookean sphere, where bifurcation is always to the right, bifurcation here may occur locally either to the right (supercritical) or to the left (subcritical) depending on the degree of anisotropy. In Section 3.6, the stability of the

foregoing solutions is examined using an energy minimization approach. The cavitation solutions are shown to be the only stable solutions for sufficiently large loads. When bifurcation at $p_0 = p_{cr}$ occurs locally to the right, a smooth cavitation occurs with cavity radius increasing continuously (from zero) as p_0 increases. When bifurcation is to the left, a cavity of *finite* radius appears at a transition load which may be less than p_{cr} . Such a discontinuous change in stable equilibrium configurations is called, as in [20], "snap cavitation", by analogy with snap-through buckling in structural mechanics. (In Sections 3.5 and 3.6, for simplicity we focus mainly on results pertaining to the specific material model described in Section 3.5. In the next Chapter, a more general treatment will be given for the problem of cavitation in a composite anisotropic sphere. As noted in Chapter 1, general results for the homogeneous sphere may thus be recovered from those in Chapter 4 by the proper choice of the parameters of Chapter 4.) In Section 3.7, the stress distribution is described. When the cavity is nucleated smoothly (as described above), the dominant stress variation is confined to a narrow boundary layer near the cavity wall. Such boundary layers have previously been encountered in cavitation problems for *isotropic* materials ([6, 21]).

3.2. Problem formulation

We are concerned with a sphere composed of a homogeneous incompressible anisotropic nonlinearly elastic material. We denote the interior of the sphere in its undeformed configuration by $D_0 = \{(R, \Theta, \Phi) \mid 0 \leq R < B, 0 < \Theta \leq 2\pi, 0 \leq \Phi \leq \pi\}$. The sphere is subjected to a prescribed uniform radial tensile dead-load of magnitude p_0 on its boundary $R = B$. We assume that the resulting deformation, which takes the point in D_0 with spherical polar coordinates (R, Θ, Φ) to the point (r, θ, ϕ) in the deformed

configuration, is radially symmetric. Thus the deformation has the form $\theta = \Theta$, $\phi = \Phi$,

$$r = r(R) > 0, 0 < R < B; \quad r(0+) \geq 0, \quad (3.2.1)$$

where $r(R)$ is to be determined.

The deformation gradient tensor \mathbf{F} associated with (3.2.1), referred to spherical polar coordinates, is given by

$$\mathbf{F} = \text{diag} \left[\dot{r}(R), \quad r(R)/R, \quad r(R)/R \right] \quad (3.2.2)$$

where $\dot{r}(R) \equiv \frac{dr}{dR}$. Incompressibility then requires that $J \equiv \det \mathbf{F} = 1$, which upon integration yields

$$r(R) = (R^3 + c^3)^{1/3}, \quad (3.2.3)$$

where $c \geq 0$ is a constant to be determined. If it is found that $c = 0$, (3.2.3) implies that the body remains a solid sphere in the current configuration. However, if c is found to be positive, then $r(0+) = c > 0$ and so there is a cavity of radius c centered at the origin in the current configuration. In this event, the cavity surface is assumed to be traction-free.

The strain-energy density per unit undeformed volume for an elastic material that is transversely isotropic about the x_1 direction is given by (see e.g. [27])

$$W = W(I_1, I_2, I_3, I_4, I_5) \quad (3.2.4)$$

where

$$\left. \begin{aligned} I_1 &= \text{tr } \mathbf{C}, \\ I_2 &= \frac{1}{2} [(\text{tr } \mathbf{C})^2 - \text{tr } \mathbf{C}^2], \\ I_3 &= \det \mathbf{C}, \\ I_4 &= C_{12}^2 + C_{13}^2, \\ I_5 &= C_{11} \end{aligned} \right\} \quad (3.2.5)$$

\mathbf{C} is the right Cauchy-Green deformation tensor $\mathbf{C} = \mathbf{F}^T \mathbf{F}$, and x_i ($i = 1, 2, 3$) are coordinates of a point in the deformed configuration associated with an orthonormal basis. For incompressible materials, we must have $I_3 = J^2 = 1$. The corresponding response equation for the Cauchy stress tensor \mathbf{T} for transversely isotropic incompressible materials is [27]

$$\mathbf{T} = -p\mathbf{1} + 2(W_1 \mathbf{B} - W_2 \mathbf{B}^{-1} + W_4 \mathbf{M} + W_5 \mathbf{N}), \quad (3.2.6)$$

where \mathbf{B} is the left Cauchy-Green deformation tensor $\mathbf{B} = \mathbf{F} \mathbf{F}^T$, $\mathbf{1}$ is the unit tensor, p is the unknown hydrostatic pressure associated with the incompressibility constraint $J = 1$, and $W_q = \partial W / \partial I_q$ ($q = 1, 2, 4, 5$). The deformation tensors \mathbf{M}, \mathbf{N} associated with the anisotropy are given by

$$M_{ij} = C_{1\alpha} (F_{i\alpha} F_{j1} + F_{j\alpha} F_{i1}) \quad (\alpha = 2, 3) \quad (3.2.7)$$

and

$$N_{ij} = F_{i1} F_{j1}, \quad (3.2.8)$$

where $i, j = 1, 2, 3$, and summation over repeated indices is used. We shall assume that the strain-energy W vanishes in the undeformed state where $I_1 = 3, I_2 = 3, I_3 = 1, I_4 = 0$, and $I_5 = 1$, so that we have the normalization condition

$$W(3, 3, 1, 0, 1) = 0. \quad (3.2.9)$$

We also assume that in the undeformed state the initial stress is a hydrostatic pressure, so that (3.2.6) gives the further normalization condition (cf. [11], p. 292)

$$W_5(3, 3, 1, 0, 1) = 0. \quad (3.2.10)$$

In (3.2.5) - (3.2.8) we now let (r, θ, ϕ) be associated with the indices $(1, 2, 3)$ so that the sphere is transversely isotropic about the radial direction. Corresponding to the

deformation field (3.2.1), we thus obtain

$$\mathbf{C} = \mathbf{B} = \text{diag} \left[\dot{r}^2, r^2/R^2, r^2/R^2 \right], \quad (3.2.11)$$

$$\mathbf{M} = \mathbf{0}, \quad (3.2.12)$$

$$\mathbf{N} = \text{diag} \left[\dot{r}^2, 0, 0 \right], \quad (3.2.13)$$

and

$$I_1 = \dot{r}^2 + 2 r^2/R^2, \quad (3.2.14)$$

$$I_2 = r^4/R^4 + 2\dot{r}^2 r^2/R^2, \quad (3.2.15)$$

$$I_3 = \dot{r}^2 r^4/R^4 = 1, \quad (3.2.16)$$

$$I_4 = 0, \quad (3.2.17)$$

$$I_5 = \dot{r}^2. \quad (3.2.18)$$

Substitution from (3.2.11) - (3.2.13) into (3.2.6) yields the nonzero components of the Cauchy stress \mathbf{T} as

$$T_{rr} = -p + 2 (\dot{r}^2 W_1 - \dot{r}^{-2} W_2 + \dot{r}^2 W_5) \quad (3.2.19)$$

and

$$T_{\theta\theta} = T_{\phi\phi} = -p + 2(\dot{r}^{-1} W_1 - \dot{r} W_2), \quad (3.2.20)$$

where the W_t ($t = 1, 2, 5$) are evaluated at the values of the invariants given by (3.2.14) - (3.2.18).

The equilibrium equations, in the absence of body forces, are

$$\text{div } \mathbf{T} = \mathbf{0}, \quad (3.2.21)$$

which in the present case reduce to

$$\frac{\partial T_{rr}}{\partial r} + \frac{2}{r} (T_{rr} - T_{\theta\theta}) = 0, \quad (3.2.22)$$

$$\frac{1}{r} \frac{\partial T_{\theta\theta}}{\partial \theta} = 0, \quad (3.2.23)$$

$$\frac{1}{r \sin \theta} \frac{\partial T_{\phi\phi}}{\partial \phi} = 0. \quad (3.2.24)$$

Equation (3.2.4), in view of equations (3.2.14)-(3.2.18), implies that W , and thus W_q , are independent of the angular variables. Thus (3.2.20), together with (3.2.23) and (3.2.24), show that $p = p(r)$ only. Since $r = r(R)$, it is convenient for us to consider $T = T(R)$ rather than the more conventional $T = T(r)$. The remaining equilibrium equation (3.2.22), on using the chain-rule, becomes

$$\frac{dT_{rr}}{dR} + \frac{2\dot{r}}{r} (T_{rr} - T_{\theta\theta}) = 0, \quad 0 < R < B. \quad (3.2.25)$$

In view of (3.2.3), (3.2.19), (3.2.20), equation (3.2.25) is a first-order nonlinear ordinary differential equation for the pressure $p(R)$.

The dead-load boundary condition now requires that

$$T_{rr}(B) = p_0 \left[\frac{B}{r(B)} \right]^2, \quad (3.2.26)$$

where the constant $p_0 > 0$ is prescribed. We note that the boundary conditions of vanishing shear tractions are satisfied identically.

Thus, the boundary value problem to be solved is the following: *For a prescribed value of the dead-load traction $p_0 > 0$, we seek a pressure field $p(R)$ and a constant $c \geq 0$ such that (3.2.25), (3.2.26) are satisfied where T_{rr} , $T_{\theta\theta}$ are given by (3.2.19), (3.2.20), (3.2.3). In addition, if $c > 0$, then the condition for a traction-free cavity surface*

$$T_{rr}(0) = 0 \quad (3.2.27)$$

must also hold.

3.3. Solutions

On using the normalization condition (3.2.10), it may readily be shown that one solution of the foregoing problem for all values of p_0 is

$$p(R) = 2[W_1(3, 3, 1, 0, 1) - W_2(3, 3, 1, 0, 1)] - p_0, \quad c = 0. \quad (3.3.1)$$

This corresponds to the trivial homogeneous state of deformation

$$r(R) = R, \quad (3.3.2)$$

with corresponding stresses $T_{rr} = T_{\theta\theta} = T_{\phi\phi} = p_0$, so that the sphere remains undeformed under a state of hydrostatic pressure.

We next describe solutions for which $c > 0$, corresponding to the presence of a traction-free cavity at the origin. For this purpose, it is convenient to introduce the notation (cf. Ball [5]),

$$\left. \begin{aligned} v = v(R) &\equiv r(R)/R = \left(1 + \frac{c^3}{R^3}\right)^{1/3} \\ v^{-2} &= \dot{r} \end{aligned} \right\}, \quad (3.3.3)$$

where the second equation in (3.3.3) results from the definition of v and (3.2.16). Using (3.3.3), the invariants (3.2.14) - (3.2.18) can be written as

$$\left. \begin{aligned} I_1 &= v^{-4} + 2v^2, \\ I_2 &= v^4 + 2v^{-2}, \\ I_3 &= 1, \\ I_4 &= 0, \\ I_5 &= v^{-4}. \end{aligned} \right\} \quad (3.3.4)$$

On using (3.2.19), (3.2.20), we adopt an approach developed in [20] and rewrite the

differential equation (3.2.25) in the form

$$\begin{aligned} \frac{d}{dR} \left\{ 2 [v^{-4} W_1 (v^{-4} + 2v^2, v^4 + 2v^{-2}, 1, 0, v^{-4}) - v^4 W_2 (v^{-4} + 2v^2, v^4 + 2v^{-2}, 1, 0, v^{-4}) \right. \\ \left. + v^{-4} W_5 (v^{-4} + 2v^2, v^4 + 2v^{-2}, 1, 0, v^{-4})] - p(R) \right\} \\ + \frac{4v^{-3}}{R} [(v^{-4} - v^2) W_1 (v^{-4} + 2v^2, v^4 + 2v^{-2}, 1, 0, v^{-4}) \\ + (v^{-2} - v^4) W_2 (v^{-4} + 2v^2, v^4 + 2v^{-2}, 1, 0, v^{-4}) \\ + v^{-4} W_5 (v^{-4} + 2v^2, v^4 + 2v^{-2}, 1, 0, v^{-4})] = 0 \text{ on } 0 < R < B. \end{aligned} \quad (3.3.5)$$

On integration of (3.3.5), we have

$$p(R) - p(0) = 2 \left\{ v^{-4}(R) (W_1 + W_5) \Big|_R - v^4(R) W_2 \Big|_R \right\} + 4J(R), \quad 0 < R < B, \quad (3.3.6)$$

where

$$J(R) = \int_0^R \left[[v^{-7}(s) - v^{-1}(s)] W_1 \Big|_s + [v^{-5}(s) - v(s)] W_2 \Big|_s + v^{-7}(s) W_5 \Big|_s \right] \frac{ds}{s}. \quad (3.3.7)$$

In (3.3.6), (3.3.7) the W_l ($l = 1, 2, 5$) are evaluated at the values of the invariants given by (3.3.4), and for simplicity we have introduced the notation

$$W_l \Big|_s = W_l (v^{-4}(s) + 2v^2(s), v^4(s) + 2v^{-2}(s), 1, 0, v^{-4}(s)). \quad (3.3.8)$$

Using (3.3.3), (3.3.6), the radial stress (3.2.19) becomes

$$T_{rr}(R) = -p(0) - 4J(R), \quad 0 < R < B. \quad (3.3.9)$$

The traction-free cavity surface condition (3.2.27), together with (3.3.9) and $J(0) = 0$, now yield

$$p(0) = 0 \quad (3.3.10)$$

so that

$$T_{rr}(R) = -4J(R), \quad 0 < R < B. \quad (3.3.11)$$

Finally, by virtue of (3.3.11), (3.3.3), we see that the dead-load boundary condition (3.2.26) at the outer surface $R = B$, is satisfied if

$$-4J(B) = p_0 [v(B)]^{-2}. \quad (3.3.12)$$

The condition (3.3.12) may be written in a compact fashion on utilizing the change of variables $s \rightarrow v$ in the integral (3.3.7). From (3.3.3) it is seen that this change of variables is one-to-one and invertible if and only if $c > 0$. Introducing the function

$$\hat{W}(x) = W(x^{-4} + 2x^2, x^4 + 2x^{-2}, 1, 0, x^{-4}), \quad (3.3.13)$$

and adopting the notation

$$\hat{W}_1(x) = \frac{d}{dx} \hat{W}(x), \quad (3.3.14)$$

it is shown in Appendix A that one may write (3.3.12) as

$$p_0 = \left[1 + \frac{c^3}{B^3} \right]^{3/2} \int_{(1 + \frac{c^3}{B^3})^{1/2}}^{\infty} \frac{\hat{W}_1(v)}{v^3 - 1} dv, \quad c > 0. \quad (3.3.15)$$

We remark that (3.3.15), here established for the anisotropic sphere, has formally the same structure as the analogous relation for the isotropic sphere (see equation (5.18) of [5] or equation (22) of [6]). For a given dead-load p_0 , solutions involving a traction-free internal cavity of radius c exist provided that c is a positive root of (3.3.15). Substitution from (3.3.10) into (3.3.6) gives the associated pressure field as

$$p(R) = 2 \left[v^{-4}(R) (W_1 + W_5)|_R - v^4(R) W_2|_R \right] + 4J(R), \quad 0 < R < B. \quad (3.3.16)$$

In summary, we have seen that for all values of the applied dead-load traction p_0 , one obtains the trivial solution (3.3.1) corresponding to the homogeneous state of deformation (3.3.2). Moreover, if positive roots c of (3.3.15) exist, then one obtains the

additional solutions involving a traction-free internal cavity described above.

3.4. The critical load and bifurcation

The *critical load* p_{cr} at which an internal cavity may be initiated is found by formally letting $c \rightarrow 0+$ in (3.3.15), and so

$$p_{cr} = \int_1^{\infty} \frac{\hat{W}_1(v)}{v^3 - 1} dv. \quad (3.4.1)$$

Since the integral (3.4.1) is improper, p_{cr} may or may not be finite, and thus cavitation may or may not take place.

As regards the lower limit in (3.4.1), it is shown in Chapter 2 (see equations (2.5.87), (2.5.94)) that

$$\hat{W}_1(1) \equiv \frac{d\hat{W}(1)}{dv} = 0, \quad \frac{d^2\hat{W}(1)}{dv^2} = 4\bar{E}, \quad (3.4.2)$$

where \bar{E} is Young's modulus in the radial direction associated with infinitesimal deformations of the transversely isotropic material at hand. Thus by l' Hopital's rule, the limit of the integrand in (3.4.1) is finite as $v \rightarrow 1$. Thus, as in the isotropic case, the finiteness of p_{cr} depends on the behavior of $\hat{W}(v)$ for *large* values of the stretch v . Suppose that the strain-energy density per unit undeformed volume for the transversely isotropic elastic material can be written in the form

$$\hat{W}(v) = a_{-m} v^{-m} + \dots + a_{-1} v^{-1} + a_0 + a_1 v + \dots + a_n v^n, \quad m, n \geq 0, \quad m + n > 0, \quad (3.4.3)$$

so that

$$\hat{W}_1(v) = -m a_{-m} v^{-m-1} - \dots - a_{-1} v^{-2} + a_1 + 2a_2 v + \dots + n a_n v^{n-1}. \quad (3.4.4)$$

From (3.4.4) we see that for large values of the stretch v , the integral (3.4.1) will converge if

$$v^{n-4} < v^{-1} . \quad (3.4.5)$$

Thus, for a strain-energy density which can be written in the form (3.4.3), we must have

$$n < 3 . \quad (3.4.6)$$

A similar condition was previously determined for the incompressible *isotropic* sphere (see equations (28), (29) of [6]). For more general W , the finiteness of p_{cr} in (3.4.1) also requires restrictions on the rate of growth of W for large stretch.

We now consider the local character of the bifurcation at $p_0 = p_{cr}$ by analyzing the curve $p_0 = p_0(c)$, given by (3.3.15), for small values of c . A Taylor expansion of (3.3.15) about $c = 0$ shows that

$$p_0 = p_{cr} + k \left[\frac{c}{B} \right]^3 + o(c^3) \text{ as } c \rightarrow 0 \quad (3.4.7)$$

where

$$k = \lim_{c \rightarrow 0} dp_0/dc^3 . \quad (3.4.8)$$

From (3.3.15) one obtains

$$k = \frac{2}{3} p_{cr} - \frac{1}{3} \lim_{v \rightarrow 1} \frac{d\hat{W}/dv}{v^3 - 1} . \quad (3.4.9)$$

On using l'Hopital's rule, we write k as

$$k = \frac{2}{3} \left[p_{cr} - \frac{1}{6} \frac{d^2 \hat{W}(1)}{dv^2} \right] , \quad (3.4.10)$$

where from (3.4.2)₂ the quantity $d^2 \hat{W}(1)/dv^2$ is finite and can be written in terms of the

infinitesimal Young's modulus in the radial direction. We see from (3.4.7) that if $k > 0$, bifurcation is locally to the right (supercritical) while if $k < 0$, bifurcation is locally to the left (subcritical). (As an illustration of these two cases, see Figures 3.3, 3.4, respectively, for values of $\rho = c/B$ close to zero.)

3.5. Illustrative example

3.5.1. A class of anisotropic incompressible elastic materials

We now consider a specific material model and provide an explicit solution for the bifurcation problem discussed in Sections 3.2-3.4. We recall from (3.2.17) that the invariant I_4 vanishes identically for the radially symmetric deformations of concern here. Thus one of the simplest strain-energy densities modeling the anisotropy of interest in this dissertation may be taken as

$$W = \frac{\mu}{2} [(I_1 - 3) + f(I_5)] , \quad (3.5.1)$$

where $\mu > 0$ is a constant and $f(I_5)$ is an arbitrary function of the fifth invariant subject only to the restrictions arising from the normalization conditions (3.2.9), (3.2.10), namely

$$f(1) = 0, \quad f'(1) = 0 , \quad (3.5.2)$$

where the prime notation denotes differentiation with respect to argument. In the special case where $f \equiv 0$, (3.5.1) reduces to the well-known neo-Hookean isotropic material model.

Rather than proceeding with a general function f in (3.5.1), we now restrict f to be a polynomial in I_5 . To satisfy the conditions (3.5.2), it can be seen that the simplest nontrivial representation for f is a quadratic function of I_5 , $f(I_5) = aI_5^2 + bI_5 + c$, where a ,

b, c are constants. On employing (3.5.2) this representation for f becomes

$$f(I_5) = a(I_5^2 - 2I_5 + 1), \quad (3.5.3)$$

where the constant $a \geq 0$ is a dimensionless parameter which serves as a measure of the degree of anisotropy of the material. Thus, from (3.5.1) and (3.5.3) we obtain the strain-energy density function

$$W = \frac{\mu}{2} \left[(I_1 - 3) + a(I_5^2 - 2I_5 + 1) \right], \quad (3.5.4)$$

which we use as an illustrative example for the remainder of this paper. When $a = 0$ in (3.5.4), one recovers the neo-Hookean (isotropic) material. We note that the above condition $a \geq 0$ is somewhat more restrictive than $a > -3/4$ determined in (2.5.117), and that μ in (3.5.1) and (3.5.4) is equivalent to the shear moduli in infinitesimal deformations of the transversely isotropic material at hand (see Section 2.5.3 and equation (2.5.112)).

The response of the material (3.5.4) to certain basic pure homogeneous deformations will now be discussed.

(i) *Uniaxial Tension:*

For uniaxial tension in the x_1 - direction (the axis of anisotropy) we have

$$T_{22} = T_{33} = 0, \quad T_{11} \neq 0, \quad \lambda_1 = \lambda > 1, \quad \lambda_2 = \lambda_3 = \lambda^{-1/2}, \quad (3.5.5)$$

where the λ_i ($i = 1, 2, 3$) are the principal stretches. For this deformation, the stress-stretch relationship for the material (3.5.4) is given by

$$T_{11}(\lambda) = \mu [(\lambda^2 - \lambda^{-1}) + 2a \lambda^2 (\lambda^2 - 1)]. \quad (3.5.6)$$

It is readily verified that $dT_{11}/d\lambda > 0$ for $\lambda > 1$ and so $T_{11}(\lambda)$ is monotone increasing in λ ,

$1 < \lambda < \infty$, for all values of the anisotropy parameter $a \geq 0$. The relationship (3.5.6) is plotted in Figure 3.1 for various values of a .

(ii) *Equibiaxial Stress (Stretch)*:

We next consider the deformation

$$T_{11} = 0, T_{22}(\lambda) = T_{33}(\lambda) \neq 0, \quad \lambda_2 = \lambda_3 = \lambda, \quad \lambda_1 = \lambda^{-2}. \quad (3.5.7)$$

We note that for the bifurcation problem of concern in this paper, we have

$$T_{rr} = 0, \quad T_{\theta\theta} = T_{\phi\phi} \neq 0, \quad \lambda_\theta = \lambda_\phi = v, \quad \lambda_r = v^{-2} \quad (3.5.8)$$

on the cavity boundary, so that locally, a state of equibiaxial stress (stretch) exists at the cavity wall. For the deformation (3.5.7), the stress-stretch relationship for the material (3.5.4) is given by

$$T(\lambda) \equiv T_{22}(\lambda) = T_{33}(\lambda) = \mu [(\lambda^2 - \lambda^{-4}) - 2a \lambda^{-4}(\lambda^{-4} - 1)]. \quad (3.5.9)$$

This relationship is plotted in Figure 3.2 for various values of the anisotropy parameter a . It can be seen that $T(\lambda)$ is monotone increasing in λ for $1 < \lambda < \infty$ provided the constant a is such that $a \leq 5.0$ (approximately). It is assumed in what follows that $0 \leq a \leq 5$. It will be seen that interesting effects of anisotropy on cavitation will occur for values of a well within this range.

We note here that for both uniaxial tension and equibiaxial stress, the stress-stretch curves involving the nominal stress $\mathbf{S} = (\det \mathbf{F}) \mathbf{F}^{-1} \mathbf{T}$ are analogous to Figures 3.1, 3.2, respectively. Finally, we also remark that the response of the material (3.5.4) in simple shear is exactly that of the neo-Hookean material.

3.5.2. Cavitation solutions

We now return to the cavitation problem for the material model (3.5.1), (3.5.2). By virtue of (3.3.4), (3.3.13), we rewrite (3.5.1) as

$$\hat{W}(v) = \frac{\mu}{2} [(v^{-4} + 2v^2 - 3) + f(v^{-4})], \quad (3.5.10)$$

so that, recalling the notation (3.3.14),

$$\hat{W}_1(v) = \frac{\mu}{2} [-4v^{-5} + 4v - 4v^{-5} f'(v^{-4})]. \quad (3.5.11)$$

Substituting (3.5.11) into (3.3.15), we obtain the relationship

$$p_0 = 2\mu \left[1 + \frac{c^3}{B^3} \right]^{3/4} \int_{(1 + \frac{c^3}{B^3})^{1/4}}^{\infty} \left[\frac{v - v^{-5}}{v^3 - 1} - \frac{v^{-5} f'(v^{-4})}{v^3 - 1} \right] dv, \quad (3.5.12)$$

so that positive roots c of (3.5.12) correspond to solutions involving a traction-free internal spherical cavity. We rewrite (3.5.12) as

$$p_0 = 2\mu \left(1 + \frac{c^3}{B^3} \right)^{3/4} (J_1 + J_2), \quad (3.5.13)$$

where

$$J_1 = \int_{(1 + \frac{c^3}{B^3})^{1/4}}^{\infty} \frac{v - v^{-5}}{v^3 - 1} dv \quad (3.5.14)$$

and

$$J_2 = \int_{(1 + \frac{c^3}{B^3})^{1/4}}^{\infty} \frac{-v^{-5} f'(v^{-4})}{v^3 - 1} dv. \quad (3.5.15)$$

Upon integration of (3.5.14), (see Appendix C for evaluation of this and all subsequent integrals), we obtain

$$J_1 = \left(1 + \frac{c^3}{B^3}\right)^{-1/3} + \frac{1}{4} \left(1 + \frac{c^3}{B^3}\right)^{-4/3}. \quad (3.5.16)$$

We now consider the special case (3.5.4) of the material model (3.5.1), so that from (3.5.3), (3.3.4) we have

$$f'(v^{-4}) = 2a (v^{-4} - 1). \quad (3.5.17)$$

Substituting (3.5.17) into (3.5.15) we obtain

$$J_2 = 2a \int_{(1 + c^3/B^3)^{1/3}}^{\infty} \frac{v^{-5} - v^{-9}}{v^3 - 1} dv. \quad (3.5.18)$$

Evaluation of (3.5.18) (see Appendix C) gives

$$\begin{aligned} J_2 = 2a & \left\{ \frac{5\pi}{6\sqrt{3}} - \left(1 + \frac{c^3}{B^3}\right)^{-1/3} + \frac{1}{2} \left(1 + \frac{c^3}{B^3}\right)^{-2/3} - \frac{1}{4} \left(1 + \frac{c^3}{B^3}\right)^{-4/3} \right. \\ & \left. + \frac{1}{5} \left(1 + \frac{c^3}{B^3}\right)^{-5/3} + \frac{1}{8} \left(1 + \frac{c^3}{B^3}\right)^{-8/3} \right. \\ & \left. - \frac{1}{\sqrt{3}} \left[\arctan \left[\frac{2(1 + c^3/B^3)^{1/3} + 1}{\sqrt{3}} \right] + \arctan \left[\frac{\sqrt{3} (1 + c^3/B^3)^{1/3}}{2 + (1 + c^3/B^3)^{1/3}} \right] \right] \right\}. \end{aligned} \quad (3.5.19)$$

Thus, for the material (3.5.4), the relationship $p_0 = p_0(c)$ between the prescribed dead-load traction p_0 and the cavity radius c is given by (3.5.13), (3.5.16), (3.5.19).

We now recall the discussion in Section 3.4 regarding the critical load p_{cr} at which an internal cavity may be initiated. First we use (3.3.4) to write (3.5.4) as

$$\hat{W}(v) = \frac{\mu}{2} [(v^{-4} + 2v^2 - 3) + a (v^{-8} - 2v^{-4} + 1)]. \quad (3.5.20)$$

Comparing (3.5.20) with (3.4.3), we have $n = 2$ and thus (3.4.6) holds, so that the integral (3.4.1) is finite for the material (3.5.4). (In fact, since $I_5 = v^{-4}$, the integral (3.4.1) will be

finite for the material (3.5.1) whenever $f(I_5)$ is a polynomial in I_5 of *any* (non-negative) degree and so the anisotropy does not affect the finiteness of p_{cr} .) On letting $c \rightarrow 0+$ in (3.5.13), (3.5.16), (3.5.19), it can be shown that

$$p_{cr} = \mu \left[\frac{5}{2} + \left[\frac{40\pi - 51\sqrt{3}}{30\sqrt{3}} \right] a \right] \approx \mu (2.5 + 0.72a). \quad (3.5.21)$$

When $a = 0$ in (3.5.4), (3.5.21), we recover the result for the neo-Hookean material (see e.g. [5], [6]).

Thus, if we consider a quasi-static loading process in which the solid sphere is subjected to a tensile dead-load p_0 that increases slowly from zero, cavity formation and growth is described by the relationship $p_0 = p_0(c)$ given by (3.5.13), (3.5.16), (3.5.19). For various values of the parameter a , the critical load p_{cr} given in (3.5.21) is the value at which the curve $p_0 = p_0(c)$ bifurcates from the straight line $c = 0$ corresponding to the trivial solution.

In what follows, it is convenient to introduce the dimensionless quantities

$$P = \frac{p_0}{\mu}, \quad P_{cr} = \frac{p_{cr}}{\mu}, \quad K = \frac{k}{\mu}, \quad \rho = \frac{c}{B}, \quad (3.5.22)$$

so that (3.5.22), (3.5.13), (3.5.16), (3.5.19) yield

$$\begin{aligned}
P = P(\rho) = 2(1 + \rho^3)^{2/3} & \left\{ (1 + \rho^3)^{-1/3} + \frac{1}{4} (1 + \rho^3)^{-4/3} + 2a \left\{ \frac{5\pi}{6\sqrt{3}} - (1 + \rho^3)^{-1/3} \right. \right. \\
& + \frac{1}{2} (1 + \rho^3)^{-2/3} - \frac{1}{4} (1 + \rho^3)^{-4/3} + \frac{1}{5} (1 + \rho^3)^{-5/3} + \frac{1}{8} (1 + \rho^3)^{-8/3} \\
& \left. \left. - \frac{1}{\sqrt{3}} \left[\arctan \left[\frac{2(1 + \rho^3)^{1/3} + 1}{\sqrt{3}} \right] + \arctan \left[\frac{\sqrt{3} (1 + \rho^3)^{1/3}}{2 + (1 + \rho^3)^{1/3}} \right] \right] \right\} \right\}.
\end{aligned} \quad (3.5.23)$$

On letting $\rho \rightarrow 0+$ in (3.5.23) one obtains

$$P_{cr} = \frac{5}{2} + \left[\frac{40\pi - 51\sqrt{3}}{30\sqrt{3}} \right] a, \quad (3.5.24)$$

which is, of course, exactly (3.5.21). By analyzing the curve (3.5.23) in the (P, ρ) - plane for small values of ρ , we can determine the local character of the bifurcation at $\rho = 0$.

Letting

$$P^*(\rho^3) \equiv P(\rho), \quad (3.5.25)$$

the Taylor expansion (3.4.7) for the material (3.5.4) can now be written as

$$P^*(\rho^3) = P_{cr} + K\rho^3 + o(\rho^3) \text{ as } \rho \rightarrow 0, \quad (3.5.26)$$

where P_{cr} is given by (3.5.24), and (3.4.10), (3.5.20), (3.5.24) give

$$K = \frac{1}{3} + \left[\frac{40\pi - 131\sqrt{3}}{45\sqrt{3}} \right] a. \quad (3.5.27)$$

Thus the curve $P = P^*(\rho^3)$ branches from the line $\rho = 0$, $P > 0$, at the point $\rho = 0$, $P = P_{cr}$, and (3.5.26), (3.5.27) show that this branching (bifurcation) is to the right (see Fig. 3.3) if $K > 0$ and is to the left (see Fig. 3.4) if $K < 0$. From (3.5.27), these

conditions on K may be written as $a < a_0$ or $a > a_0$ respectively, where

$$a_0 = \frac{15\sqrt{3}}{131\sqrt{3} - 40\pi} \approx 0.257. \quad (3.5.28)$$

(Note that a_0 is well within the range of values for a assumed earlier in this section.)

Thus, *for sufficiently small values of the anisotropy parameter a , bifurcation is locally to the right as for the neo-Hookean material. As the degree of anisotropy increases beyond $a = a_0$, the bifurcation character changes to being locally to the left.* In Figs. 3.3 and 3.4 we have plotted the curve (3.5.23) for two representative choices of the parameter a . In Fig. 3.4, there exists a turning point (P_t, ρ_t) of the curve at which

$$\frac{dP}{d\rho} = 0. \quad (3.5.29)$$

The point (P_t, ρ_t) is thus determined by solving (3.5.29) for the root ρ_t and then using (3.5.23) to give $P_t = P(\rho_t)$.

To conclude this section, we examine the curve (3.5.23) for large values of ρ . A detailed analysis given in Appendix B shows that

$$P \sim 2\rho \text{ as } \rho \rightarrow \infty, \quad (3.5.30)$$

so that the curve (3.5.23) is asymptotic to a straight line with slope = 2, *for all values of the parameter a .* Thus the initial character of the bifurcation at $(P, \rho) = (P_{cr}, 0)$ does not affect the large ρ asymptotic behavior of $P(\rho)$.

3.6. Energy and stability of solutions

To examine the stability of the cavitation solutions, we now carry out an energy analysis. Returning to the considerations of Sections 3.2 - 3.4 for general W , we find that the total energy associated with any equilibrium configuration of the body is given by

$$\begin{aligned}
 E(c) = & 4\pi \int_0^B W(\dot{r}^2 + 2r^2/R^2, r^4/R^4 + 2\dot{r} r^2/R^2, 1, 0, \dot{r}^2) R^2 dR \\
 & - 4\pi B^2 p_0 [r(B) - B].
 \end{aligned}
 \tag{3.6.1}$$

The first term on the right in (3.6.1) is the total strain-energy while the second term is the work done by the dead-load tractions. For the trivial solution (3.3.1) with deformation (3.3.2), we see that

$$E(0) = 0 \tag{3.6.2}$$

on using the normalization (3.2.9). We will see in this section that equilibrium solutions with an internal cavity of radius $c > 0$ may lead to either positive or negative values for $E(c)$. Following the approach of [20], we now extend our interpretation of the energy function $E(c)$, given by (3.6.1), to hold for all values of $c \geq 0$ and not just for those values associated with equilibrium solutions. We shall seek values of $c \geq 0$ that, for a given $p_0 > 0$, minimize the extended function $E(c)$.

Recalling the notation (3.3.13), (3.3.3), we may write equation (3.6.1) as

$$\begin{aligned}
 E(c) = & 4\pi c^3 \int_{(1+c^3/B^3)^{1/3}}^{\infty} v^2 (v^3 - 1)^{-2} W(v^{-4} + 2v^2, v^4 + 2v^{-2}, 1, 0, v^{-4}) dv \\
 & - 4\pi B^2 p_0 [r(B) - B], \quad c > 0.
 \end{aligned}
 \tag{3.6.3}$$

An analogous expression has been obtained in Ball [5] for the isotropic homogeneous sphere, and also by Horgan and Pence [20] for the isotropic composite sphere. (See equations (5.5) and (5.19) of [5] and equation (2.27) of [20].)

In what follows, we confine attention to the illustrative example described in Section 3.5. For the transversely isotropic sphere with strain-energy density given by

(3.5.4) (or equivalently, by (3.5.20)), the expression (3.6.3) for $E(c)$ yields

$$E(c) = 4\pi c^3 \frac{\mu}{2} \int_{(1+c^3/B^3)^{1/3}}^{\infty} (v^3 - 1)^{-2} [(v^{-2} + 2v^4 - 3v^2) + a(v^{-6} - 2v^{-2} + v^2)] dv \\ - 4\pi B^2 p_0 [(B^3 + c^3)^{1/3} - B], \quad c > 0. \quad (3.6.4)$$

Upon integration of (3.6.4) (see Appendix C) and introduction of the dimensionless quantity

$$\Sigma = \frac{E}{(4/3) \pi B^3 \mu}, \quad (3.6.5)$$

we obtain

$$\Sigma(\rho) = \alpha(\rho) + P\beta(\rho), \quad \rho \geq 0 \quad (3.6.6)$$

where

$$\alpha(\rho) = 3(1 + \rho^3)^{2/3} - \frac{3}{2} (1 + \rho^3)^{-1/3} - \frac{3}{2} + a \left\{ \frac{10\sqrt{3} \pi}{9} + \frac{5 + 8\rho^3}{10} (1 + \rho^3)^{-5/3} \right. \\ \left. + 2\rho^3 (1 + \rho^3)^{-2/3} + 3(1 + \rho^3)^{-1/3} - 4(1 + \rho^3)^{2/3} + \frac{1}{2} \right. \\ \left. - \frac{4}{\sqrt{3}} \rho^3 \left[\arctan \frac{\sqrt{3}(1 + \rho^3)^{1/3}}{2 + (1 + \rho^3)^{1/3}} + \arctan \frac{2(1 + \rho^3)^{1/3} + 1}{\sqrt{3}} \right] \right\}, \quad (3.6.7)$$

and

$$\beta(\rho) = -3[(1 + \rho^3)^{1/3} - 1]. \quad (3.6.8)$$

Thus the energy minimization problem for the material (3.5.4) can be stated in a purely algebraic setting: *for fixed $P > 0$, we seek those values of $\rho \geq 0$ that minimize $\Sigma(\rho)$.*

We begin by examining the end-point $\rho = 0$ where $\Sigma(0) = 0$. Using a superposed dot to denote differentiation with respect to ρ , it can be shown that

$$\dot{\Sigma}(0+) = \ddot{\Sigma}(0+) = 0, \quad \ddot{\Sigma}(0+) = 6(P_{cr} - P), \quad (3.6.9)$$

where we recall that for the material (3.5.4), P_{cr} is given by (3.5.24). Thus $\rho = 0$ is a local minimum if $P < P_{cr}$ and a local maximum if $P > P_{cr}$. Observe that

$$\rho = 0, \quad P > 0, \quad (3.6.10)$$

corresponds to the trivial solution (3.3.1).

We now consider the possible existence of internal extrema and thus seek values of $\rho > 0$ for which

$$\dot{\Sigma}(\rho) = \dot{\alpha}(\rho) + P \dot{\beta}(\rho) = 0. \quad (3.6.11)$$

From (3.6.8), $\dot{\beta}(\rho) < 0$ for $\rho > 0$ so that (3.6.11) may be written as

$$P = - \frac{\dot{\alpha}(\rho)}{\dot{\beta}(\rho)}, \quad \rho > 0. \quad (3.6.12)$$

We observe that the expression for $P(\rho)$ given by (3.6.12), derived from the preceding energy considerations, can be seen to be identical to the expression (3.5.23), which was obtained from the solution (3.3.15) determined directly in Section 3.3. Thus, as expected, the extremals provided by (3.6.12) correspond to the equilibrium solutions with an internal cavity.

Analyzing the dimensionless energy $\Sigma(\rho)$ given by (3.6.6) - (3.6.8) near $\rho = 0$ and using (3.5.26), we obtain

$$\Sigma(\rho) = -\frac{1}{2} K \rho^6 + O(\rho^9) \quad \text{as } \rho \rightarrow 0, \quad (3.6.13)$$

where K is given by (3.5.27). Thus, recalling the results at the end of Section 3.5, where the curve (3.6.12) (or equivalently (3.5.23)) was shown to bifurcate from the trivial solution (3.6.10) at the point $\rho = 0, P = P_{cr}$, (3.6.13) shows that $\Sigma < 0$ on this curve near $\rho = 0$ if the bifurcation is to the right ($K > 0$ or $a < a_0$) and $\Sigma > 0$ if the bifurcation is to

the left ($K < 0$ or $a > a_0$). Furthermore, examining (3.6.6) - (3.6.8) for large values of ρ , and using (3.5.30), an analysis similar to that of Appendix B shows that

$$\Sigma \sim -3\rho^2 \text{ as } \rho \rightarrow \infty, \quad (3.6.14)$$

so that Σ will always be negative on the curve (3.5.23) for sufficiently large values of ρ , *independent of the values of a* . Thus the initial character of the bifurcation at $(P, \rho) = (P_{cr}, 0)$ does not affect the large ρ asymptotic behavior of Σ on the curve (3.5.23).

The results obtained thus far in this section for the transversely isotropic sphere with strain-energy density given by (3.5.4) are analogous to those established by Horgan and Pence [20] for an isotropic composite neo-Hookean sphere. (See Section 3 of [20]). We now state two properties established in [20] which will be utilized in our discussion of stability of the equilibrium solutions (3.6.10), (3.5.23). These properties may be verified using arguments analogous to those given in [20, pp. 72-74].

Property A: The curve $P = P(\rho)$ is a locus of local *minima* of $\Sigma(\rho)$ for fixed P whenever $dP/d\rho > 0$, and is a locus of local *maxima* of $\Sigma(\rho)$ for fixed P whenever $dP/d\rho < 0$.

Property B: On the curve $P = P(\rho)$, the values of $\Sigma(\rho)$ are *decreasing* with ρ whenever $dP/d\rho > 0$ and are *increasing* with ρ whenever $dP/d\rho < 0$.

We begin our discussion of stability by considering the case where the function $P(\rho)$ in (3.5.23) is monotonically increasing so that the bifurcated curve (3.5.23) is as shown in Fig. 3.3. As seen from Fig. 3.3, the number of equilibrium solutions depends on the value of P . For $P < P_{cr}$, the only solution is the trivial solution $\rho = 0$. For $P > P_{cr}$, there are exactly two solutions, namely the trivial solution $\rho = 0$ and in addition a single

bifurcated solution involving an internal cavity. As was shown previously in this section, the trivial solution minimizes Σ among all possible (radially symmetric) configurations when $P < P_{cr}$. For $P > P_{cr}$, the trivial solution provides a local maximum for Σ among this same class of configurations, whereas the bifurcated solution yields a local minimum from Property A, and hence the absolute minimum. Thus we say that the trivial solution is *stable* for $P < P_{cr}$. For $P > P_{cr}$, the trivial solution is *unstable* while the bifurcated solution is *stable*. Thus for all values of P there exists exactly one stable solution. We now consider this result in the context of the quasi-static process in which the sphere is subjected to a tensile dead-load surface traction $p_0 = P\mu$ which increases slowly from zero. As p_0 is increased from zero to $P_{cr}\mu$, the stable equilibrium configuration is that produced by the homogeneous deformation (3.3.2). At $p_0 = P_{cr}\mu$ an internal void is nucleated, and as p_0 is further increased from $P_{cr}\mu$, the cavity radius $c = B\rho$ increases from zero in a continuous fashion.

Analogous results to the above, as well as to the remainder of this section, have been obtained and discussed for the isotropic composite neo-Hookean sphere in [20]. (See Sections 3 and 4 of [20]). Our subsequent discussion follows closely that of [20].

We now consider the case where the function $P(\rho)$ in (3.5.23) is monotone decreasing for $0 < \rho < \rho_t$, and monotone increasing for $\rho > \rho_t$ as in Fig. 3.4. As seen from Fig. 3.4, the number of equilibrium solutions depends on the values of P in the following way: for $0 < P < P_t$, the only solution is the trivial solution $\rho = 0$; for $P_t < P < P_{cr}$, there are exactly three solutions, namely, the trivial solution $\rho = 0$ and in addition two bifurcated solutions each involving an internal cavity; finally, for $P > P_{cr}$, there are exactly two solutions, namely the trivial solution and a single

bifurcated solution involving an internal cavity. As noted earlier, the trivial solution provides a local minimum for Σ and hence is stable for $0 < P < P_{cr}$, while for $P > P_{cr}$ the trivial solution provides a local maximum for Σ and thus is unstable. By virtue of Property A, the bifurcated curve (3.5.23) provides a local maximum for Σ if $0 < \rho < \rho_t$ and hence the associated solution is unstable, while for $\rho > \rho_t$, this curve provides a local minimum for Σ and hence this solution is stable. Thus if $0 < P < P_t$ or if $P > P_{cr}$, there is exactly one stable equilibrium solution, while if $P_t < P < P_{cr}$ there are two stable equilibrium solutions. To differentiate between these two stable solutions, we say that a solution is *absolutely stable* (AS) if it provides the absolute minimum for Σ whereas it is said to be *metastable* (MS) if it provides a local minimum for Σ which is not the absolute minimum. To address the transition between metastability and absolute stability, we refer to Fig. 3.5, where ρ_t and P_t are as before, and ρ_c denotes the value of $\rho > 0$ for which $P(\rho) = P_{cr}$. Then there exists a unique value of P , namely $P = P_N$, obeying $P_t < P_N < P_{cr}$, such that for $P < P_N$ the trivial solution is absolutely stable, while for $P > P_N$ the absolutely stable solution occurs on the bifurcated branch. Since $\Sigma = 0$ for the trivial solution $\rho = 0$, the preceding result follows from the existence of a unique value of ρ , namely $\rho = \rho_N$, satisfying $\rho_t < \rho_N < \rho_c$, such that $\Sigma(\rho) > 0$ for $\rho_t < \rho < \rho_N$ and $\Sigma(\rho) < 0$ for $\rho_N < \rho < \rho_c$ on the curve $P = P(\rho)$ given by (3.5.23). The existence of ρ_N follows immediately from Properties A and B.

We again consider the previously envisioned quasi-static loading process for the transversely isotropic sphere whose equilibrium solutions give rise to a bifurcation diagram of the type shown in Fig. 3.5. If one supposes that the body always assumes an absolutely stable configuration, the trivial homogeneous deformation (3.3.2) persists for $0 < p_0 < P_N \mu$. As p_0 passes through $P_N \mu$, the foregoing notion of stability predicts the

sudden appearance of a cavity of finite radius $c = B\rho_N$. As p_0 is further increased, the cavity radius increases in a continuous fashion. On the other hand, one may suppose that the trivial homogeneous deformation persists until it becomes unstable at $p_0 = P_{cr} \mu$, in which case the initial cavity radius is predicted to be $c = B\rho_c$, with subsequent growth occurring in a continuous fashion as p_0 is further increased. Regardless of the stability criterion adopted, one obtains a discontinuous transition from the stable trivial solution $\rho = 0$, $P < P_{cr}$ to the stable bifurcated solution $P = P(\rho)$, $\rho > \rho_t$. A similar discontinuous transition was also obtained in [20], [21] for a composite isotropic incompressible sphere and by Antman and Negron-Marrero [4] for compressible anisotropic spheres and cylinders. Such behavior was called "snap cavitation" in [20], [21] by analogy with the snap-through buckling phenomenon of structural mechanics.

3.7. Stress distribution

We proceed now to discuss the stress distribution in the anisotropic sphere. We begin by recalling some results obtained in Sections 3.2-3.4 for general W . At the beginning of Section 3.3, we saw that the stresses corresponding to the trivial solution (3.3.1) were given as

$$T_{rr} = T_{\theta\theta} = T_{\phi\phi} = p_0 . \quad (3.7.1)$$

Thus, prior to cavitation, we have simply the constant stress distribution (3.7.1). Subsequent to cavitation, (3.3.11), (3.3.7), and the considerations of Appendix A give the radial stress as

$$T_{rr}(R) = \int_{(1 + c^3/B^3)^{1/3}}^{\infty} \frac{\hat{W}_1(v)}{v^3 - 1} dv , \quad (3.7.2)$$

where we recall the notation (3.3.13), (3.3.14). Observe that for fixed R , $0 < R \leq B$, letting $c \rightarrow 0+$ formally in (3.7.2) results in the right-hand side of (3.4.1), so that

$$\lim_{c \rightarrow 0+} T_{\pi}(R) = p_{cr}, \quad 0 < R \leq B. \quad (3.7.3)$$

We shall use (3.7.3) later on in this section. Now, from (3.2.19), (3.2.20), (3.3.3), we can write the hoop stresses as

$$T_{\theta\theta}(R) = T_{\phi\phi}(R) = 2 \left[(v^2 - v^{-4}) W_1|_R - (v^{-2} - v^4) W_2|_R - v^{-4} W_5|_R \right] + T_{\pi}(R), \quad (3.7.4)$$

where $T_{\pi}(R)$ is given by (3.7.2) and we recall the notation (3.3.8).

In what follows, we confine attention to the illustrative example of Section 3.5. On comparing (3.7.2) and (3.3.15), it follows immediately from (3.5.13), (3.5.16), (3.5.19) that for the material (3.5.4) we have

$$\begin{aligned} T_{\pi}(R) = 2\mu & \left[\left[1 + \frac{c^3}{R^3} \right]^{-1/3} + \frac{1}{4} \left[1 + \frac{c^3}{R^3} \right]^{-4/3} + 2a \left\{ \frac{5\pi}{6\sqrt{3}} - \left[1 + \frac{c^3}{R^3} \right]^{-1/3} \right. \right. \\ & + \frac{1}{2} \left[1 + \frac{c^3}{R^3} \right]^{-2/3} - \frac{1}{4} \left[1 + \frac{c^3}{R^3} \right]^{-4/3} + \frac{1}{5} \left[1 + \frac{c^3}{R^3} \right]^{-5/3} + \frac{1}{8} \left[1 + \frac{c^3}{R^3} \right]^{-8/3} \\ & \left. \left. + \frac{1}{\sqrt{3}} \left[\arctan \left[\frac{2(1 + c^3/R^3)^{1/3} + 1}{\sqrt{3}} \right] + \arctan \left[\frac{\sqrt{3} (1 + c^3/R^3)^{1/3}}{2 + (1 + c^3/R^3)^{1/3}} \right] \right] \right] \right]. \end{aligned} \quad (3.7.5)$$

Now, from (3.5.4) it is readily verified that

$$W_1 = \frac{\mu}{2}, \quad W_2 = 0, \quad W_5 = \mu a (I_5 - 1), \quad (3.7.6)$$

so that (3.7.6), (3.7.4), (3.3.4), (3.3.3) combine to give the hoop stresses for the material (3.5.4) as

$$T_{\theta\theta}(R) = T_{\phi\phi}(R) = \mu \left\{ \left[1 + \frac{c^3}{R^3} \right]^{2/3} - \left[1 + \frac{c^3}{R^3} \right]^{-4/3} - 2a \left[\left[1 + \frac{c^3}{R^3} \right]^{-8/3} - \left[1 + \frac{c^3}{R^3} \right]^{-4/3} \right] \right\} + T_{rr}(R), \quad (3.7.7)$$

where $T_{rr}(R)$ is given by (3.7.5).

The stresses (3.7.5), (3.7.7) are plotted in Figure 3.6 for a representative value of the anisotropy parameter $a < a_0$. We observe from Fig. 3.6 that T_{rr} is a monotone increasing function of R on $0 \leq R \leq B$, while $T_{\theta\theta} = T_{\phi\phi}$ are monotone decreasing functions of R on this range. Notice also from Fig. 3.6 that $T_{\theta\theta}(R) = T_{\phi\phi}(R) > T_{rr}(R)$ for $c > 0$. This latter fact may also be verified analytically, for all values of a , as follows: from (3.7.7) we obtain

$$T_{\theta\theta}(R) - T_{rr}(R) = T(\lambda), \quad (3.7.8)$$

where $T(\lambda)$ is given by (3.5.9), with $\lambda \equiv v(R) = \left[1 + \frac{c^3}{R^3} \right]^{1/3}$. Thus, as seen from Fig.

3.2, $T(\lambda) > 0$ for $\lambda > 1$, so that (3.7.8) implies that

$$T_{\theta\theta}(R) = T_{\phi\phi}(R) > T_{rr}(R) \text{ for } c > 0. \quad (3.7.9)$$

Similar results were obtained for the composite neo-Hookean isotropic sphere in [21, Fig. 4].

Another interesting feature concerning the stresses $T_{rr}(R)$, $T_{\theta\theta}(R)$, $T_{\phi\phi}(R)$ immediately after cavitation is the presence of a boundary layer near the cavity wall when smooth cavitation (i.e., $K > 0$ or $a < a_0$) has taken place. Observe from (3.7.3), (3.5.21) that for the material (3.5.4),

$$\lim_{c \rightarrow 0+} T_{rr}(R) = \mu \left[\frac{5}{2} + \left[\frac{40\pi - 51\sqrt{3}}{30\sqrt{3}} \right] a \right], \quad 0 < R \leq B. \quad (3.7.10)$$

Since the boundary condition (3.2.27) of a traction-free cavity surface guarantees $T_{rr}(0) = 0$, the radial stress thus experiences a rapid growth in a narrow region near the cavity wall for applied dead-loads p_0 slightly larger than p_{cr} . From (3.7.7) it is clear that a similar boundary layer exists in the stress components $T_{\theta\theta}$, $T_{\phi\phi}$. These boundary layers in the stresses are illustrated in Figures 3.7 and 3.8 for a representative value of the anisotropy parameter a . Similar boundary layer behavior in the stresses was observed in [21], [6]. (See Sec. 4 and Fig. 5 of [21], Figs. 3 and 4 of [6].) As noted in [21], such severe boundary layers for the stresses do *not* occur in the case of snap cavitation ($K < 0$ or $a > a_0$) since in this case the deformed cavity radius jumps to a finite value upon cavity formation.

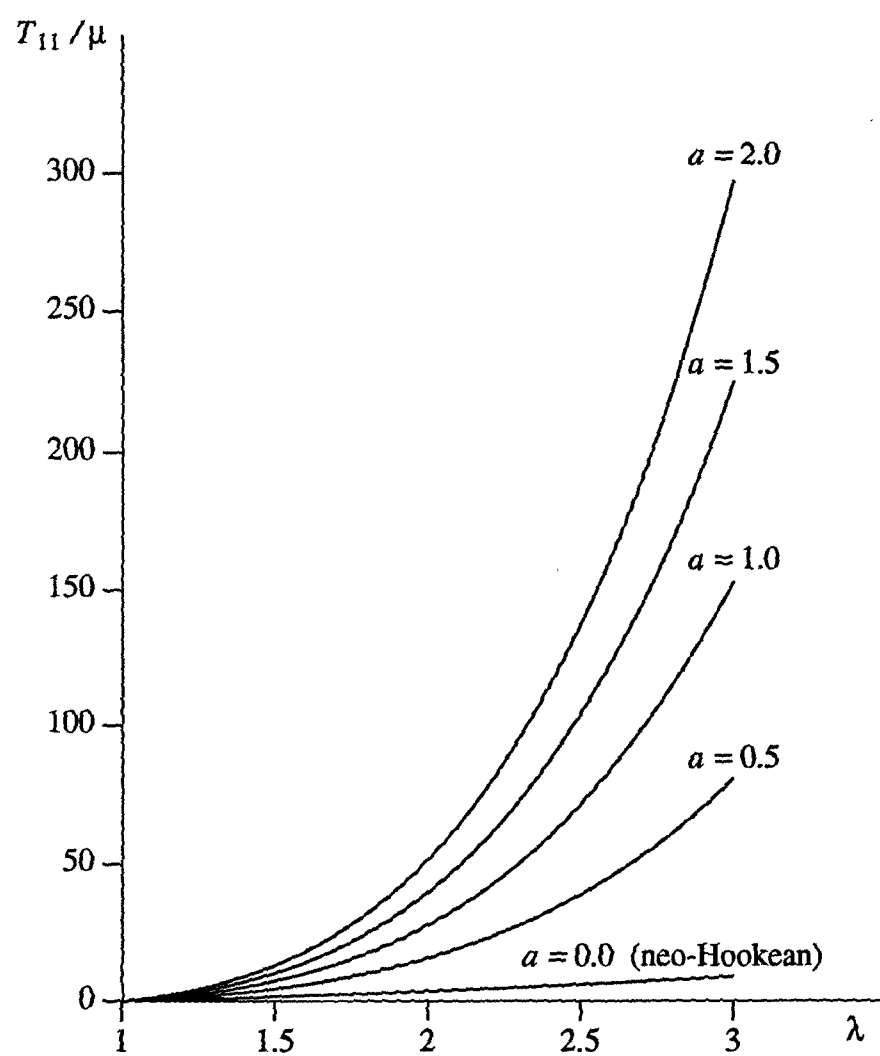


Figure 3.1. Nondimensional stress $\frac{T_{11}(\lambda)}{\mu}$ vs. stretch λ for uniaxial tension for the anisotropic material with strain-energy density given by (3.5.4).

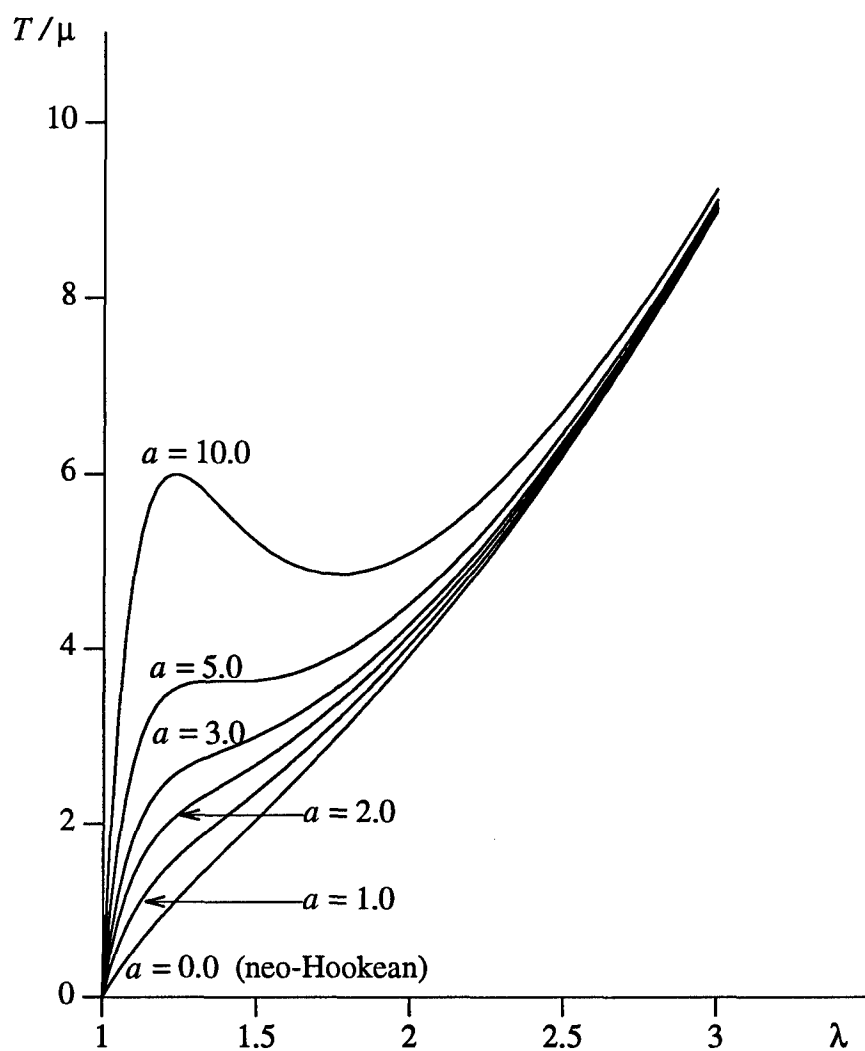


Figure 3.2. Nondimensional stress $\frac{T(\lambda)}{\mu}$ vs. stretch λ for equibiaxial stress (stretch) for the anisotropic material with strain-energy density given by (3.5.4).

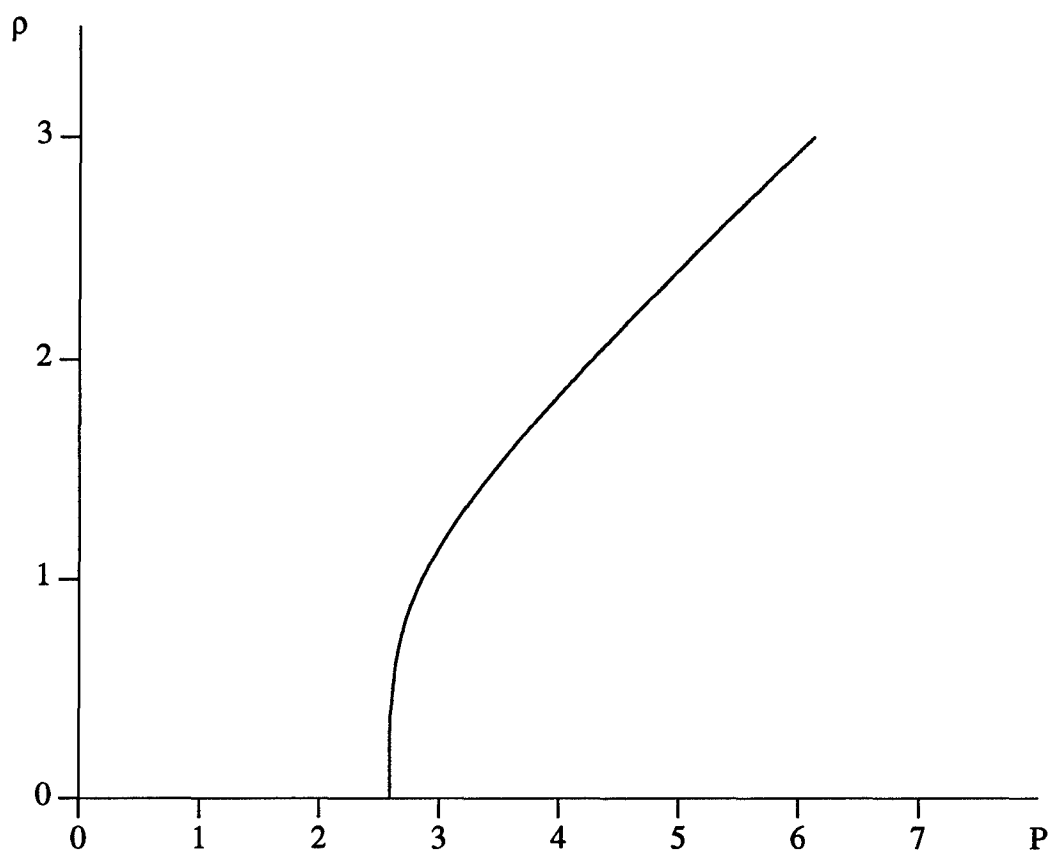


Figure 3.3. Variation of the deformed cavity radius $\rho = c/B$ with applied dead-load traction $P = p_o/\mu$ for the anisotropic sphere with strain-energy density given by (3.5.4) with $a = 0.125$.

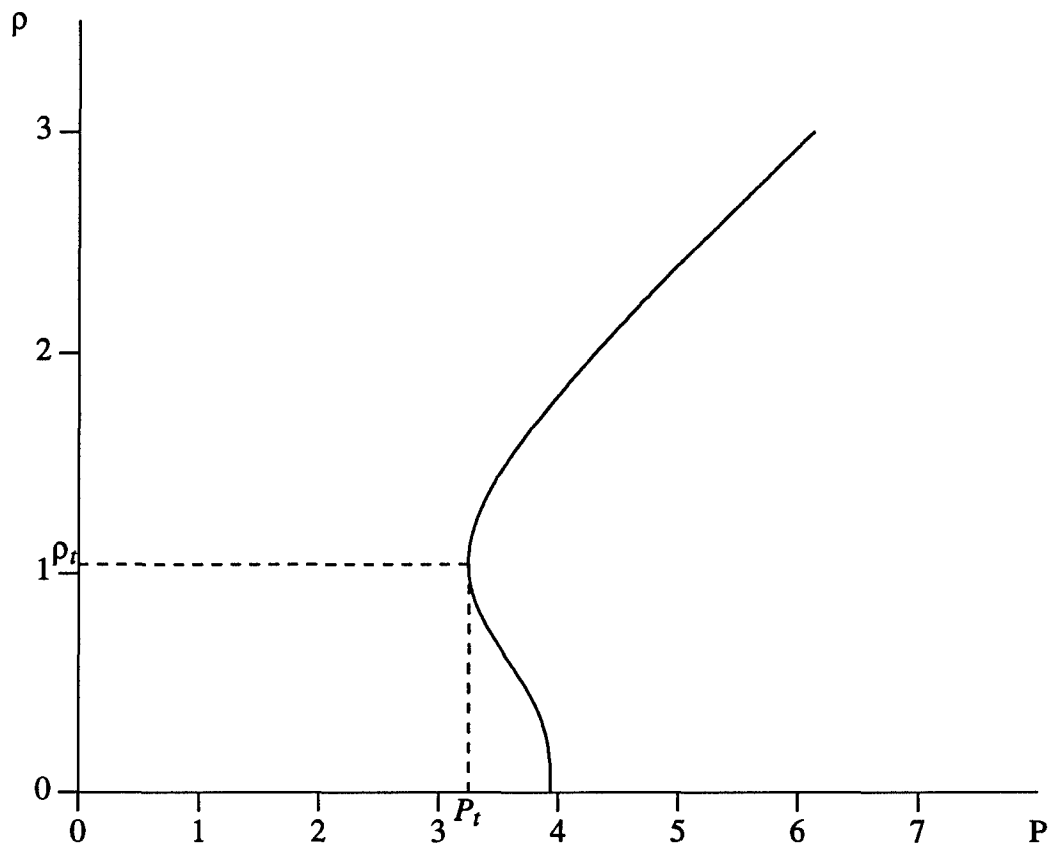


Figure 3.4. Variation of the deformed cavity radius $\rho = c/B$ with applied dead-load traction $P = p_o/\mu$ for the anisotropic sphere with strain-energy density given by (3.5.4) with $a = 2.0$.

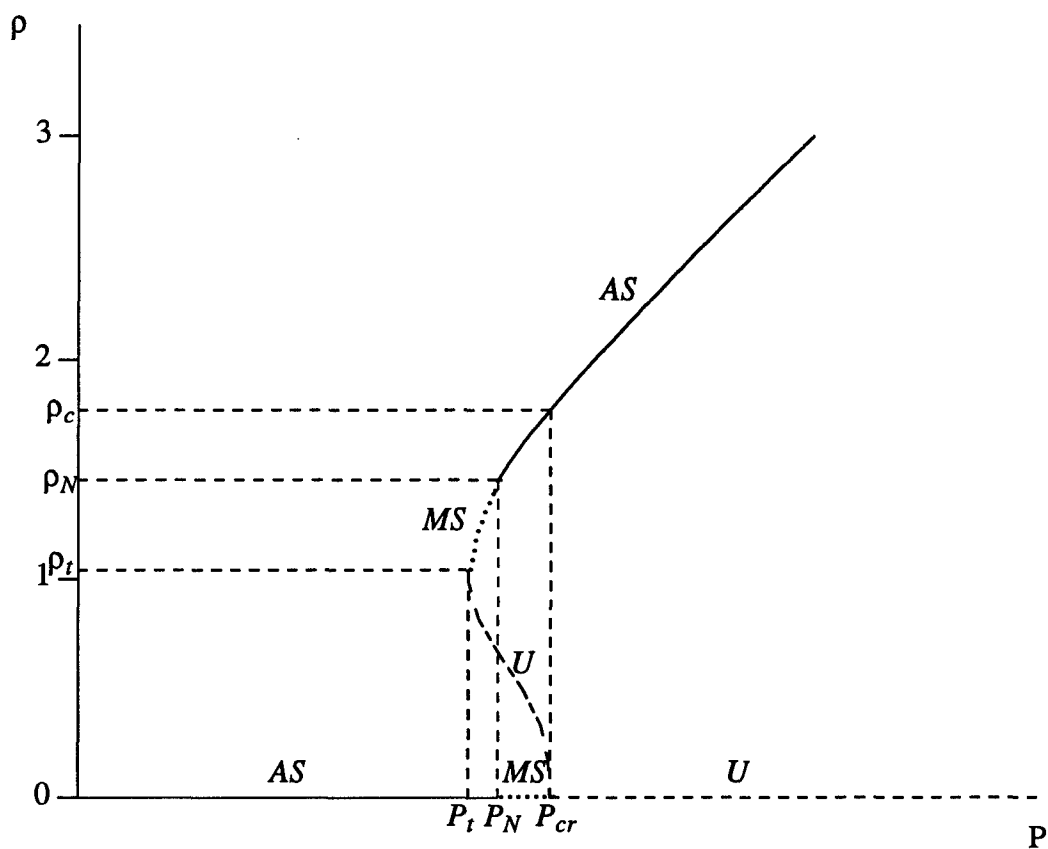


Figure 3.5. Stability zones for the case when bifurcation to the left occurs.

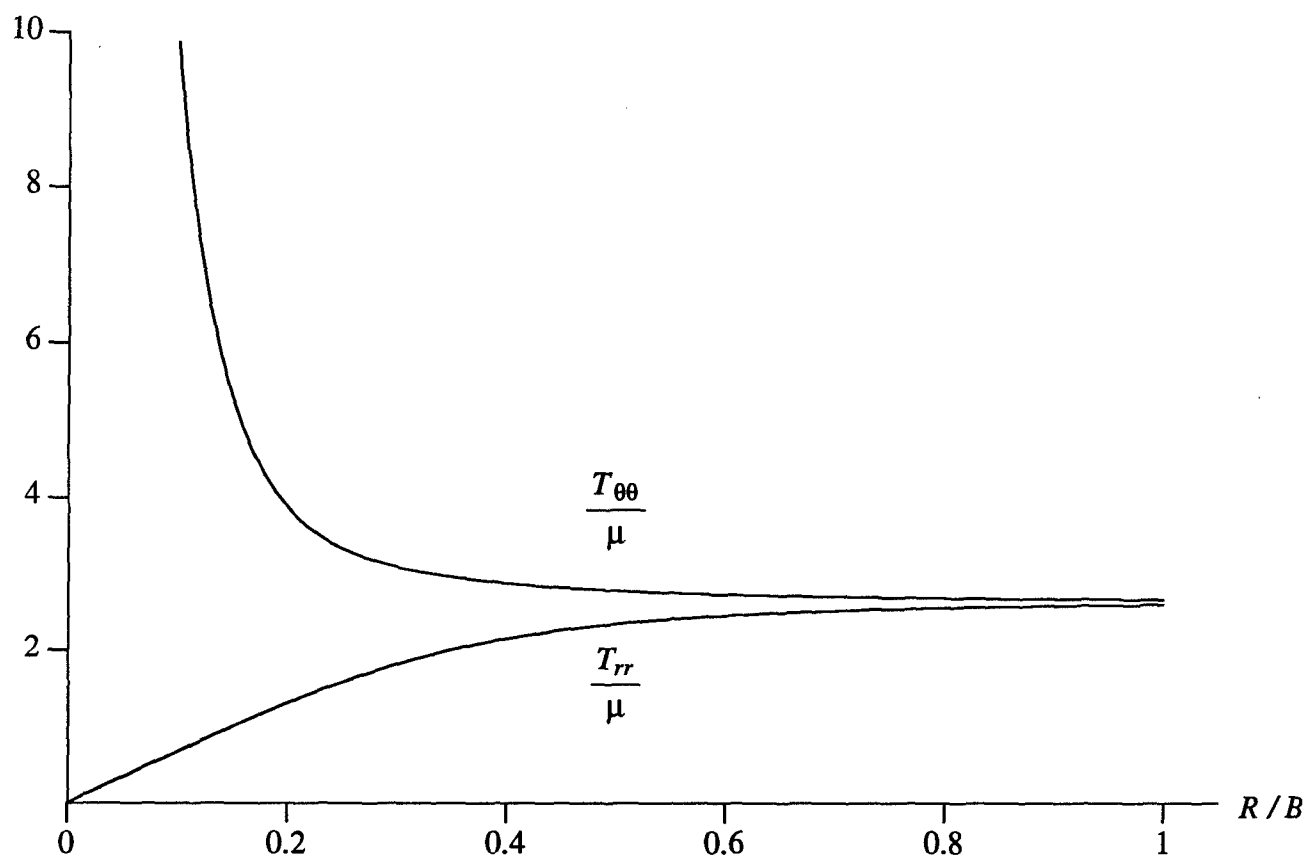


Figure 3.6. Variation of the stresses $T_{rr}(R)$, $T_{\theta\theta}(R)$ with undeformed radius R subsequent to cavitation for the anisotropic material with strain-energy density given by (3.5.4) with $a = 0.2$. Here, $P = 2.646$, $P_{cr} = 2.644$, $\rho = c/B = 0.3$.

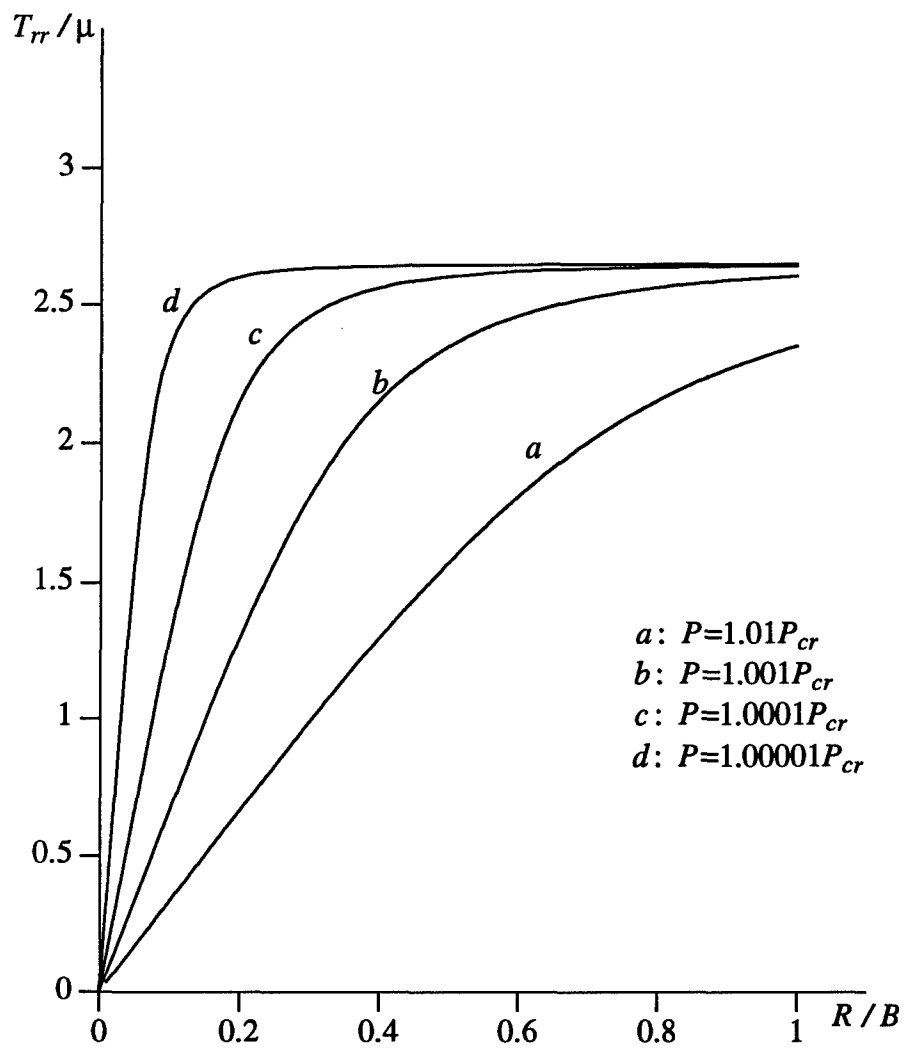


Figure 3.7. Variation of the radial stress $T_{rr}(R)$ with undeformed radius R subsequent to cavitation for the anisotropic material with strain-energy density given by (3.5.4) with $a = 0.2$. Here, $P_{cr} = 2.644$.

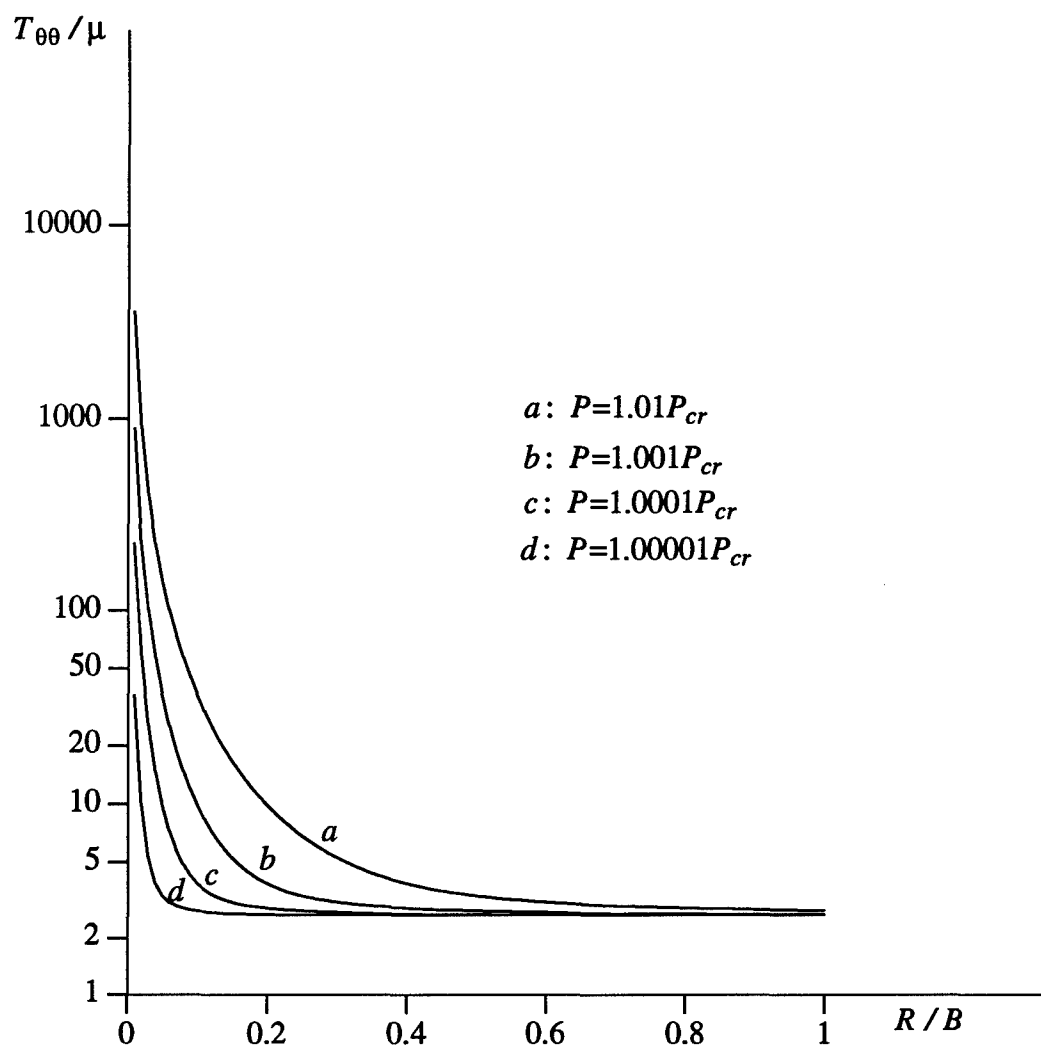


Figure 3.8. Variation of the hoop stress $T_{\theta\theta}(R)$ with undeformed radius R subsequent to cavitation for the anisotropic material with strain-energy density given by (3.5.4) with $a = 0.2$. Here, $P_{cr} = 2.644$.

Chapter 4

COMPOSITE ANISOTROPIC SPHERE

4.1. Introduction

In the previous chapter, the effects of *material anisotropy* on cavitation for *incompressible* nonlinearly elastic spheres was examined. That investigation was motivated by the work of Antman and Negron-Marrero [4] on *compressible* transversely isotropic nonlinearly elastic solids and by the studies of Horgan and Pence [20-22] on *composite* incompressible nonlinearly elastic spheres with *isotropic* phases. The purpose of the present Chapter is to investigate the combined effects of *anisotropy* and *material inhomogeneity* on cavitation. A more complicated sequence of cavitation instabilities might be expected to occur due to the interaction of these effects and we show that this is indeed the case.

In Section 4.2, we formulate the basic boundary value problem of concern. We consider a composite sphere composed of two incompressible anisotropic nonlinearly elastic phases, each of which is transversely isotropic about the radial direction. The sphere is subjected to a prescribed uniform radial tensile dead-load p_0 on its boundary. In Section 4.3, it is shown that one solution to this problem, for all values of p_0 , corresponds to a trivial homogeneous state in which the sphere remains undeformed but stressed. However, as seen previously for the *homogeneous* anisotropic sphere, for sufficiently large values of p_0 , one has in addition other possible radially symmetric configurations involving an internal traction-free cavity. Again, such solutions bifurcate from the homogeneous solution at p_{cr} , a critical value of p_0 . The possibility for these

bifurcated solutions to exist depends *only on the constitutive law for the material at the core* of the composite sphere (Section 4.4). In Section 4.4, we also give conditions to determine whether bifurcation is supercritical or subcritical. In Section 4.5, the stability of the foregoing solutions is examined using an energy minimization approach. For a composite sphere described by a *general* transversely isotropic strain-energy density function, W , the cavitation solutions are shown to be the only stable (radially symmetric) solutions for sufficiently large loads. In Section 4.6, we present an example which illustrates explicitly the preceding results. The specific anisotropic material model described in Chapter 3, Section 5, is considered for each phase of the composite, and explicit results are obtained for the relationship $p_0 = p_0(c)$ between the applied tensile load p_0 and the deformed cavity radius c . We also obtain an explicit result for the relationship between the total energy Σ and the cavity radius. We recall that for the isotropic composite sphere discussed in [20], and the homogeneous anisotropic sphere described in Chapter 3, Section 5, when bifurcation at $p_0 = p_{cr}$ occurs locally to the right, a *smooth cavitation* takes place with cavity radius increasing continuously (from zero) as p_0 increases. Here however the situation is quite different. We exhibit *three* possible configurations the sphere may assume when bifurcation occurs locally to the right. First, a smooth cavitation may take place. Second, a *snap cavitation* may occur in which there is a cavity of *finite* radius upon first appearance at a transition load which is *less* than p_{cr} . Third, the sphere may undergo a smooth cavitation initially, and then experience a discontinuous jump in cavity radius. That is, the cavity radius "snaps" from one finite value to another (larger) finite value at a load p_0 *greater* than p_{cr} . The last two phenomena were not seen for the spheres discussed in [20] and Chapter 3. When bifurcation is to the left, the sphere experiences a snap cavitation so that again a cavity of

finite radius appears at a transition load which is less than p_{cr} . In Section 4.7, the stress distribution is described. When a cavity is nucleated, in the case of smooth cavitation, a predominant stress variation exists in a narrow boundary layer near the cavity wall. Also, the effect of cavitation at the center on possible interface debonding is considered. It is assumed that debonding occurs uniformly whenever the normal stress at the interface reaches a threshold value. A condition on the strain-energy is given so that in a quasi-static loading process, cavitation relieves the interfacial normal stress so that subsequent interfacial debonding is precluded. The boundary layers in the stresses as well as the stress relaxation in the normal stress at the interface subsequent to cavitation are illustrated for the specific material model of Section 4.6.

4.2. Problem formulation

We are concerned with a sphere composed of an incompressible anisotropic nonlinearly elastic material. As in Chapter 3, we denote the interior of the sphere in its undeformed configuration by $D_0 = \{(R, \Theta, \Phi) \mid 0 \leq R < B, 0 < \Theta \leq 2\pi, 0 \leq \Phi \leq \pi\}$. The sphere is subjected to a prescribed uniform radial tensile dead-load of magnitude p_0 on its boundary $R = B$. We assume that the resulting deformation, which takes the point in D_0 with spherical polar coordinates (R, Θ, Φ) to the point (r, θ, ϕ) in the deformed configuration, is radially symmetric. Thus the deformation has the form $\theta = \Theta, \phi = \Phi$,

$$r = r(R) > 0, 0 < R < B; \quad r(0+) \geq 0, \quad (4.2.1)$$

where $r(R)$ is to be determined.

As in Chapter 3, the deformation gradient tensor \mathbf{F} associated with (4.2.1), referred to spherical polar coordinates, is given by

$$\mathbf{F} = \text{diag} \left[\dot{r}(R), r(R)/R, r(R)/R \right] \quad (4.2.2)$$

where $\dot{r}(R) \equiv \frac{dr}{dR}$. Incompressibility then requires that $J \equiv \det \mathbf{F} = 1$, which upon integration yields

$$r(R) = (R^3 + c^3)^{1/3}, \quad (4.2.3)$$

where $c \geq 0$ is a constant to be determined. As in Chapter 3, if it is found that $c = 0$, (4.2.3) implies that the body remains a solid sphere in the current configuration. However, if c is found to be positive, then $r(0+) = c > 0$ and so there is a cavity of radius c centered at the origin in the current configuration. In this event, the cavity surface is assumed to be traction-free.

The incompressible material of concern here is assumed to be transversely isotropic in the radial direction, and possibly inhomogeneous in the radial direction as well. The strain-energy density per unit undeformed volume for such an elastic material is denoted by

$$W = W(I_1, I_2, I_3, I_4, I_5; R) \quad (4.2.4)$$

where the explicit dependence of W on the radial coordinate R reflects the possible material inhomogeneity. We shall assume that the strain-energy W vanishes in the undeformed state where $I_1 = 3$, $I_2 = 3$, $I_3 = 1$, $I_4 = 0$, and $I_5 = 1$, so that we have the normalization condition

$$W(3, 3, 1, 0, 1; R) = 0 \quad \forall R \geq 0. \quad (4.2.5)$$

As in Chapter 3, we also assume that in the undeformed state the initial stress is a hydrostatic pressure, so that we have the further normalization condition

$$W_5(3, 3, 1, 0, 1; R) = 0 \quad \forall R \geq 0. \quad (4.2.6)$$

We shall be concerned in what follows with the case of a composite sphere composed of two different transversely isotropic incompressible materials perfectly bonded across the interface $R = A$ ($A < B$). The material properties in each individual phase are assumed to have smooth radial dependence. Thus $W(I_1, I_2, I_3, I_4, I_5; R)$ is assumed to be smooth on $0 < R < A$, $A < R < B$ while suffering a jump discontinuity at the interface $R = A$. Observe that, by virtue of (4.2.3), the deformation field is continuous at this interface. In the remainder of this section, we proceed formally and assume that W possesses sufficient regularity properties to permit the subsequent analysis.

The response equation for the Cauchy stress tensor \mathbf{T} for transversely isotropic incompressible materials is, as given previously,

$$\mathbf{T} = -p\mathbf{1} + 2(W_1 \mathbf{B} - W_2 \mathbf{B}^{-1} + W_4 \mathbf{M} + W_5 \mathbf{N}), \quad (4.2.7)$$

where, as before, \mathbf{B} is the left Cauchy-Green deformation tensor $\mathbf{B} = \mathbf{F} \mathbf{F}^T$, $\mathbf{1}$ is the unit tensor, p is the unknown hydrostatic pressure associated with the incompressibility constraint $J = 1$, and $W_q = \partial W / \partial I_q$ ($q = 1, 2, 4, 5$). The deformation tensors \mathbf{B} , $\mathbf{C} = \mathbf{F}^T \mathbf{F}$, \mathbf{M} , and \mathbf{N} , and the invariants I_i , ($i=1, \dots, 5$), are given in Chapter 3, Section 2, in general, as well as for the particular deformation and transverse isotropy of concern. Thus, for the sphere which is transversely isotropic about the radial direction, we have, corresponding to the deformation field (4.2.1),

$$\mathbf{C} = \mathbf{B} = \text{diag} \left[\dot{r}^2, r^2/R^2, r^2/R^2 \right], \quad (4.2.8)$$

$$\mathbf{M} = \mathbf{0}, \quad (4.2.9)$$

$$\mathbf{N} = \text{diag} \left[\dot{r}^2, 0, 0 \right], \quad (4.2.10)$$

and

$$I_1 = \dot{r}^2 + 2 r^2 / R^2, \quad (4.2.11)$$

$$I_2 = r^4 / R^4 + 2 \dot{r}^2 r^2 / R^2, \quad (4.2.12)$$

$$I_3 = \dot{r}^2 r^4 / R^4 = 1, \quad (4.2.13)$$

$$I_4 = 0, \quad (4.2.14)$$

$$I_5 = \dot{r}^2. \quad (4.2.15)$$

Substitution from (4.2.8) - (4.2.10) into (4.2.7) yields the nonzero components of the Cauchy stress \mathbf{T} as

$$T_{rr} = -p + 2 (\dot{r}^2 W_1 - \dot{r}^{-2} W_2 + \dot{r}^2 W_5) \quad (4.2.16)$$

and

$$T_{\theta\theta} = T_{\phi\phi} = -p + 2(\dot{r}^{-1} W_1 - \dot{r} W_2), \quad (4.2.17)$$

where the W_t ($t = 1, 2, 5$) are evaluated at the values of the invariants given by (4.2.11) - (4.2.15), and we note that W_t is also dependent on the radial coordinate R . The derivatives in (4.2.16), (4.2.17) are understood to be one-sided derivatives at the material interface $R = A$.

The equilibrium equations, in the absence of body forces, are

$$\text{div } \mathbf{T} = \mathbf{0}, \quad (4.2.18)$$

which in the present case reduce to

$$\frac{\partial T_{rr}}{\partial r} + \frac{2}{r} (T_{rr} - T_{\theta\theta}) = 0, \quad (4.2.19)$$

$$\frac{1}{r} \frac{\partial T_{\theta\theta}}{\partial \theta} = 0, \quad (4.2.20)$$

$$\frac{1}{r \sin \theta} \frac{\partial T_{\phi\phi}}{\partial \phi} = 0. \quad (4.2.21)$$

As seen in Chapter 3, Section 2, we again have W_q independent of the angular variables, and thus it follows from (4.2.17) and (4.2.20) - (4.2.21) that the pressure $p=p(r)$ only. There may be a jump discontinuity at the interface $R = A$ in $p(r)$. Elsewhere the pressure is assumed sufficiently smooth. Since $r=r(R)$, we again consider $T=T(R)$ (and $p=p(R)$). The remaining equilibrium equation (4.2.19), on using the chain-rule, becomes

$$\frac{dT_{rr}}{dR} + \frac{2\dot{r}}{r} (T_{rr} - T_{\theta\theta}) = 0, \quad \text{on } 0 < R < A, \quad A < R < B. \quad (4.2.22)$$

Equation (4.2.22) is a first-order nonlinear ordinary differential equation for the pressure $p(R)$. Also for equilibrium, the normal traction component at the material interface must be continuous, i.e.,

$$T_{rr}(A-) = T_{rr}(A+). \quad (4.2.23)$$

The dead-load boundary condition now requires that

$$T_{rr}(B) = p_0 \left[\frac{B}{r(B)} \right]^2, \quad (4.2.24)$$

where the constant $p_0 > 0$ is prescribed. We note that the boundary conditions of vanishing shear tractions are satisfied identically.

Thus, the boundary value problem to be solved is the following: *For a prescribed value of the dead-load traction $p_0 > 0$, we seek a pressure field $p(R)$ and a constant $c \geq 0$ such that (4.2.22) - (4.2.24) are satisfied where T_{rr} , $T_{\theta\theta}$ are given by (4.2.16), (4.2.17), (4.2.3). In addition, if $c > 0$, then the condition for a traction-free cavity surface*

$$T_{rr}(0) = 0 \quad (4.2.25)$$

must also hold.

4.3. Solutions

On using the normalization condition (4.2.6), it may readily be shown that one solution of the foregoing problem for all values of p_0 is

$$p(R) = 2[W_1(3, 3, 1, 0, 1; R) - W_2(3, 3, 1, 0, 1; R)] - p_0, \quad c = 0. \quad (4.3.1)$$

This corresponds to the trivial homogeneous state of deformation

$$r(R) = R, \quad (4.3.2)$$

with corresponding stresses $T_{rr} = T_{\theta\theta} = T_{\phi\phi} = p_0$, so that the sphere remains undeformed under a state of hydrostatic pressure. Note that even though the pressure p given in (4.3.1) is in general discontinuous across the interface $R = A$, the corresponding stresses are continuous.

We next describe solutions for which $c > 0$, corresponding to the presence of a traction-free cavity at the origin. We again employ the notation used in Chapter 3 for convenience:

$$\left. \begin{aligned} v = v(R) &\equiv r(R)/R = \left(1 + \frac{c^3}{R^3}\right)^{1/3} \\ v^{-2} &= \dot{r} \end{aligned} \right\}, \quad (4.3.3)$$

and thus rewrite the invariants (4.2.11) - (4.2.15) as

$$\left. \begin{aligned} I_1 &= v^{-4} + 2v^2, \\ I_2 &= v^4 + 2v^{-2}, \\ I_3 &= 1, \\ I_4 &= 0, \\ I_5 &= v^{-4}. \end{aligned} \right\} \quad (4.3.4)$$

Following the techniques of Chapter 3, Section 3, we rewrite the differential equation (4.2.22) in the form

$$\begin{aligned} \frac{d}{dR} \left\{ 2 [v^{-4} W_1 (v^{-4} + 2v^2, v^4 + 2v^{-2}, 1, 0, v^{-4}; R) - v^4 W_2 (v^{-4} + 2v^2, v^4 + 2v^{-2}, 1, 0, v^{-4}; R) \right. \\ \left. + v^{-4} W_5 (v^{-4} + 2v^2, v^4 + 2v^{-2}, 1, 0, v^{-4}; R)] - p(R) \right\} \\ + \frac{4v^{-3}}{R} [(v^{-4} - v^2) W_1 (v^{-4} + 2v^2, v^4 + 2v^{-2}, 1, 0, v^{-4}; R) \\ + (v^{-2} - v^4) W_2 (v^{-4} + 2v^2, v^4 + 2v^{-2}, 1, 0, v^{-4}; R) \\ + v^{-4} W_5 (v^{-4} + 2v^2, v^4 + 2v^{-2}, 1, 0, v^{-4}; R)] = 0 \text{ on } 0 < R < A, A < R < B. \end{aligned} \quad (4.3.5)$$

On integration of (4.3.5), we have

$$p(R) - p(0) = 2 \left\{ v^{-4}(R) (W_1 + W_5) \Big|_R - v^4(R) W_2 \Big|_R \right\} + 4J(R), \quad 0 < R < A, \quad (4.3.6)$$

and

$$\begin{aligned} p(R) - [p]_{A-}^{A+} - p(0) = 2 \left\{ v^{-4}(R) (W_1 + W_5) \Big|_R - v^4(R) W_2 \Big|_R \right. \\ \left. - v^{-4}(A) [W_1 + W_5]_{A-}^{A+} + v^4(A) [W_2]_{A-}^{A+} \right\} + 4J(R), \quad A < R < B, \end{aligned} \quad (4.3.7)$$

where

$$J(R) = \int_0^R \left[\left[v^{-7}(s) - v^{-1}(s) \right] W_1 \Big|_s + \left[v^{-5}(s) - v(s) \right] W_2 \Big|_s + v^{-7}(s) W_5 \Big|_s \right] \frac{ds}{s}, \quad (4.3.8)$$

on $0 < R < B$, and $[f(s)]_{A-}^{A+} = f(A+) - f(A-)$. In (4.3.6) - (4.3.8) the W_l ($l = 1, 2, 5$) are

evaluated at the values of the invariants given by (4.3.4), and for simplicity we retain an obvious modification of the notation introduced in Chapter 3, i.e.,

$$W_I|_s = W_I(v^{-4}(s) + 2v^2(s), v^4(s) + 2v^{-2}(s), 1, 0, v^{-4}(s); s). \quad (4.3.9)$$

On substitution into (4.2.16), and using (4.3.3), the radial stress becomes

$$T_{rr}(R) = -p(0) - 4J(R), \quad 0 < R < A, \quad (4.3.10)$$

$$T_{rr}(R) = -p(0) - [p]_{A-}^{A+} + 2 \left\{ v^{-4}(A) [W_1 + W_5]_{A-}^{A+} - v^4(A) [W_2]_{A-}^{A+} \right\} - 4J(R), \quad A < R < B. \quad (4.3.11)$$

The interface condition (4.2.23) now shows that

$$- [p]_{A-}^{A+} + 2 \left\{ v^{-4}(A) [W_1 + W_5]_{A-}^{A+} - v^4(A) [W_2]_{A-}^{A+} \right\} = 0, \quad (4.3.12)$$

so that (4.3.11) becomes

$$T_{rr}(R) = -p(0) - 4J(R), \quad A < R < B. \quad (4.3.13)$$

The traction-free cavity surface condition (4.2.25), together with (4.3.10) and $J(0) = 0$, now yield $p(0) = 0$, so that

$$T_{rr}(R) = -4J(R), \quad 0 < R < B. \quad (4.3.14)$$

Finally, by virtue of (4.3.14), (4.3.3), we see that the dead-load boundary condition (4.2.24) at the outer surface $R = B$ is satisfied if

$$-4J(B) = p_0 [v(B)]^{-2}. \quad (4.3.15)$$

As in Chapter 3, Section 3, the condition (4.3.15) may be written compactly on utilizing the $s \rightarrow v$ change of variables in the integral (4.3.8). Introducing the function

$$\hat{W}(x; y) = W(x^{-4} + 2x^2, x^4 + 2x^{-2}, 1, 0, x^{-4}; y), \quad (4.3.16)$$

and adopting the notation

$$\hat{W}_1(x; y) = \frac{\partial}{\partial x} \hat{W}(x; y) \quad (4.3.17)$$

as in [20], it follows similarly from the arguments contained in Appendix A that one may write (4.3.15) as

$$p_0 = \left[1 + \frac{c^3}{B^3}\right]^{2/3} \int_{(1 + \frac{c^3}{B^3})^{1/3}}^{\infty} \frac{\hat{W}_1(v; \frac{c}{(v^3 - 1)^{1/3}})}{v^3 - 1} dv, \quad c > 0. \quad (4.3.18)$$

We remark that (4.3.18), here established for the anisotropic composite sphere, has formally the same structure as the analogous relation for the isotropic composite sphere (see equation (2.23) of [20]). As discussed in [20], the integrand in this equation is, in general, discontinuous at the interface $v = (1 + \frac{c^3}{A^3})^{1/3}$. Equation (4.3.18) was first established in [5] for the case of the homogeneous isotropic sphere (see equation (5.18) of [5]). Thus, for a given dead-load p_0 , solutions involving a traction-free internal cavity of radius c exist provided that c is a positive root of (4.3.18). The associated pressure field is given by

$$p(R) = 2 \left[v^{-4}(R) (W_1 + W_5)|_R - v^4(R) W_2|_R \right] + 4J(R) \quad (4.3.19)$$

on $0 < R < A$, $A < R < B$.

In summary, we have seen that for all values of the applied dead-load traction p_0 , one obtains the trivial solution (4.3.1) corresponding to the homogeneous state of deformation (4.3.2). Moreover, if positive roots c of (4.3.18) exist, then one obtains the *additional* solutions involving a traction-free internal cavity described above.

4.4. The critical load and bifurcation

Henceforth we confine attention to a composite sphere composed of two *homogeneous* anisotropic phases. To remove the explicit radial dependence from the strain-energy, we now write $W = W(I_1, I_2, I_3, I_4, I_5; R)$ for the composite sphere as

$$\begin{aligned} W &= W^1(I_1, I_2, I_3, I_4, I_5), \quad 0 \leq R < A \\ W &= W^2(I_1, I_2, I_3, I_4, I_5), \quad A < R \leq B. \end{aligned} \quad (4.4.1)$$

Using the definitions in (4.3.16), (4.3.17), and (4.4.1), we rewrite (4.3.18) as

$$p_0 = \left[1 + \frac{c^3}{B^3}\right]^{\frac{2}{3}} \left[\int_{(1 + \frac{c^3}{A^3})^{\frac{1}{3}}}^{\infty} \frac{\hat{W}_1^1(v)}{v^3 - 1} dv + \int_{(1 + \frac{c^3}{B^3})^{\frac{1}{3}}}^{(1 + \frac{c^3}{A^3})^{\frac{1}{3}}} \frac{\hat{W}_1^2(v)}{v^3 - 1} dv \right], \quad c > 0 \quad (4.4.2)$$

The *critical load* p_{cr} at which an internal cavity may be initiated is then found by formally letting $c \rightarrow 0+$ in (4.4.2), and so

$$p_{cr} = \int_1^{\infty} \frac{\hat{W}_1^1(v)}{v^3 - 1} dv. \quad (4.4.3)$$

As seen in Chapter 3, p_{cr} may or may not be finite, and thus cavitation may or may not take place since the integral (4.4.3) is improper. We see from (4.4.3) that the finiteness of p_{cr} and its value depend *only upon the material at the core of the composite sphere*. Such a result was also obtained in [21] for a composite sphere with isotropic phases (see also [34]). In Section 4.5, we derive an alternative formula for the critical load involving the strain-energy function $\hat{W}^1(v)$ instead of its derivative, as in (4.4.3).

As discussed in Chapter 3, Section 4, and shown in Chapter 2, the integrand in (4.4.3) is finite as $v \rightarrow 1$. Thus, as before, the behavior of $\hat{W}^1(v)$ for *large* values of the

stretch v determines whether cavitation will or will not take place. That is, restrictions on the rate of growth of $\hat{W}^1(v)$ for large stretch, similar to those described in Chapter 3, Section 4, are required.

We now consider the local character of the bifurcation at $p_0 = p_{cr}$ by analyzing the curve $p_0 = p_0(c)$, given by (4.3.18), for small values of c . We first introduce the dimensionless parameters

$$\rho = \frac{c}{B}, \quad \alpha = \frac{B}{A}, \quad (\alpha > 1) \quad (4.4.4)$$

and define

$$p_0(c) \equiv p_0^*(\rho^3) = (1 + \rho^3)^{2/3} \left[\int_{(1 + \alpha^3 \rho^3)^{1/3}}^{\infty} \frac{\hat{W}_1^1(v)}{v^3 - 1} dv + \int_{(1 + \rho^3)^{1/3}}^{(1 + \alpha^3 \rho^3)^{1/3}} \frac{\hat{W}_1^2(v)}{v^3 - 1} dv \right]. \quad (4.4.5)$$

A Taylor expansion of (4.4.5) about $\rho^3 = 0$ shows that

$$p_0 = p_{cr} + k \rho^3 + o(\rho^3) \text{ as } \rho^3 \rightarrow 0 \quad (4.4.6)$$

where

$$k = \lim_{\rho^3 \rightarrow 0} dp_0^*/d\rho^3. \quad (4.4.7)$$

From (4.4.5) one obtains

$$k = \frac{2}{3} p_{cr} - \frac{1}{3} \alpha^3 \lim_{v \rightarrow 1} \frac{d\hat{W}_1^1/dv}{v^3 - 1} + \frac{1}{3} (\alpha^3 - 1) \lim_{v \rightarrow 1} \frac{d\hat{W}_1^2/dv}{v^3 - 1}. \quad (4.4.8)$$

On using l'Hopital's rule and defining

$$f = \alpha^{-3}, \quad 0 < f < 1 \quad (4.4.9)$$

as the volume fraction of the core material to the total material, we write k as

$$k = \frac{2}{3} \left[p_{cr} - \frac{1}{6} f^{-1} \frac{d^2 \hat{W}_1^1(1)}{dv^2} + \frac{1}{6} (f^{-1} - 1) \frac{d^2 \hat{W}_1^2(1)}{dv^2} \right], \quad (4.4.10)$$

where, from the considerations of Chapter 3, Section 4, and Chapter 2, the quantities $d^2\hat{W}^i(1)/dv^2$, ($i=1,2$), are positive and finite, and each can be written in terms of the associated infinitesimal Young's moduli in the radial direction. We see from (4.4.6) that if $k > 0$, bifurcation is locally to the right (supercritical) while if $k < 0$, bifurcation is locally to the left (subcritical). Equations corresponding to (4.4.6), (4.4.10) were also determined in [21] for the case of an isotropic composite sphere, as well as in Chapter 3 for the case of a homogeneous transversely isotropic sphere. (To recover the latter, set the volume fraction $f = 1$ in (4.4.10) and compare (4.4.6), (4.4.10) with (3.4.7), (3.4.10).) We now make the further definitions

$$K = \frac{k}{d^2\hat{W}^1(1)/dv^2} \quad , \quad \omega = \frac{d^2\hat{W}^2(1)/dv^2}{d^2\hat{W}^1(1)/dv^2} \quad , \quad (4.4.11)$$

$$\hat{p}_{cr} = \frac{p_{cr}}{d^2\hat{W}^1(1)/dv^2} \quad , \quad \hat{p} = \frac{p_0}{d^2\hat{W}^1(1)/dv^2} \quad ,$$

so that

$$K = \frac{2}{3} \left[\hat{p}_{cr} - \frac{1}{6} f^{-1} + \frac{1}{6} (f^{-1} - 1) \omega \right] . \quad (4.4.12)$$

Letting $f \rightarrow 1$ in (4.4.12), we obtain the value of K appropriate to the homogeneous transversely isotropic sphere composed of the core material, namely

$$K_h \equiv \frac{2}{3} \left(\hat{p}_{cr} - \frac{1}{6} \right) . \quad (4.4.13)$$

In contrast to the case for a homogeneous *isotropic* sphere for which $K_h > 0$ so that bifurcation is only to the right, (see § 5.2 of [5] or eqn. (25) of [21]), we saw in Chapter 3 that for the *anisotropic* sphere, bifurcation can occur either to the right *or* to the left. Thus, for the anisotropic sphere, K_h can be either positive or negative.

Returning to (4.4.12), we now discuss the circumstances which determine whether the bifurcation for the composite sphere is locally to the right or to the left. It is convenient to treat these cases with reference to the schematic diagrams in Figures 4.1 and 4.2. Figure 4.1 corresponds to the case in which bifurcation for the *homogeneous sphere composed of the core material would be to the right*, and Figure 4.2 to the case in which such a sphere would bifurcate to the *left*. In these figures, the semi-infinite strips $0 < f < 1$, $0 < \omega < \infty$, are divided into two regions, I, II by the curve

$$f(\omega) = \frac{\omega - 1}{\omega - 6\hat{p}_{cr}} \quad (4.4.14)$$

on which $K = 0$. When $K_h > 0$ (Fig. 4.1), the curve (4.4.14) is monotone *decreasing* on the region of interest, and when $K_h < 0$ (Fig. 4.2), the curve (4.4.14) is monotone *increasing* with $f(\omega) \rightarrow 1$ as $\omega \rightarrow \infty$. In view of the remark made above following (4.4.13), we note that *there is no diagram analogous to Fig. 4.2 for the composite isotropic sphere considered in [20, 21]*. In both Figures 4.1 and 4.2, if (ω, f) lies in region I, then $K > 0$ and so bifurcation for the composite sphere is to the right, while if (ω, f) lies in region II, then $K < 0$ and so bifurcation is to the left.

As in [21], we may discuss these diagrams with reference to a composite sphere of either fixed geometric properties together with varying material properties or vice versa. We first consider Figure 4.1 so that $K_h > 0$ ($\Rightarrow \hat{p}_{cr} > 1/6$). Taking the former view, we see that for

$$f \geq \frac{1}{6\hat{p}_{cr}} \quad (4.4.15)$$

bifurcation is always to the right. *Thus, if the volume fraction of the core to the total volume exceeds $1/6\hat{p}_{cr}$, bifurcation is locally to the right regardless of the material*

properties of the outer material. Taking the latter view, we also see that for $\omega \geq 1$, i.e., for

$$\frac{d^2 \hat{W}^2(1)}{dv^2} \geq \frac{d^2 \hat{W}^1(1)}{dv^2} \quad (4.4.16)$$

bifurcation is always to the right. It is shown in Chapter 2 that for the transverse isotropy of concern, one has

$$\frac{d^2 \hat{W}(1)}{dv^2} = 4\bar{E} \quad (4.4.17)$$

where \bar{E} is Young's modulus in the direction of anisotropy, i.e., the radial direction, associated with infinitesimal deformations of the transversely isotropic material at hand.

We thus make the following definition for the composite sphere,

$$\begin{aligned} \bar{E}_1 &: \bar{E} \text{ for core material,} \\ \bar{E}_2 &: \bar{E} \text{ for surrounding material.} \end{aligned} \quad (4.4.18)$$

Thus, from (4.4.16) - (4.4.18), if the material in the surrounding shell is stiffer in tension in the radial direction than the core material, ($\bar{E}_2 \geq \bar{E}_1$), bifurcation is to the right irrespective of geometry.

On the other hand, the condition for bifurcation to the left requires *both* geometric and material restrictions. These may be written as

$$f < \frac{\omega - 1}{\omega - 6\hat{p}_{cr}} \quad (4.4.19)$$

and

$$\omega < 1. \quad (4.4.20)$$

Thus, the occurrence of bifurcation to the left in a composite sphere corresponding to

Figure 4.1 requires *a sufficiently small core surrounded by a shell of sufficiently compliant material*.

We next consider similar implications of Figure 4.2, so that now the core material alone would undergo bifurcation to the left ($K_h < 0 \Rightarrow \hat{p}_{cr} < 1/6$). In contrast to the case of Fig. 4.1, we cannot determine a single condition for bifurcation to the right to occur. Thus, we must have

$$f < \frac{\omega - 1}{\omega - 6\hat{p}_{cr}} \quad (4.4.21)$$

and

$$\omega > 1. \quad (4.4.22)$$

In other words, the occurrence of bifurcation to the right in a composite sphere corresponding to Fig. 4.2 requires *a sufficiently small core surrounded by a shell of sufficiently stiff material*.

The situation for bifurcation to the left is much different. Although we can draw no conclusions based on geometric properties alone, we can deduce that for

$$\omega \leq 1 \quad (\Rightarrow \bar{E}_2 \leq \bar{E}_1), \quad (4.4.23)$$

bifurcation is always to the left. *Thus, if the material in the surrounding shell is more compliant in tension in the radial direction than the core material, bifurcation is to the left irrespective of geometry.*

Finally from Fig. 4.2, if

$$\omega > 1 \quad (\Rightarrow \bar{E}_2 > \bar{E}_1) \quad (4.4.24)$$

and

$$f > \frac{\omega - 1}{\omega - 6\hat{p}_{cr}}, \quad (4.4.25)$$

we also have a bifurcation to the left occurring. Thus, bifurcation to the left in a composite sphere corresponding to Figure 4.2 is also possible provided there is *a sufficiently large core surrounded by a shell of sufficiently stiff material*.

We conclude this section by again emphasizing that the behavior of the composite sphere is highly dependent upon the core material. Whether cavitation will or will not take place depends *solely* on the core material. The value of the critical load depends only on the core material. Furthermore, material properties of the core alone determine which of the schematic diagrams (Fig. 4.1 or Fig. 4.2) applies.

4.5. Energy and stability of solutions

To examine the stability of the cavitation solutions, we now carry out an energy analysis for *general* transversely isotropic strain-energy, W . As in Chapter 3, Section 6, the total energy associated with any radially symmetric equilibrium configuration of the body is given by

$$\begin{aligned} E(c) = 4\pi \int_0^B W(\dot{r}^2 + 2r^2/R^2, r^4/R^4 + 2\dot{r}^2 r^2/R^2, 1, 0, \dot{r}^2; R) R^2 dR \\ - 4\pi B^2 p_0 [r(B) - B]. \end{aligned} \quad (4.5.1)$$

For the trivial solution (4.3.1) with deformation (4.3.2), we have

$$E(0) = 0 \quad (4.5.2)$$

on using the normalization (4.2.4). Following the approach taken in Chapter 3, Section 6,

we now consider (4.5.1) to hold for all values of $c \geq 0$, and thus seek values of $c \geq 0$ that, for a given $p_0 > 0$, minimize the extended energy function $E(c)$.

Recalling the notation (4.3.16), (4.3.3), we may write equation (4.5.1) as

$$E(c) = 4\pi c^3 \int_{(1+c^3/B^3)^{1/3}}^{\infty} v^2 (v^3 - 1)^{-2} \hat{W}(v; \frac{c}{(v^3-1)^{1/3}}) dv - 4\pi B^2 p_0 [r(B) - B], \quad c > 0. \quad (4.5.3)$$

Henceforth, for simplicity of notation, we omit the explicit dependence of \hat{W} on its second argument. Upon introduction of the dimensionless quantity

$$\Sigma = \frac{E}{(4/3) \pi B^3 d^2 \hat{W}^1(1) / dv^2}, \quad (4.5.4)$$

and using (4.4.1), (4.4.4), and (4.2.3), we rewrite (4.5.3) as

$$\begin{aligned} \frac{d^2 \hat{W}^1(1)}{dv^2} \Sigma(\rho) = 3\rho^3 \left\{ \int_{(1+\rho^3)^{1/3}}^{\infty} v^2 (v^3 - 1)^{-2} \hat{W}^2(v) dv \right. \\ \left. + \int_{(1+\alpha^3 \rho^3)^{1/3}}^{\infty} v^2 (v^3 - 1)^{-2} \hat{W}^1(v) dv \right\} - 3p_0 [(1+\rho^3)^{1/3} - 1]. \end{aligned} \quad (4.5.5)$$

We now let

$$\Sigma(\rho) = \frac{1}{d^2 \hat{W}^1(1) / dv^2} [\Phi(\rho) + p_0 \Psi(\rho)], \quad \rho \geq 0 \quad (4.5.6)$$

where

$$\Phi(\rho) = 3\rho^3 \left\{ \int_{(1+\rho^3)^{1/3}}^{(1+\alpha^3\rho^3)^{1/3}} \frac{v^2 \hat{W}^2(v)}{(v^3-1)^2} dv + \int_{(1+\alpha^3\rho^3)^{1/3}}^{\infty} \frac{v^2 \hat{W}^1(v)}{(v^3-1)^2} dv \right\} \quad (4.5.7)$$

and

$$\Psi(\rho) = -3[(1+\rho^3)^{1/3} - 1]. \quad (4.5.8)$$

We thus state the energy minimization problem as: *for fixed $p_0 > 0$, we seek those values of $\rho \geq 0$ that minimize $\Sigma(\rho)$.*

Proceeding as in Chapter 3, we first examine the end-point $\rho = 0$ where $\Sigma(0) = 0$. It is shown in Appendix D that

$$\dot{\Sigma}(0+) = \ddot{\Sigma}(0+) = 0, \quad \dddot{\Sigma}(0+) = 6(\hat{p}_{cr} - \hat{p}), \quad (4.5.9)$$

where the superposed dot again denotes differentiation with respect to ρ , and \hat{p}_{cr} , \hat{p} are given by (4.4.11), (4.4.3). Thus $\rho = 0$ is a local minimum if $\hat{p} < \hat{p}_{cr}$ ($p_0 < p_{cr}$) and a local maximum if $\hat{p} > \hat{p}_{cr}$ ($p_0 > p_{cr}$). Observe that

$$\rho = 0, \quad p_0 > 0, \quad (4.5.10)$$

corresponds to the trivial solution (4.3.1).

We now consider the possible existence of internal extrema and thus seek values of $\rho > 0$ for which

$$\dot{\Sigma}(\rho) = 0 \quad \text{and so} \quad \dot{\Phi}(\rho) + p_0 \dot{\Psi}(\rho) = 0. \quad (4.5.11)$$

From (4.5.8), $\dot{\Psi}(\rho) < 0$ for $\rho > 0$ so that (4.5.11) may be written as

$$p_0 = -\frac{\dot{\Phi}(\rho)}{\dot{\Psi}(\rho)}, \quad \rho > 0. \quad (4.5.12)$$

We again note that the expression (4.5.12) for $p_0(\rho)$ derived from energy considerations

can be shown to be identical to the expression (4.3.18) determined directly in Section 4.3. Thus, as expected, the extremals provided by (4.5.12) correspond to equilibrium solutions with an internal cavity.

We next analyze the dimensionless energy $\Sigma(\rho)$ given by (4.5.6) - (4.5.8) near $\rho^3 = 0$. A straightforward calculation shows that

$$\Psi(\rho) \equiv \Psi^*(\rho^3) = -\rho^3 + \frac{1}{3}\rho^6 + O(\rho^9) \text{ as } \rho^3 \rightarrow 0. \quad (4.5.13)$$

On using (4.5.13) and (4.4.6), the last term in (4.5.6) has the asymptotic expression

$$p_0(\rho)\Psi(\rho) = -p_{cr}\rho^3 + \left(\frac{1}{3}p_{cr} - k\right)\rho^6 + O(\rho^9) \text{ as } \rho^3 \rightarrow 0, \quad (4.5.14)$$

where k is given by (4.4.10). We next consider the Taylor expansion

$$\Phi(\rho) \equiv \Phi^*(\rho^3) = \Phi^*(0) + \frac{d\Phi^*}{d\rho^3}(0)\rho^3 + \frac{1}{2}\frac{d^2\Phi^*}{d(\rho^3)^2}(0)\rho^6 + O(\rho^9) \text{ as } \rho^3 \rightarrow 0. \quad (4.5.15)$$

It is easily seen that

$$\Phi^*(0) = 0. \quad (4.5.16)$$

This follows from the fact that $\Sigma(0) = 0$ and so from (4.5.6), $\Phi(0) + p_0\Psi(0) = 0$; however, (4.5.8) implies that $\Psi(0) = 0$, so that (4.5.16) must hold.

Now, differentiating (4.5.7) we obtain

$$\begin{aligned} \frac{d\Phi^*}{d\rho^3} = & 3 \left\{ \int_{(1+\rho^3)^{1/6}}^{(1+\alpha^3\rho^3)^{1/6}} \frac{v^2 \hat{W}^2(v)}{(v^3-1)^2} dv + \int_{(1+\alpha^3\rho^3)^{1/6}}^{\infty} \frac{v^2 \hat{W}^1(v)}{(v^3-1)^2} dv \right\} \\ & + \frac{1}{\rho^3} \left\{ \alpha^{-3} \left[\hat{W}^2(v) - \hat{W}^1(v) \right] \Big|_{v(A)=(1+\alpha^3\rho^3)^{1/6}} - \hat{W}^2(v) \Big|_{v(B)=(1+\rho^3)^{1/6}} \right\}, \end{aligned} \quad (4.5.17)$$

so that

$$\begin{aligned} \frac{d\Phi^*}{d\rho^3}(0) = & 3 \int_1^\infty \frac{v^2}{(v^3 - 1)^2} \hat{W}^1(v) dv \\ & + \lim_{\rho^3 \rightarrow 0} \frac{\alpha^{-3} [\hat{W}^2((1+\alpha^3 \rho^3)^{1/3}) - \hat{W}^1((1+\alpha^3 \rho^3)^{1/3})] - \hat{W}^2((1+\rho^3)^{1/3})}{\rho^3}. \end{aligned} \quad (4.5.18)$$

Integrating the first term on the right hand side by parts gives

$$\int_1^\infty 3v^2 (v^3 - 1)^{-2} \hat{W}^1(v) dv = \lim_{v \rightarrow 1} \frac{\hat{W}^1(v)}{v^3 - 1} - \lim_{v \rightarrow \infty} \frac{\hat{W}^1(v)}{v^3 - 1} + \int_1^\infty \frac{\hat{W}_1^1(v)}{v^3 - 1} dv, \quad (4.5.19)$$

where we note from (4.4.3) that the last term in the above equation is p_{cr} . Since $\hat{W}^i(1) = 0$ ($i=1,2$) from (4.2.5) and (4.3.16), using L'Hopital's rule and (3.4.2)₁ shows that the first term on the right in (4.5.19) is zero. Also, it follows from considerations similar to those of Section 4.4 that for a finite p_{cr} , i.e., for cavitation to take place, we must have

$$\hat{W}^1(v) = O(v^n), \quad n < 3, \quad \text{as } v \rightarrow \infty. \quad (4.5.20)$$

Thus, the second term on the right in (4.5.19) is also zero so that we arrive at the following *alternative formula for the critical load* (when the strain-energy satisfies the growth assumption (4.5.20)):

$$\int_1^\infty \frac{3v^2}{(v^3 - 1)^2} \hat{W}^1(v) dv = \int_1^\infty \frac{\hat{W}_1^1(v)}{v^3 - 1} dv \equiv p_{cr}. \quad (4.5.21)$$

Now, the limit in (4.5.18) is zero by arguments similar to those used following equation (4.5.19). Thus, on using the formula (4.5.21) for the critical load, (4.5.18) reduces to

$$\frac{d\Phi^*}{d\rho^3}(0) = p_{cr}. \quad (4.5.22)$$

We next differentiate (4.5.17) and obtain

$$\frac{d^2\Phi^*}{d(\rho^3)^2} = \frac{1}{3} \left\{ \frac{[\hat{W}_1^2(v) - \hat{W}_1^1(v)]|_{v(A)=(1+\alpha^3\rho^3)^{1/3}}}{\rho^3 (1+\alpha^3\rho^3)^{2/3}} - \frac{\hat{W}_1^2(v)|_{v(B)=(1+\rho^3)^{1/3}}}{\rho^3 (1+\rho^3)^{2/3}} \right\}, \quad (4.5.23)$$

so that taking the limit as $\rho^3 \rightarrow 0$ and applying L'Hopital's rule gives

$$\frac{d^2\Phi^*}{d(\rho^3)^2}(0) = \frac{1}{9} \left\{ \alpha^3 \left[\frac{d^2\hat{W}^2}{dv^2}(1) - \frac{d^2\hat{W}^1}{dv^2}(1) \right] - \frac{d^2\hat{W}^2}{dv^2}(1) \right\}. \quad (4.5.24)$$

Combining (4.5.15), (4.5.16), (4.5.22), (4.5.24), and (4.4.9) then gives

$$\Phi^*(\rho^3) = p_{cr}\rho^3 + \frac{1}{18} \left\{ f^{-1} \left[\frac{d^2\hat{W}^2}{dv^2}(1) - \frac{d^2\hat{W}^1}{dv^2}(1) \right] - \frac{d^2\hat{W}^2}{dv^2}(1) \right\} \rho^6 + O(\rho^9) \quad (4.5.25)$$

as $\rho^3 \rightarrow 0$.

Finally, using (4.5.14) and (4.5.25) in (4.5.6), we obtain

$$\Sigma(\rho) \equiv \Sigma^*(\rho^3) = -\frac{1}{2} K \rho^6 + O(\rho^9) \text{ as } \rho^3 \rightarrow 0, \quad (4.5.26)$$

where K is given by (4.4.12). The above result, which holds for a composite sphere consisting of two *general* homogeneous transversely isotropic phases, generalizes those found previously in [20], (see eq. (3.17)) for a composite sphere composed of two neo-Hookean phases, and in Chapter 3, (see equation (3.6.13)), for the homogeneous transversely isotropic sphere composed of the specific material described in Chapter 3, Section 5. Equations (4.5.21) and (4.5.26) of course hold for the general problem considered in Chapter 3 (i.e., $\alpha = 1$, $\hat{W}^2 \equiv 0$). In this case, \hat{W}^1 represents the stored-energy function for the homogeneous transversely isotropic sphere, and K appearing in (4.5.26) is given by (4.4.13), (see (4.4.12) and the sentence following (4.4.12)). Returning to the problem at hand and recalling the results at the end of Section 4.4,

where the curve (4.5.12) (or equivalently (4.4.2)) was shown to bifurcate from the trivial solution (4.5.10) at the point $\rho = 0$, $p_0 = p_{cr}$, (4.5.26) shows that $\Sigma < 0$ on this curve near $\rho = 0$ if the bifurcation is to the right ($K > 0$) and $\Sigma > 0$ if the bifurcation is to the left ($K < 0$). We have thus established, in general, all of the energy results which were essential for the specific material models in [20] (and in Chapter 3, Section 6) to establish Properties A and B, which we now restate for convenience:

Property A: The curve $\hat{p} = \hat{p}(\rho)$ is a locus of local *minima* of $\Sigma(\rho)$ for fixed \hat{p} whenever $d\hat{p}/d\rho > 0$, and is a locus of local *maxima* of $\Sigma(\rho)$ for fixed \hat{p} whenever $d\hat{p}/d\rho < 0$.

Property B: On the curve $\hat{p} = \hat{p}(\rho)$, the values of $\Sigma(\rho)$ are *decreasing* with ρ whenever $d\hat{p}/d\rho > 0$ and are *increasing* with ρ whenever $d\hat{p}/d\rho < 0$.

With the above results we have that, in general, where the curve $\hat{p} = \hat{p}(\rho)$ is monotone decreasing, the cavitated solution is unstable, and where $\hat{p} = \hat{p}(\rho)$ is monotone increasing, the cavitated solution is stable. If there exist two stable solutions corresponding to a particular load, we again say that a solution is *absolutely stable* (AS) if it provides the absolute minimum for Σ and is *metastable* (MS) if it provides a local minimum for Σ which is not the absolute minimum. In cases such as this, there may be a discontinuous transition in cavity radius in moving from one stable solution to another. The transition between metastability and absolute stability will be addressed more completely in the illustrative example considered in the following section.

4.6. Illustrative example

In this section, we illustrate the foregoing results for a specific material model. Consider a composite sphere whose phases are described by the transversely isotropic strain-energy density function discussed in Section 3.5.1. Explicitly, we have

$$W = \begin{cases} \frac{\mu_1}{2} \left[(I_1 - 3) + a_1 (I_5^2 - 2I_5 + 1) \right] , & 0 \leq R < A \\ \frac{\mu_2}{2} \left[(I_1 - 3) + a_2 (I_5^2 - 2I_5 + 1) \right] , & A < R \leq B \end{cases} \quad (4.6.1)$$

where I_1 , I_5 are given by (4.2.11), (4.2.15), the μ_i ($i = 1, 2$) are positive constants, and the a_i with $0 \leq a_i \leq 5.0$ ($i=1, 2$) are dimensionless parameters which serve as measures of the degree of anisotropy in the respective phases. When $a_1 = 0$, $a_2 = 0$, one recovers the neo-Hookean composite sphere treated in [20, 21]. Recalling the notation (4.3.3), (4.3.16), and using (4.3.4), we rewrite (4.6.1) as

$$\hat{W}(v) = \begin{cases} \hat{W}^1(v) = \frac{\mu_1}{2} [(v^{-4} + 2v^2 - 3) + a_1 (v^{-8} - 2v^{-4} + 1)] , & 0 \leq R < A \\ \hat{W}^2(v) = \frac{\mu_2}{2} [(v^{-4} + 2v^2 - 3) + a_2 (v^{-8} - 2v^{-4} + 1)] , & A < R \leq B \end{cases} \quad (4.6.2)$$

where, from the considerations of Chapter 2,

$$d^2 \hat{W}^i(1)/dv^2 = 4\bar{E}_i = 4\mu_i(3 + 4a_i) > 0 \quad (i = 1, 2) \quad (4.6.3)$$

for this material. We recall that the \bar{E}_i are Young's moduli in the radial direction.

On substitution from (4.6.2) into (4.5.7) and from (4.6.3) with $i = 1$ into (4.5.6), and making the definitions

$$\beta = \frac{\mu_2}{\mu_1}, \quad z(x) = (1 + x^3)^{1/3}, \quad (4.6.4)$$

we find that (4.5.6) - (4.5.8) and the considerations of Appendix C give the total energy for the composite sphere as

$$\Sigma(\rho) = \frac{1}{4(3 + 4a_1)} \left[\frac{\Phi(\rho)}{\mu_1} + \frac{p_0}{\mu_1} \Psi(\rho) \right] \quad (4.6.5)$$

where

$$\begin{aligned} \frac{\Phi(\rho)}{\mu_1} = & \frac{3}{2} \left\{ -\alpha^{-3} (\beta - 1) \left[2z^2(\alpha\rho) - z^{-1}(\alpha\rho) - 1 \right] + \beta \left[2z^2(\rho) - z^{-1}(\rho) - 1 \right] \right. \\ & - (\beta a_2 - a_1) \left[\frac{1}{3}\alpha^{-3} z^{-5}(\alpha\rho) + \frac{8}{3}\rho^3 \left[\frac{1}{5}z^{-5}(\alpha\rho) + \frac{1}{2}z^{-2}(\alpha\rho) \right. \right. \\ & \left. \left. - \frac{1}{\sqrt{3}} \arctan \frac{\sqrt{3} z(\alpha\rho)}{2 + z(\alpha\rho)} - \frac{1}{\sqrt{3}} \arctan \frac{2z(\alpha\rho) + 1}{\sqrt{3}} \right] + \alpha^{-3} (2z^{-1}(\alpha\rho) - \frac{8}{3}z^2(\alpha\rho) + \frac{1}{3}) \right] \\ & + \beta a_2 \left[\frac{1}{3}z^{-5}(\rho) + \frac{8}{3}\rho^3 \left[\frac{1}{5}z^{-5}(\rho) + \frac{1}{2}z^{-2}(\rho) - \frac{1}{\sqrt{3}} \arctan \frac{\sqrt{3} z(\rho)}{2 + z(\rho)} - \frac{1}{\sqrt{3}} \arctan \frac{2z(\rho) + 1}{\sqrt{3}} \right] \right. \\ & \left. \left. + 2z^{-1}(\rho) - \frac{8}{3}z^2(\rho) + \frac{1}{3} \right] + \frac{20\pi}{9\sqrt{3}} a_1 \rho^3 \right\} \end{aligned} \quad (4.6.6)$$

and $\Psi(\rho)$ is given by (4.5.8). Furthermore, from either (4.5.12) or (4.4.5), and making the definitions

$$\left. \begin{aligned} F[z(x)] &= z^{-1}(x) + \frac{1}{4} z^{-4}(x), \\ G[z(x)] &= F[z(x)] - \frac{1}{2} z^{-2}(x) - \frac{1}{5} z^{-5}(x) - \frac{1}{8} z^{-8}(x) \\ &\quad + \frac{1}{\sqrt{3}} \left[\arctan \frac{2z(x) + 1}{\sqrt{3}} + \arctan \frac{\sqrt{3} z(x)}{2 + z(x)} \right], \end{aligned} \right\} \quad (4.6.7)$$

we obtain the corresponding load/cavity relationship as

$$\begin{aligned} \frac{p_0(\rho)}{\mu_1} = 2z^2(\rho) \left\{ \left[1 - \beta \right] F [z(\alpha\rho)] + \beta F [z(\rho)] \right. \\ \left. + 2 \left[\beta a_2 - a_1 \right] G [z(\alpha\rho)] - 2\beta a_2 G [z(\rho)] + \frac{5\pi}{3\sqrt{3}} a_1 \right\}. \end{aligned} \quad (4.6.8)$$

For small values of ρ we have (see (4.4.6), (4.5.26) respectively)

$$\hat{p}(\rho) = \hat{p}_{cr} + K\rho^3 + o(\rho^3) \text{ as } \rho^3 \rightarrow 0, \quad (4.6.9)$$

$$\Sigma(\rho) = -\frac{1}{2} K\rho^6 + o(\rho^6) \text{ as } \rho^3 \rightarrow 0, \quad (4.6.10)$$

where, for the material at hand,

$$\begin{aligned} \hat{p}_{cr} = \frac{1}{4(3 + 4a_1)} \left[\frac{5}{2} + \left[\frac{40\pi - 51\sqrt{3}}{30\sqrt{3}} \right] a_1 \right] \\ \text{so that } \frac{p_{cr}}{\mu_1} = \left[\frac{5}{2} + \left[\frac{40\pi - 51\sqrt{3}}{30\sqrt{3}} \right] a_1 \right] \end{aligned} \quad (4.6.11)$$

and

$$K = \frac{2}{3} \left[\hat{p}_{cr} - \frac{1}{6} f^{-1} + \frac{1}{6} (f^{-1} - 1) \beta \frac{(3 + 4a_2)}{(3 + 4a_1)} \right]. \quad (4.6.12)$$

We now examine the curve (4.6.8) and corresponding energy for the material (4.6.1) for large values of ρ . A detailed analysis of (4.6.8) similar to that discussed in Appendix B for the homogeneous sphere, shows that for large values of ρ ,

$$\frac{p_0(\rho)}{\mu_1} \sim 2 \left[\beta(1 - \alpha^{-1}) + \alpha^{-1} \right] \rho \text{ as } \rho \rightarrow \infty, \quad (4.6.13)$$

while the expression for the energy on this curve for large ρ follows from (4.6.5), (4.6.6), (4.6.13), and (4.5.8) as

$$\frac{\mathcal{E}(\rho)}{\mu_1} \sim -3 [\beta(1 - \alpha^{-1}) + \alpha^{-1}] \rho^2 \text{ as } \rho \rightarrow \infty. \quad (4.6.14)$$

In (4.6.14), $\mathcal{E}(\rho) / \mu_1$ is defined to be the quantity in brackets in (4.6.5). The expressions (4.6.13), (4.6.14) are identical to those found in [20] for the composite neo-Hookean sphere. (See eqs. (3.18), (3.19); the additional factor of two in the equations in [20] is due to the authors' use of a shear modulus one-half that of the actual infinitesimal shear modulus). Thus, the anisotropy considered here does not affect the large ρ asymptotic behavior of the bifurcation curve, nor the energy on it. Since $\alpha > 1$, $\beta > 0$ we see that $\beta(1 - \alpha^{-1}) + \alpha^{-1} > 0$. Thus, the curve (4.6.8) is asymptotic to a straight line with positive slope, while the energy will always be negative on this curve for sufficiently large values of ρ . Thus, as seen in [20] and in Chapter 3, the initial character of the bifurcation does not affect the large ρ asymptotic behavior. Note that we recover the results (3.5.30), (3.6.14) for the homogeneous anisotropic sphere on setting $\alpha = 1$ in (4.6.13), (4.6.14) respectively.

In Figures 4.3 - 4.6 we have plotted the curve (4.6.8) for four different pairs of values of the anisotropy coefficients a_1 , a_2 , and the parameter ω defined in (4.4.11). (Note that for the material (4.6.1), we have

$$\omega = \beta \frac{(3 + 4a_2)}{(3 + 4a_1)} \quad (4.6.15)$$

so that choosing any three of the parameters in (4.6.15) specifies the last.) All graphs in Sections 4.6 and 4.7 correspond to a representative value $f = 0.1$ for the volume fraction of the core material to the total material. The situations corresponding to Figures 4.3 and 4.4 were discussed extensively in Chapter 3. We will treat these briefly in what follows, and pay closer attention to the more novel phenomena displayed in Figures 4.5 and 4.6.

In the case of Fig. 4.3, the composite sphere undergoes a bifurcation to the right and a smooth cavitation occurs. Here, an internal cavity is nucleated at the critical load, with its radius increasing continuously from zero as p_0 is further increased. In Fig. 4.4, the composite sphere undergoes a bifurcation to the left. There exists a turning point (p_t, ρ_t) of the curve at which

$$\frac{dp_0}{d\rho} = 0, \quad (4.6.16)$$

and a cavity of finite radius is nucleated at a transition load \tilde{p} , with $p_t < \tilde{p} < p_{cr}$. The existence of a unique value $p = \tilde{p}$ was established in [20] for the composite neo-Hookean sphere, and, as discussed in Chapter 3, follows from the Properties A and B given in Chapter 3 and at the end of Section 4.5. (The nondimensional analog of \tilde{p} was called P_N in Chapter 3). Stability arguments of the type carried out in Chapter 3 again show that a "snap cavitation" occurs in which a discontinuous change in stable equilibrium configurations takes place.

We consider now the situation in which the curve (4.6.8) bifurcates to the *right* from the trivial solution (4.5.10) at the point $(p_{cr}, 0)$, *and has two turning points*, (p_{t1}, ρ_{t1}) , (p_{t2}, ρ_{t2}) , at which (4.6.16) holds. This is the case in Figures 4.5(a) and 4.6(a). In each of these figures, the curve (4.6.8) is monotonically increasing for $0 < \rho < \rho_{t2}$ and $\rho > \rho_{t1}$, and is monotonically decreasing for $\rho_{t2} < \rho < \rho_{t1}$. *Note that in Figure 4.5(a), p_{t1} and p_{t2} both fall to the right of p_{cr} , while in Figure 4.6(a), p_{cr} falls between p_{t1} and p_{t2} .*

We first consider Figure 4.5(a), for which the number of equilibrium solutions depends on the values of p_0 in the following way: for $0 < p_0 < p_{cr}$, the only solution is the trivial solution $\rho = 0$; for $p_{cr} < p_0 < p_{t1}$, there are exactly *two* solutions, namely, the

trivial solution $\rho = 0$ and an additional bifurcated solution involving an internal cavity; for $p_{t1} < p_0 < p_{t2}$, there are exactly *four* solutions, namely, the trivial solution $\rho = 0$ and in addition three bifurcated solutions each involving an internal cavity; finally, for $p_0 > p_{t2}$, there are exactly *two* solutions, namely the trivial solution and a single bifurcated solution involving an internal cavity. Again, the trivial solution provides a local minimum for Σ and hence is stable for $0 < p_0 < p_{cr}$, while for $p_0 > p_{cr}$ the trivial solution provides a local maximum for Σ and thus is unstable. By virtue of Property A, the bifurcated curve (4.6.8) again provides a local maximum for Σ if $\rho_{t2} < \rho < \rho_{t1}$ and hence the associated solution is unstable, while for $0 < \rho < \rho_{t2}$ and $\rho > \rho_{t1}$, this curve provides a local minimum for Σ and hence this solution is stable. Thus if $0 < p_0 < p_{t1}$ or if $p_0 > p_{t2}$, there is exactly one stable equilibrium solution, while if $p_{t1} < p_0 < p_{t2}$ there are two stable equilibrium solutions, each involving an internal cavity.

We now address the transition between metastability and absolute stability in the region $p_{t1} \leq p_0 \leq p_{t2}$. We again refer to Fig. 4.5(a). Observe that the stable branches on the region of interest correspond to the intervals $\bar{\rho}_{t1} \leq \rho \leq \rho_{t2}$ and $\rho_{t1} \leq \rho \leq \bar{\rho}_{t2}$, where $\bar{\rho}_{t1}$, $\bar{\rho}_{t2}$ are the points at which $p_0(\bar{\rho}_{t1}) = p_{t1}$, $p_0(\bar{\rho}_{t2}) = p_{t2}$, respectively, and where (4.6.16) is *not* satisfied. From Property B and $\Sigma(0) = 0$, we have that $\Sigma(\rho)$ decreases from zero on the interval $0 \leq \rho \leq \rho_{t2}$. Property B and (4.6.14) give that $\Sigma(\rho)$ is decreasing with ρ for $\rho > \rho_{t1}$, and $\Sigma(\rho)$ is negative for sufficiently large ρ . (Note that $\Sigma(\rho_{t1})$ can be either positive or negative.) We now define a transition load $p_0 = p_{tr}$, satisfying $p_{t1} \leq p_{tr} \leq p_{t2}$, such that for $p_{t1} \leq p_0 \leq p_{tr}$, we have $\Sigma(\rho)$ on $\bar{\rho}_{t1} \leq \rho \leq \rho_{tr}$ less than $\Sigma(\rho)$ on $\rho_{t1} \leq \rho \leq \bar{\rho}_{tr}$, and for $p_{tr} \leq p_0 \leq p_{t2}$, we have $\Sigma(\rho)$ on $\rho_{tr} \leq \rho \leq \rho_{t2}$ greater than $\Sigma(\rho)$ on $\bar{\rho}_{tr} \leq \rho \leq \bar{\rho}_{t2}$, where ρ_{tr} , $\bar{\rho}_{tr}$ ($\bar{\rho}_{tr} > \rho_{tr}$) are the values of ρ occurring on the stable branches for which $p_0(\rho) = p_{tr}$. In other words, p_{tr} is the value of the dead-load at which the energy on the

upper portion of the bifurcation curve becomes less than that on the lower portion of this curve, and thus the value after which the upper branch remains the absolutely stable solution. The preceding is sketched in Fig. 4.5(b). Note that if $p_{tr} = p_{t1}$, then $\bar{\rho}_{tr} = \rho_{t1}$ and the upper branch is absolutely stable for $\rho > \rho_{t1}$, and if $p_{tr} = p_{t2}$, then $\rho_{tr} = \rho_{t2}$ and the lower branch is the absolutely stable solution for $0 < \rho \leq \rho_{t2}$.

Consider now the quasi-static loading process in which the composite sphere is subjected to a tensile dead-load surface traction p_0 which increases slowly from zero. We again refer to Fig. 4.5(b). The trivial homogeneous deformation (4.3.2) persists as p_0 is increased from zero, until the critical load, $p_0 = p_{cr}$, is reached. Then an internal void is nucleated, with cavity radius increasing continuously from zero as p_0 increases, until $p_0 = p_{tr}$. At this point there are two possibilities. First, if one supposes that the body always assumes an absolutely stable configuration, then as p_0 passes through p_{tr} , a discontinuous growth in cavity radius from $c = B\rho_{tr}$ to $c = B\bar{\rho}_{tr}$ is predicted, with cavity radius increasing continuously as p_0 is further increased. On the other hand, if one supposes that continuous deformation of the body persists as long as possible, then the cavity radius grows continuously as p_0 is increased until $p_0 = p_{t2}$ and then experiences a jump from $c = B\rho_{t2}$ to $c = B\bar{\rho}_{t2}$ as p_0 passes through p_{t2} . The cavity radius then increases continuously as p_0 is further increased. Note that the foregoing two possibilities coincide if $p_{tr} = p_{t2}$.

We next consider Figure 4.6(a), for which the number of equilibrium solutions depends on the values of p_0 in the following way: for $0 < p_0 < p_{t1}$, the only solution is the trivial solution $\rho = 0$; for $p_{t1} < p_0 < p_{cr}$, there are exactly *three* solutions, namely, the trivial solution $\rho = 0$ and in addition two bifurcated solutions each involving an

internal cavity; for $p_{cr} < p_0 < p_{t2}$, there are exactly *four* solutions, namely, the trivial solution $\rho = 0$ and in addition three bifurcated solutions each involving an internal cavity; finally, for $p_0 > p_{t2}$, there are exactly *two* solutions, namely the trivial solution and a single bifurcated solution involving an internal cavity. As noted earlier, the trivial solution provides a local minimum for Σ and hence is stable for $0 < p_0 < p_{cr}$, while for $p_0 > p_{cr}$ the trivial solution provides a local maximum for Σ and thus is unstable. Again by Property A, the bifurcated curve (4.6.8) provides a local maximum for Σ if $\rho_{t2} < \rho < \rho_{t1}$ and hence the associated solution is unstable, while for $0 < \rho < \rho_{t2}$ and $\rho > \rho_{t1}$, this curve provides a local minimum for Σ and hence this solution is stable. Thus if $0 < p_0 < p_{t1}$ or if $p_0 > p_{t2}$, there is exactly one stable equilibrium solution, while if $p_{t1} < p_0 < p_{cr}$ there are two stable equilibrium solutions, one involving an internal cavity, and if $p_{cr} < p_0 < p_{t2}$ there are two stable equilibrium solutions, each involving an internal cavity.

To address the transition between metastability and absolute stability, we refer to Figs. 4.6(b),(c), where ρ_{t1} , ρ_{t2} , p_{t1} , p_{t2} are as before, and ρ_{c1} denotes the value of $\rho > 0$ occurring on the stable branch for which $p_0(\rho) = p_{cr}$, while ρ_{c2} denotes the value of $\rho > 0$ such that $p_0(\rho) = p_{cr}$ occurs on the unstable branch. In Figure 4.6(c) we have graphed the energy, $\mathcal{E}(\rho) / \mu_1 = [\Phi(\rho) + p_0(\rho) \Psi(\rho)] / \mu_1$, for $\rho > 0$ on the curve shown in Fig. 4.6(b). Note that the following analysis depends only on the sign of $\Sigma(\rho) = \mathcal{E} / [4\mu_1(3 + 4a_1)]$ which has the same sign as \mathcal{E} , so that all necessary information on Σ can be extracted from Fig. 4.6(c). We shall now show that there exists a unique value of p_0 , namely $p_0 = \tilde{p}_1$, satisfying $p_{t1} < \tilde{p}_1 < p_{t2}$, such that, if $\tilde{p}_1 < p_{cr}$, the trivial solution is absolutely stable for $p_0 < \tilde{p}_1$, while for $p_0 > \tilde{p}_1$, the absolutely stable solution occurs on the bifurcated branch. (We note here that we shall confine attention to the case

$\tilde{p}_1 < p_{cr}$ in what follows; stability for the case $\tilde{p}_1 > p_{cr}$ is analogous to the situation previously described for Figure 4.5(b)). The desired result is established by the following argument: First, since $\Sigma(0) = 0$, we have $\Sigma(\rho_{c2}) < 0$ from Property B. Second, from Property A, we know that for $p_0 = p_{cr}$ fixed, $\rho = \rho_{c2}$ corresponds to a local maximum of the energy while $\rho = 0$ and $\rho = \rho_{c1}$ correspond to local minima. Thus, in particular, $\Sigma(\rho_{c2}) > \Sigma(0) = 0$. [We remark here that the energy curve *for fixed* p_0 is distinctly different from that displayed in Fig. 4.6(c). In Fig. 4.6(c), *every* value of ρ corresponds to a particular maximum or minimum of the energy associated with a corresponding value of the load p_0 . To see this, compare Fig. 4.6(c) to Fig. 4.6(d), which represents the energy curve $\Sigma(\rho)$ vs. ρ for fixed $p_0 = p_{cr}$. Figure 4.6(d) indeed shows that ρ_{c1} , ρ_{c2} correspond to extrema of the energy for p_0 fixed at $p_0 = p_{cr}$. Note also that although Fig. 4.6(d) implies $\Sigma(\rho_{c1}) < \Sigma(0) = 0$, this is not necessarily true for all curves of the type shown in Fig. 4.6(a).] Returning now to our argument, we have from $\Sigma(\rho_{c2}) < 0$, $\Sigma(\rho_{c2}) > 0$, and Property B, that there exists a unique value of $\rho = \tilde{\rho}_2$, satisfying $\rho_{c2} < \tilde{\rho}_2 < \rho_{c2}$, for which $\Sigma(\tilde{\rho}_2) = 0$. (See Fig. 4.6(c)). We now consider the value of the load associated with $\tilde{\rho}_2$, defined to be $p_0(\tilde{\rho}_2) \equiv \tilde{p}_2$. Again from Property A for $p_0 = \tilde{p}_2$ fixed, $0 = \Sigma(\tilde{\rho}_2) > \Sigma(\tilde{\rho}_2'')$, where $\tilde{\rho}_2''$ is the largest value of ρ such that $p_0(\rho) = \tilde{p}_2$. (See Figs. 4.6(b),(c)). We also observe that the preceding along with Property B give $\Sigma(\rho_{t1}) > 0$. Therefore, by Property B, there exists a unique value of $\rho = \tilde{\rho}_1$, satisfying $\rho_{t1} < \tilde{\rho}_1 < \tilde{\rho}_2''$, for which $\Sigma(\tilde{\rho}_1) = 0$. The associated load is then $p_0(\tilde{\rho}_1) \equiv \tilde{p}_1$. (See Figs. 4.6(b),(c)). Thus, the energy on the bifurcated curve is such that $\Sigma(\rho) < 0$ for $0 < \rho < \tilde{\rho}_2$ and for $\rho > \tilde{\rho}_1$, while $\Sigma(\rho) > 0$ for $\tilde{\rho}_2 < \rho < \tilde{\rho}_1$. This completes the argument since the energy associated with the trivial solution is everywhere zero.

Consider now the previously envisioned quasi-static loading process. We thus refer to Figure 4.6(e), where, as remarked earlier, we have $\bar{p}_1 < p_{cr}$. If one supposes that the body always assumes an absolutely stable configuration, then the trivial homogeneous deformation (4.3.2) persists for $0 < p_0 < \bar{p}_1$. As p_0 passes through \bar{p}_1 , the foregoing notion of stability predicts the sudden appearance of a cavity of finite radius $c = B\bar{p}_1$. As p_0 is further increased, the cavity radius increases in a continuous fashion. On the other hand, one may suppose that the trivial homogeneous deformation (4.3.2) persists until it becomes unstable at $p_0 = p_{cr}$. *In this case, there are two possibilities as p_0 passes through p_{cr}* , similar to those discussed for Fig. 4.5(b). First, if one supposes that the body then assumes an absolutely stable configuration, the sudden appearance of a cavity of finite radius $c = Bp_{c1}$ is predicted, with cavity radius increasing in a continuous fashion as p_0 is further increased. On the other hand, one may suppose that continuous deformation of the body persists as long as possible so that an internal void is nucleated at $p_0 = p_{cr}$ and the cavity radius grows continuously from zero until $p_0 = p_{t2}$ and then experiences a jump from $c = Bp_{t2}$ to $c = B\bar{p}_{t2}$, as p_0 passes through p_{t2} . The cavity radius then increases continuously as p_0 is further increased.

We have seen in the foregoing that there are *four* distinct types of bifurcation that can occur (Figs. 4.3 - 4.6). Note that these four possibilities exist *regardless* of which of the schematic diagrams (Fig. 4.1 or Fig. 4.2) applies. In each of the diagrams, points in region II give rise to only *one* type of bifurcation (i.e. that shown in Fig. 4.4), while points in region I have three types of bifurcation associated with them (i.e. those shown in Figs. 4.3, 4.5, 4.6). We also remark that although there corresponds a different diagram resembling either Fig. 4.1 or Fig. 4.2 *for every value of a_1* , these two diagrams exhaust the possibilities. For $a_1 < a_0$, we have a figure similar to Fig. 4.1, and for

$a_1 > a_0$, we have a figure similar to Fig. 4.2. We recall from Chapter 3 that for a homogeneous sphere consisting of the inner material only, a_0 is the transition value of the anisotropy parameter, a , which governs whether bifurcation for this sphere is to the right ($a < a_0$) or to the left ($a > a_0$). The numerical value of a_0 is given by (3.5.28). Finally, we observe that regardless of the stability criterion adopted, a discontinuous growth in cavity radius is predicted in three of the four types of bifurcation discussed.

We conclude this section by addressing more closely how the anisotropy considered here results in the four different bifurcations we have seen. As stated above, when the parameter pair (ω, f) lies in region II in either of the schematic diagrams Figs. 4.1, 4.2, we have seen only one type of bifurcation. However, when (ω, f) lies in region I, there are three possibilities. We now examine the role of the anisotropy parameters a_1, a_2 , in determining which of the three types of bifurcation associated with regions I occurs. For this purpose, we refer to Figures 4.5(a), 4.7, and 4.8. These three figures correspond to *the same value of a_1 , the same parameter pair (ω, f) , and different values of a_2* . Note that the value of β necessarily changes if one holds a_1 and ω fixed, and varies a_2 (see the comment following (4.6.15)). As the value of a_2 is decreased from $a_2 = 3.7$ in Fig. 4.5(a), to $a_2 = 1.475$ in Fig. 4.7, the value of p_{t1} approaches that of p_{t2} , so that the region in which there is more than one stable solution, i.e., $p_{t1} \leq p_0 \leq p_{t2}$, becomes much smaller. When a_2 is further decreased to $a_2 = 0.14$ in Fig. 4.8, the curve (4.6.8) is monotone increasing, so that bifurcation here is of the type displayed in Fig. 4.3. We also note that, if we held the values of a_1, ω , and f associated with Fig. 4.6(a) fixed and varied a_2 as above, this would give rise to figures similar to those shown in Figs. 4.7, 4.8. Thus, we conclude that it is the *magnitude of the anisotropy parameter a_2 associated with the surrounding shell* that is important in determining the region in which multiple

stable solutions occur and thus the monotonicity of the curve (4.6.8). For large values of a_2 in the range $0 \leq a_2 \leq 5$, one obtains figures like Fig. 4.5(a) or Fig. 4.6(a), while for small a_2 one obtains figures like Fig. 4.8. In addition, we observe from Figs. 4.5(a), 4.6(a) that the *magnitude of the anisotropy parameter a_1 associated with the core material* is also crucial in determining which of these two more novel types of bifurcation occurs. These two figures correspond to *the same values of a_2 , β , and f , but different values of a_1* (and again, necessarily different values of ω). The above statement follows from the fact that the point at which the curve (4.6.8) bifurcates from the trivial solution, i.e., at $p_0 / \mu_1 = p_{cr} / \mu_1$, is *solely* dependent upon the value of a_1 (see (4.6.11)₂ as well as the last paragraph of Section 4.4). Thus, the magnitude of a_1 determines whether $p_{cr} < p_{t1}$ or $p_{cr} > p_{t1}$, which in turn implies whether we have a figure like Fig. 4.5(a) or Fig. 4.6(a), respectively. Finally, we observe that for a composite sphere corresponding to a diagram like that of Fig. 4.1, so that $a_1 < a_0 \approx 0.257$, the changes in character of the bifurcations are not as drastic as those associated with Fig. 4.2 since variations in the magnitude of a_1 are limited.

4.7. Stress distribution

We conclude this chapter with a discussion of the stress distribution in the composite anisotropic sphere. Recall that at the beginning of Section 4.3, we saw that the stresses corresponding to the trivial solution (4.3.1) were given as

$$T_{rr} = T_{\theta\theta} = T_{\phi\phi} = p_0 . \quad (4.7.1)$$

Thus, prior to cavitation, we have simply the constant stress distribution (4.7.1). Subsequent to cavitation ($c > 0$), (4.3.14), (4.3.8), and the considerations of Appendix A

give the radial stress as

$$T_{rr}(R) = \int_{(1 + c^3/R^3)^{1/3}}^{\infty} (v^3 - 1)^{-1} \hat{W}_1 \left(v; \frac{c}{(v^3 - 1)^{1/3}} \right) dv, \text{ on } 0 \leq R \leq B, \quad (4.7.2)$$

where we recall the notation (4.3.16), (4.3.17). On using (4.4.2), we may write (4.7.2) for the composite anisotropic sphere as

$$T_{rr}(R) = \begin{cases} \int_{(1 + c^3/R^3)^{1/3}}^{\infty} (v^3 - 1)^{-1} \hat{W}_1^1(v) dv, & \text{on } 0 \leq R \leq A, \\ p_0 (1 + c^3/B^3)^{-2/3} + \int_{(1 + c^3/R^3)^{1/3}}^{(1 + c^3/B^3)^{1/3}} (v^3 - 1)^{-1} \hat{W}_1^2(v) dv, & \text{on } A \leq R \leq B. \end{cases} \quad (4.7.3)$$

Now, from (4.2.16), (4.2.17), (4.3.3), we can write the hoop stresses as

$$T_{\theta\theta}(R) = T_{\phi\phi}(R) = 2 \left[(v^2 - v^{-4}) W_1 \Big|_R - (v^{-2} - v^4) W_2 \Big|_R - v^{-4} W_5 \Big|_R \right] + T_{rr}(R), \quad (4.7.4)$$

where $T_{rr}(R)$ is given by (4.7.2) or (4.7.3), and we recall the notation (4.3.9). From (4.7.3), (4.7.4) and our assumptions on the smoothness properties of W , we see that T_{rr} is a continuous function of R on $0 \leq R \leq B$, with a discontinuity in slope at the interface $R = A$, while $T_{\theta\theta}(R) = T_{\phi\phi}(R)$ suffers a jump discontinuity at the interface. The stress distributions (4.7.3), (4.7.4) are given explicitly (see (4.7.12), (4.7.13) below) for the material model (4.6.1) and are illustrated in Figures 4.9 and 4.10. Further discussion of these figures will be carried out below.

Another interesting feature of the stresses immediately after cavitation is the presence of a boundary layer near the cavity wall in the case of smooth cavitation. To see this, we observe that for fixed R , $0 < R \leq B$, letting $c \rightarrow 0+$ formally in (4.7.3) results in the right-hand side of (4.4.3), so that

$$\lim_{c \rightarrow 0^+} T_{rr}(R) = p_{cr}, \quad 0 < R \leq B. \quad (4.7.5)$$

Since $T_{rr}(0) = 0$, (4.7.5) shows that, when smooth cavitation takes place (so that the cavity radius increases continuously from zero in a neighborhood of p_{cr}), the radial stress suffers a rapid growth near the cavity wall for applied dead loads p_0 slightly larger than p_{cr} . This boundary layer behavior is shown in Figure 4.11 for a particular case of the material model (4.6.1). From (4.7.4), it is clear that a similar boundary layer exists in the stress components $T_{\theta\theta}(R)$, $T_{\phi\phi}(R)$.

We next consider the radial stress at the interface. From (4.7.3), we have

$$T_{rr}(A) = \int_{(1 + c^3/A^3)^{1/3}}^{\infty} (v^3 - 1)^{-1} \hat{W}_1^1(v) dv. \quad (4.7.6)$$

We wish now to determine a sufficient condition on the strain-energy so that the maximum interfacial stress is reached at the point at which cavitation occurs. This will be the case if $T_{rr}(A)$ is monotone decreasing with respect to cavity radius $c > 0$. It is readily verified that

$$\frac{dT_{rr}(A)}{dc} = -\frac{1}{c} (1 + c^3/A^3)^{-2/3} \hat{W}_1^1(v) \Big|_{v(A) = (1 + c^3/A^3)^{1/3}} \quad (4.7.7)$$

so that for $c > 0$, $dT_{rr}(A)/dc < 0$ if and only if

$$\hat{W}_1^1(v) > 0 \quad \text{for all } v > 1. \quad (4.7.8)$$

Now, from (4.7.1), we have prior to cavitation,

$$T_{rr}(A) = p_0, \quad c = 0, \quad (4.7.9)$$

and from (4.7.5), subsequent to cavitation,

$$\lim_{c \rightarrow 0^+} T_{rr}(A) = p_{cr} \equiv \lim_{c \rightarrow 0^+} p_0(c), \quad c > 0. \quad (4.7.10)$$

There are now three possibilities to consider. First, in the case of smooth cavitation, the radial stress at the interface $T_{rr}(A)$ increases linearly with p_0 until $p_0 = p_{cr}$, $T_{rr}(A)$ is continuous at $p_0 = p_{cr}$, and then decreases for $p_0 > p_{cr}$. (See Figure 4.12). Second, for the case of snap cavitation, where a cavity of finite radius $c = c_0 > 0$ appears at a transition load $\tilde{p}_0 < p_{cr}$, (\tilde{p}_0 is analogous to the quantities \tilde{p} or \tilde{p}_1 discussed in Section 4.6 in connection with Figs. 4.4 or 4.6, respectively) equation (4.7.10) is no longer relevant. The interfacial stress $T_{rr}(A)$ increases linearly with p_0 until $p_0 = \tilde{p}_0$, at which point it suffers a jump discontinuity. If condition (4.7.8) holds, it is easily seen that the integrand in (4.7.6) is positive on the range of integration, so that the jump in $T_{rr}(A)$ is negative. Thus upon appearance of a cavity with finite radius, ($c = c_0 > 0$, $p_0 = \tilde{p}_0$), the value of $T_{rr}(A)$ necessarily decreases. (See Figure 4.13). Third, consider the radial stress at the interface for the case in which the sphere undergoes a bifurcation of the type portrayed in Fig. 4.5. Here $T_{rr}(A)$ increases linearly with p_0 until $p_0 = p_{cr}$, $T_{rr}(A)$ is continuous at $p_0 = p_{cr}$, and decreases until p_0 reaches a transition value (greater than p_{cr}) where it again suffers a jump discontinuity. (See Figure 4.14).

As observed in [21], the foregoing considerations have immediate implications relating to the issue of possible debonding at the material interface $R = A$. (We remark that in [21] a figure of the type displayed in Fig. 4.14 did not arise). Suppose that the interface bond is sustained only so long as the normal stress at the interface remains less than a threshold value, T_d , a measure of the strength of the interface bond. Then debonding would occur if

$$T_{rr}(A) = T_d . \quad (4.7.11)$$

Consider again a quasi-static loading process in which p_0 increases slowly from zero. If

$T_d < p_{cr}$ for smooth cavitation ($T_d < \tilde{p}_0$ for snap cavitation) then debonding occurs when $p_0 = T_d$ and cavitation is not relevant. However, if $T_d > p_{cr}$ for smooth cavitation ($T_d > \tilde{p}_0$ for snap cavitation), then when (4.7.8) holds, the resulting stress relief at the interface precludes the criterion (4.7.11) from being met and thus eliminates the possibility of interface debonding.

We conclude this section by returning to the material model (4.6.1). Recalling the notations (4.6.4) and (4.6.7), the stresses (4.7.3), (4.7.4) for a composite sphere composed of such a material can be written as

$$\frac{T_{rr}(R)}{\mu_1} = \begin{cases} 2 \left\{ F\left[z\left(\frac{B}{R}\rho\right)\right] + 2a_1\left(\frac{5\pi}{6\sqrt{3}} - G\left[z\left(\frac{B}{R}\rho\right)\right]\right) \right\}, & 0 \leq R \leq A, \\ 2 \left\{ (1-\beta) F[z(\alpha\rho)] + \beta F\left[z\left(\frac{B}{R}\rho\right)\right] + \frac{5\pi}{3\sqrt{3}} a_1 \right. \\ \left. + 2(a_2\beta - a_1) G[z(\alpha\rho)] - 2a_2\beta G\left[z\left(\frac{B}{R}\rho\right)\right] \right\}, & A \leq R \leq B, \end{cases} \quad (4.7.12)$$

and

$$\frac{T_{\theta\theta}(R)}{\mu_1} = \frac{T_{\phi\phi}(R)}{\mu_1} = \begin{cases} z^2\left(\frac{B}{R}\rho\right) - z^{-4}\left(\frac{B}{R}\rho\right) - 2a_1\left[z^{-8}\left(\frac{B}{R}\rho\right) - z^{-4}\left(\frac{B}{R}\rho\right)\right] + \frac{T_{rr}(R)}{\mu_1}, & 0 \leq R < A, \\ \beta\left[z^2\left(\frac{B}{R}\rho\right) - z^{-4}\left(\frac{B}{R}\rho\right)\right] - 2a_2\beta\left[z^{-8}\left(\frac{B}{R}\rho\right) - z^{-4}\left(\frac{B}{R}\rho\right)\right] \\ + \frac{T_{rr}(R)}{\mu_1}, & A < R \leq B. \end{cases} \quad (4.7.13)$$

These stresses are shown in Figures 4.9 and 4.10 for parameter values corresponding to the bifurcation diagrams Figs. 4.4 and 4.6, respectively. In Fig. 4.9, these stresses are plotted for a case with $\beta < 1$ ($\mu_2 < \mu_1$). When $\beta > 1$ ($\mu_2 > \mu_1$), the jump in $T_{\theta\theta} = T_{\phi\phi}$ at the material interface $R = A$ is in the opposite direction to that in Fig. 4.9, while the

slope discontinuity in T_{rr} has opposite character. In Fig. 4.10, we have $\beta = 1.0$, and the jump discontinuity in $T_{\theta\theta} = T_{\phi\phi}$ nearly vanishes. This dependence of the hoop stress discontinuity on the relative sizes of μ_1, μ_2 , i.e., on the size of β compared to unity, was seen in the hoop stresses corresponding to the composite neo-Hookean sphere discussed in [21]. Thus, the anisotropy considered here has a negligible effect on the jump discontinuity in the hoop stresses at the material interface. This can be seen from (4.7.13) since it is the βz^2 term in the second of (4.7.13) which contributes most significantly to the discontinuity.

Finally, it is easily verified that the condition (4.7.8) holds for the material (4.6.1), so that we *do have* normal stress relaxation at the material interface subsequent to cavitation for all materials of the type (4.6.1). Thus, as seen earlier, regardless of the stability criterion adopted, there are essentially three possible ways in which the composite sphere may deform. First, a smooth cavitation may take place. Second, an immediate snap cavitation at some load *less than* the critical load may occur. Third, a smooth cavitation may initially take place, followed by a "snap" from one finite cavity radius to another at some load *greater than* the critical load. The interfacial normal stress for these three cases are shown in Figures 4.12, 4.13, and 4.14 for spheres with parameter values corresponding to the bifurcation diagrams Figs. 4.3, 4.4, and 4.5, respectively.

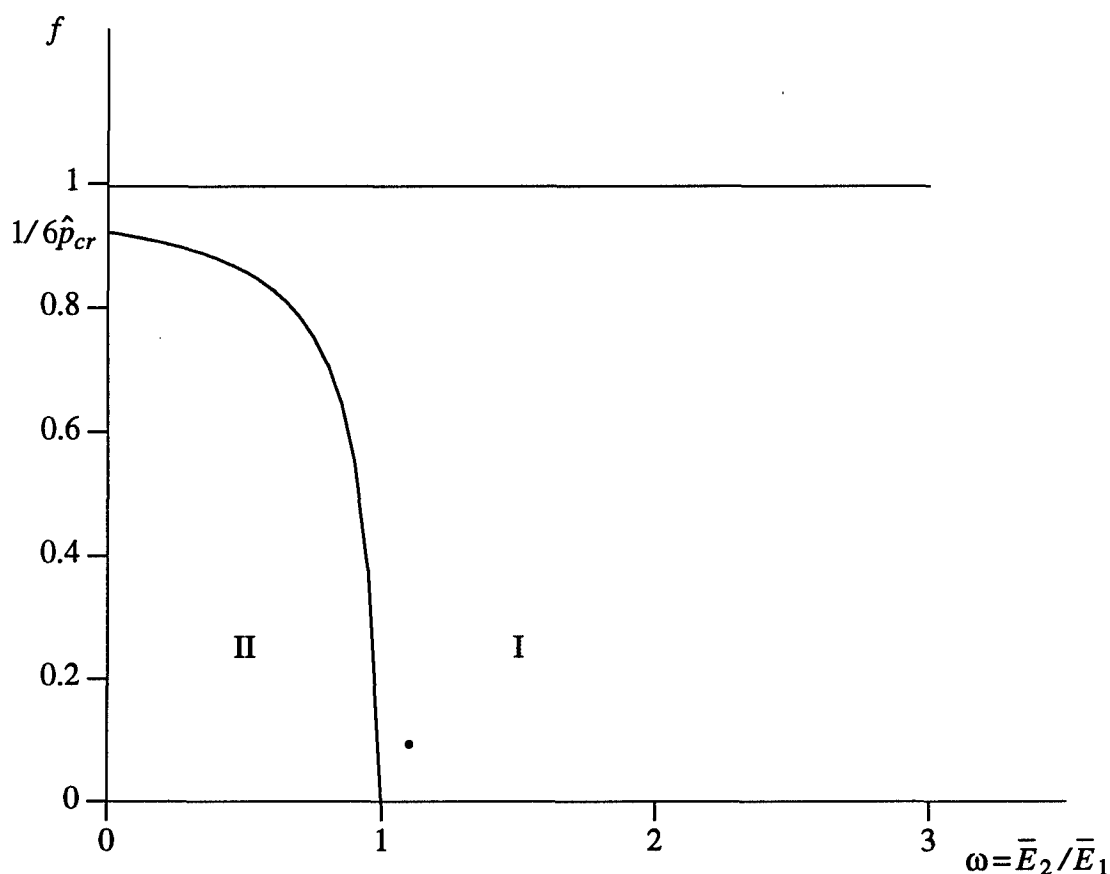


Figure 4.1. Semi-infinite strip $0 < f = \frac{A^3}{B^3} < 1$, $\omega = \frac{d^2 \hat{W}^2(1)/dv^2}{d^2 \hat{W}^1(1)/dv^2} = \frac{\mu_2(3+4a_2)}{\mu_1(3+4a_1)} > 0$.

For parameter pairs (ω, f) in region I, bifurcation occurs to the right, while in region II, bifurcation occurs to the left. For the curve shown, $p_{cr}/\mu_1 = 4(3+4a_1)\hat{p}_{cr}$, $a_1 = 0.157$, $\hat{p}_{cr} = 0.18$. Figure 4.1 corresponds to the case in which bifurcation for the *homogeneous sphere composed of the core material* would be to the right ($\hat{p}_{cr} > 1/6$). The point shown in region I is the parameter pair associated with Fig. 4.3.

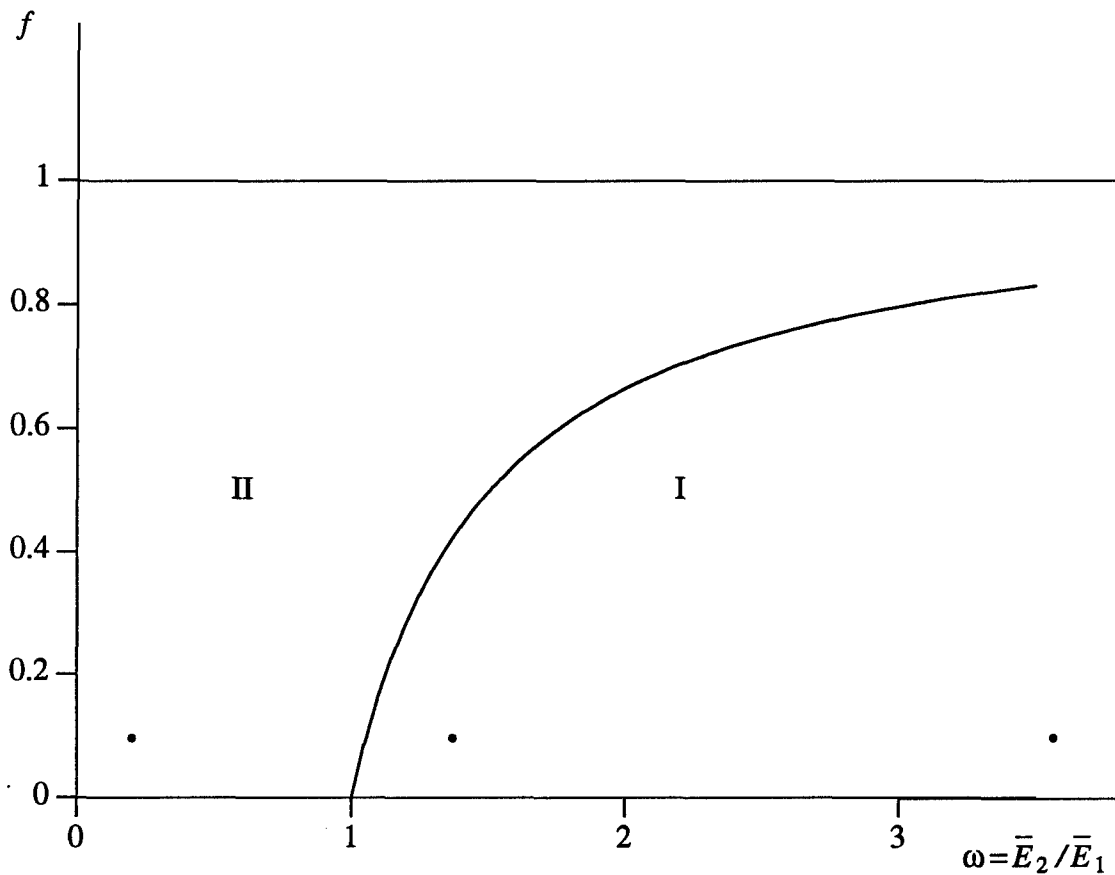


Figure 4.2. Semi-infinite strip $0 < f = \frac{A^3}{B^3} < 1$, $\omega = \frac{d^2 \hat{W}^2(1)/dv^2}{d^2 \hat{W}^1(1)/dv^2} = \frac{\mu_2(3+4a_2)}{\mu_1(3+4a_1)} > 0$.

For parameter pairs (ω, f) in region I, bifurcation occurs to the right, while in region II, bifurcation occurs to the left. Figure 4.2 corresponds to the case in which bifurcation for the *homogeneous sphere composed of the core material would be to the left* ($\hat{p}_{cr} < 1/6$). The point shown in region II is the parameter pair (ω, f) associated with Fig. 4.4, while the points in region I, ordered with increasing ω , are the parameter pairs associated with Figs. 4.6 and 4.5, respectively.

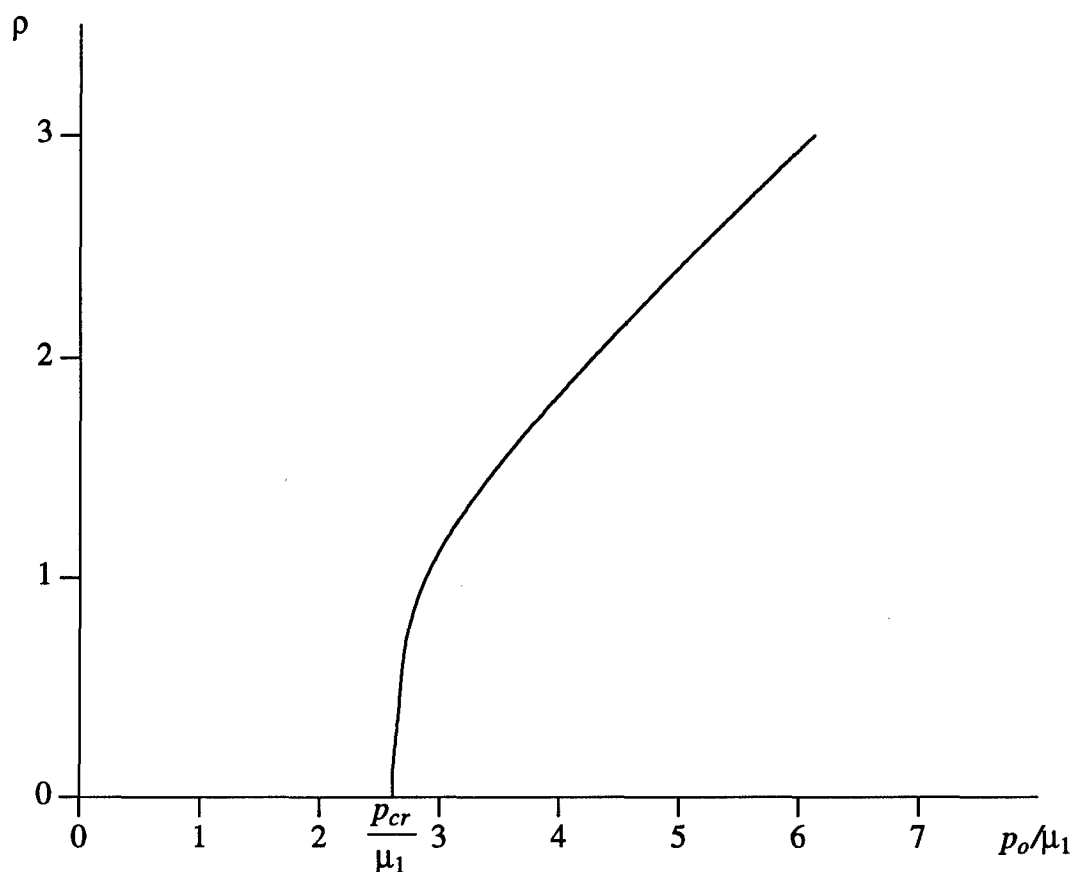


Figure 4.3. Variation of the deformed cavity radius $\rho = c/B$ with applied dead-load traction p_o/μ_1 for the anisotropic composite sphere described by (4.6.1). Here $a_1 = 0.157$, $a_2 = 0.2477$, $\beta = \frac{\mu_2}{\mu_1} = 1.0$, $f = \frac{A^3}{B^3} = \alpha^{-3} = 0.1$, $\omega = \frac{\mu_2(3+4a_2)}{\mu_1(3+4a_1)} = 1.1$. Also $p_{cr}/\mu_1 = 2.61$.

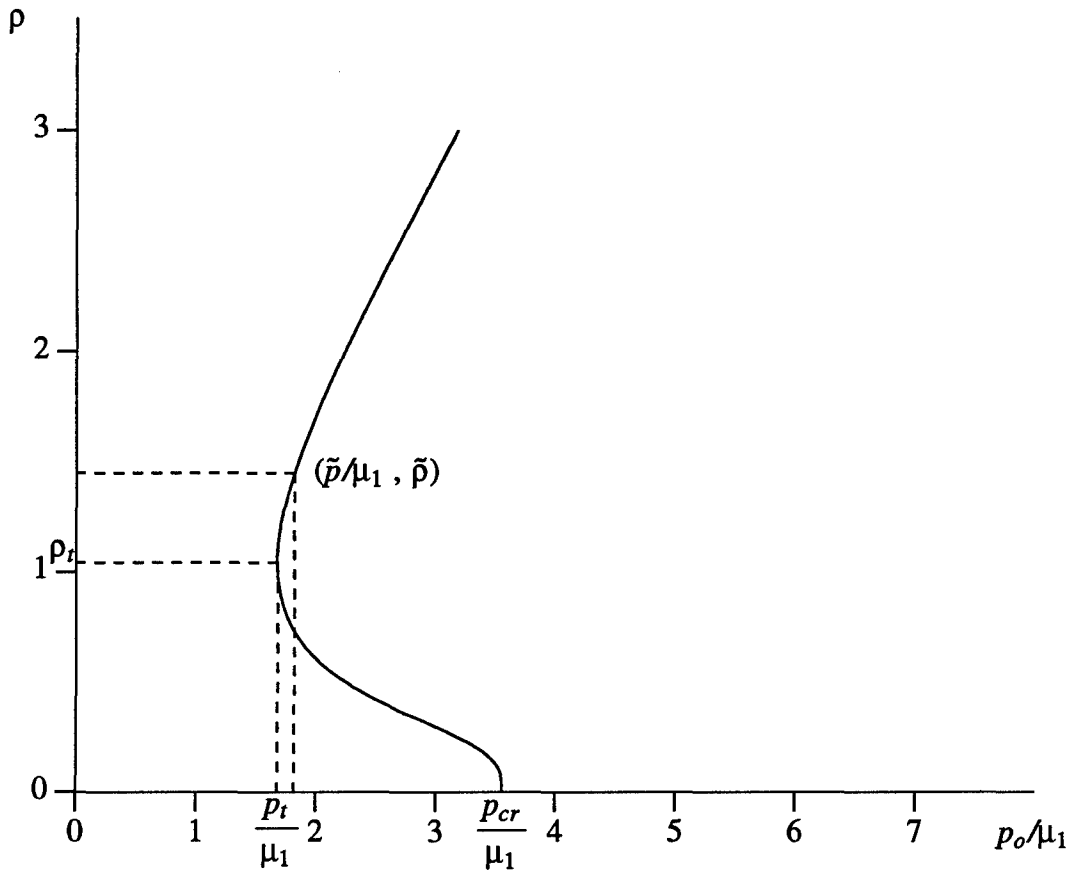


Figure 4.4. Variation of the deformed cavity radius $\rho = c/B$ with applied dead-load traction p_o/μ_1 for the anisotropic composite sphere described by (4.6.1).

Here $a_1 = 1.475$, $a_2 = 3.7$, $\beta = \frac{\mu_2}{\mu_1} = 0.1$, $f = \frac{A^3}{B^3} = \alpha^{-3} = 0.1$, $\omega = \frac{\mu_2(3+4a_2)}{\mu_1(3+4a_1)} = 0.2$.

Also $p_{cr}/\mu_1 = 3.56$, $(p_t/\mu_1, \rho_t) = (1.68, 1.04)$, $(\tilde{p}/\mu_1, \tilde{\rho}) = (1.82, 1.45)$.

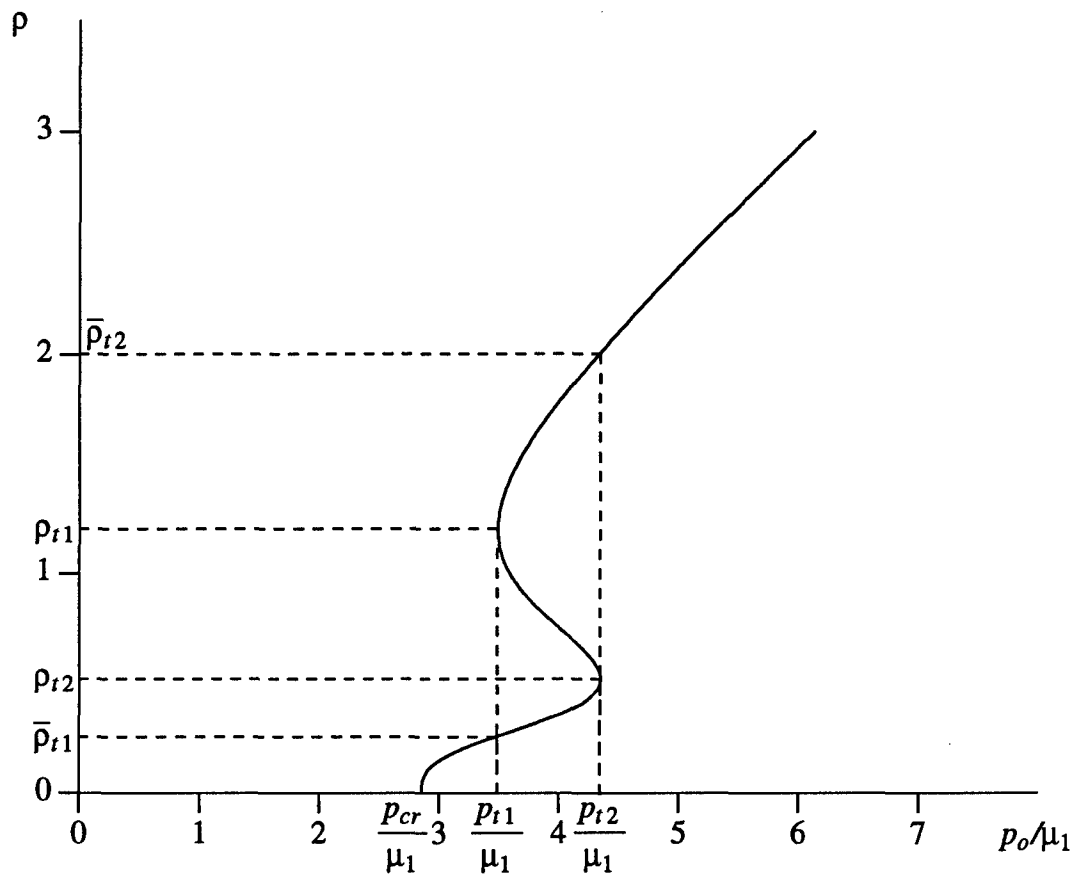


Figure 4.5(a). Variation of the deformed cavity radius $\rho = c/B$ with applied dead-load traction p_o/μ_1 for the anisotropic composite sphere described by (4.6.1).

Here $a_1 = 0.5$, $a_2 = 3.7$, $\beta = \frac{\mu_2}{\mu_1} = 1.0$, $f = \frac{A^3}{B^3} = \alpha^{-3} = 0.1$, $\omega = \frac{\mu_2(3+4a_2)}{\mu_1(3+4a_1)} = 3.56$.

Also $p_{cr}/\mu_1 = 2.86$, $(p_{t1}/\mu_1, \rho_{t1}) = (3.49, 1.21)$, $(p_{t2}/\mu_1, \rho_{t2}) = (4.35, 0.52)$, $\bar{\rho}_{t1} = 0.25$, $\bar{\rho}_{t2} = 2.01$.

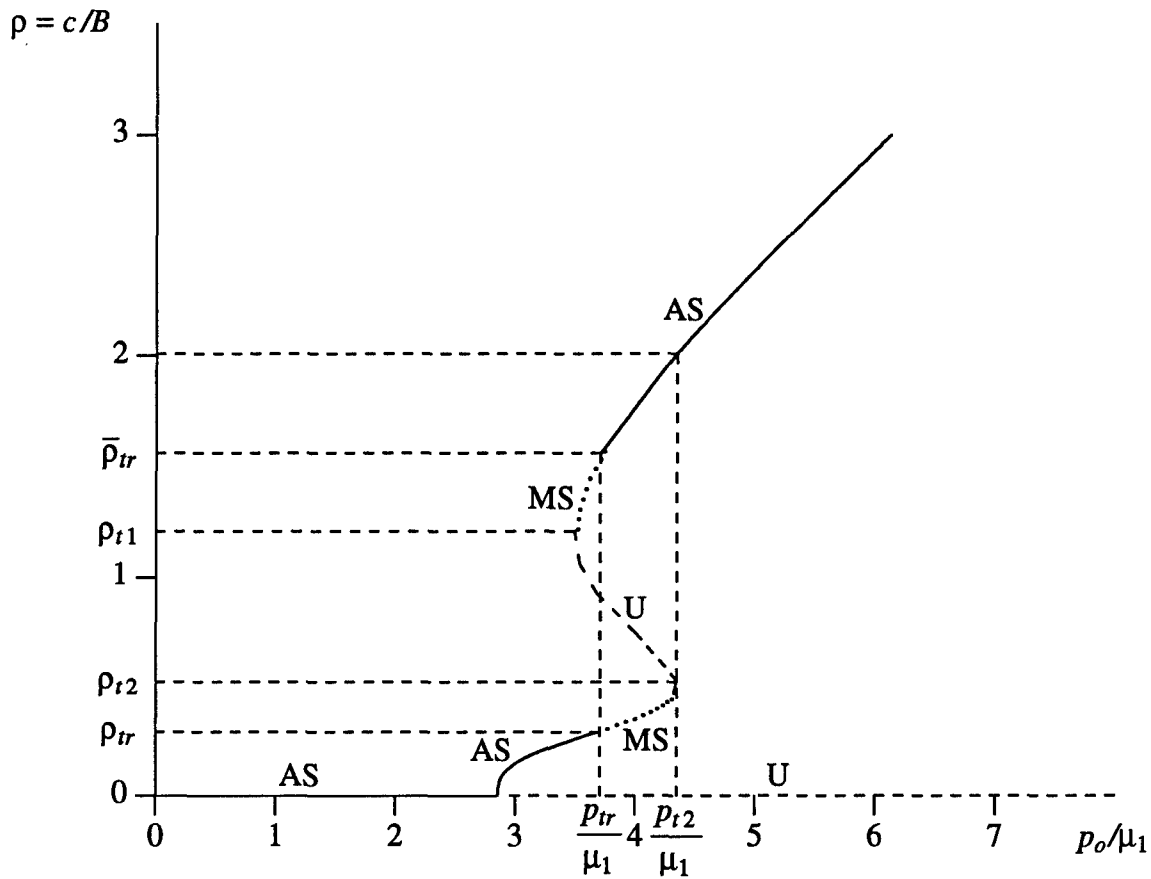


Figure 4.5(b). Stability zones corresponding to bifurcation diagrams of the type displayed in Figure 4.5(a).

Here $a_1 = 0.5$, $a_2 = 3.7$, $\beta = \frac{\mu_2}{\mu_1} = 1.0$, $f = \frac{A^3}{B^3} = \alpha^{-3} = 0.1$, $\omega = \frac{\mu_2(3+4a_2)}{\mu_1(3+4a_1)} = 3.56$.

Also $p_{tr}/\mu_1 = 3.71$, $\rho_{tr} = 0.29$, $\bar{\rho}_{tr} = 1.56$.

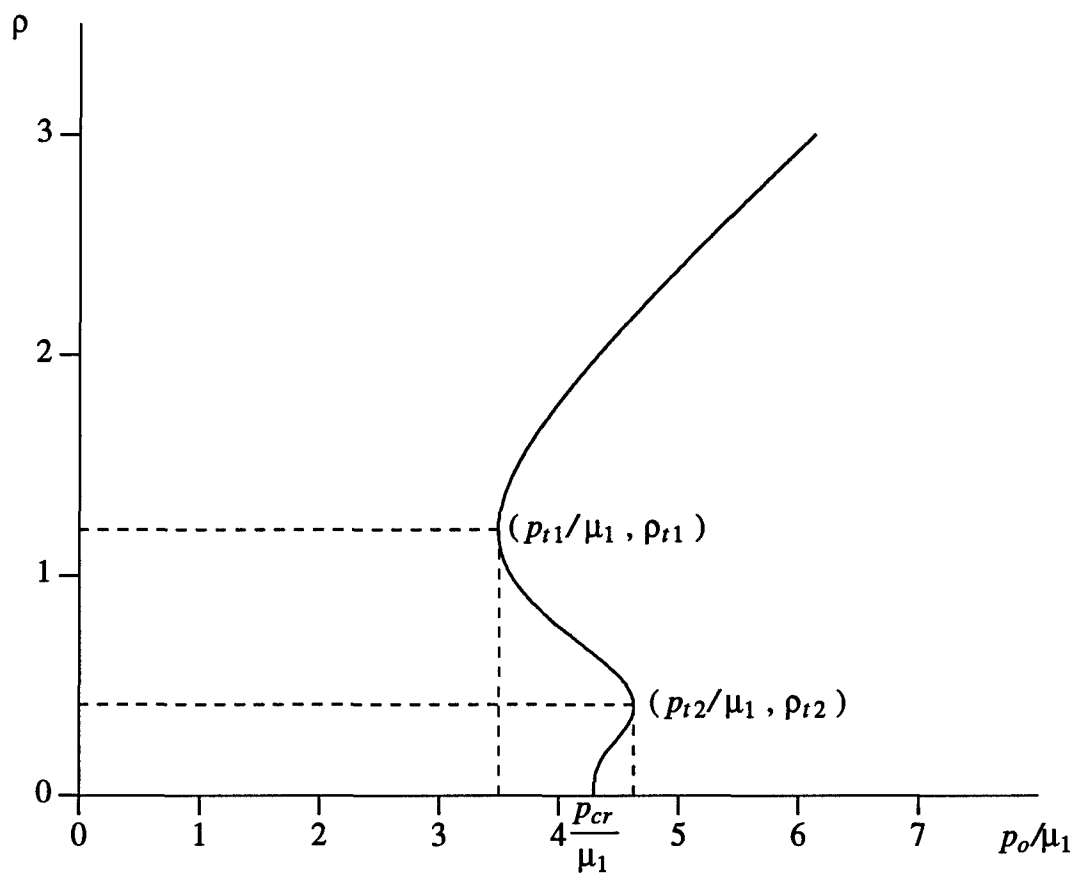


Figure 4.6(a). Variation of the deformed cavity radius $\rho = c/B$ with applied dead-load traction p_o/μ_1 for the anisotropic composite sphere described by (4.6.1).

Here $a_1 = 2.5$, $a_2 = 3.7$, $\beta = \frac{\mu_2}{\mu_1} = 1.0$, $f = \frac{A^3}{B^3} = \alpha^{-3} = 0.1$, $\omega = \frac{\mu_2(3+4a_2)}{\mu_1(3+4a_1)} = 1.37$.
 Also $p_{cr}/\mu_1 = 4.30$, $(p_{t1}/\mu_1, \rho_{t1}) = (3.50, 1.21)$, $(p_{t2}/\mu_1, \rho_{t2}) = (4.63, 0.41)$.

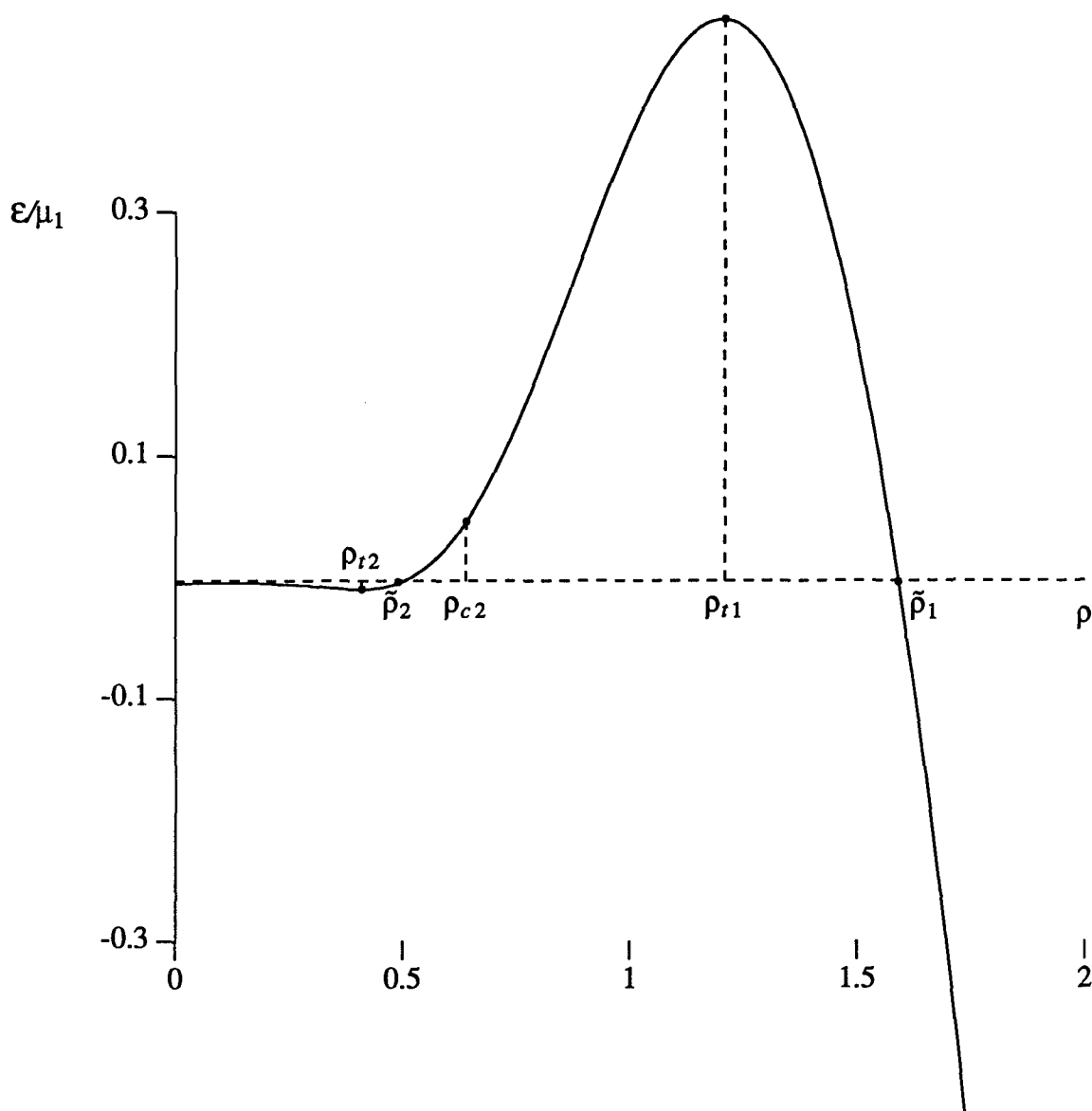


Figure 4.6(c). Energy $\frac{\varepsilon(\rho)}{\mu_1} = \frac{\Phi(\rho)}{\mu_1} + \frac{p_0(\rho)}{\mu_1} \Psi(\rho)$, on the curve (4.6.8) for the parameter values of Figure 4.6(a).

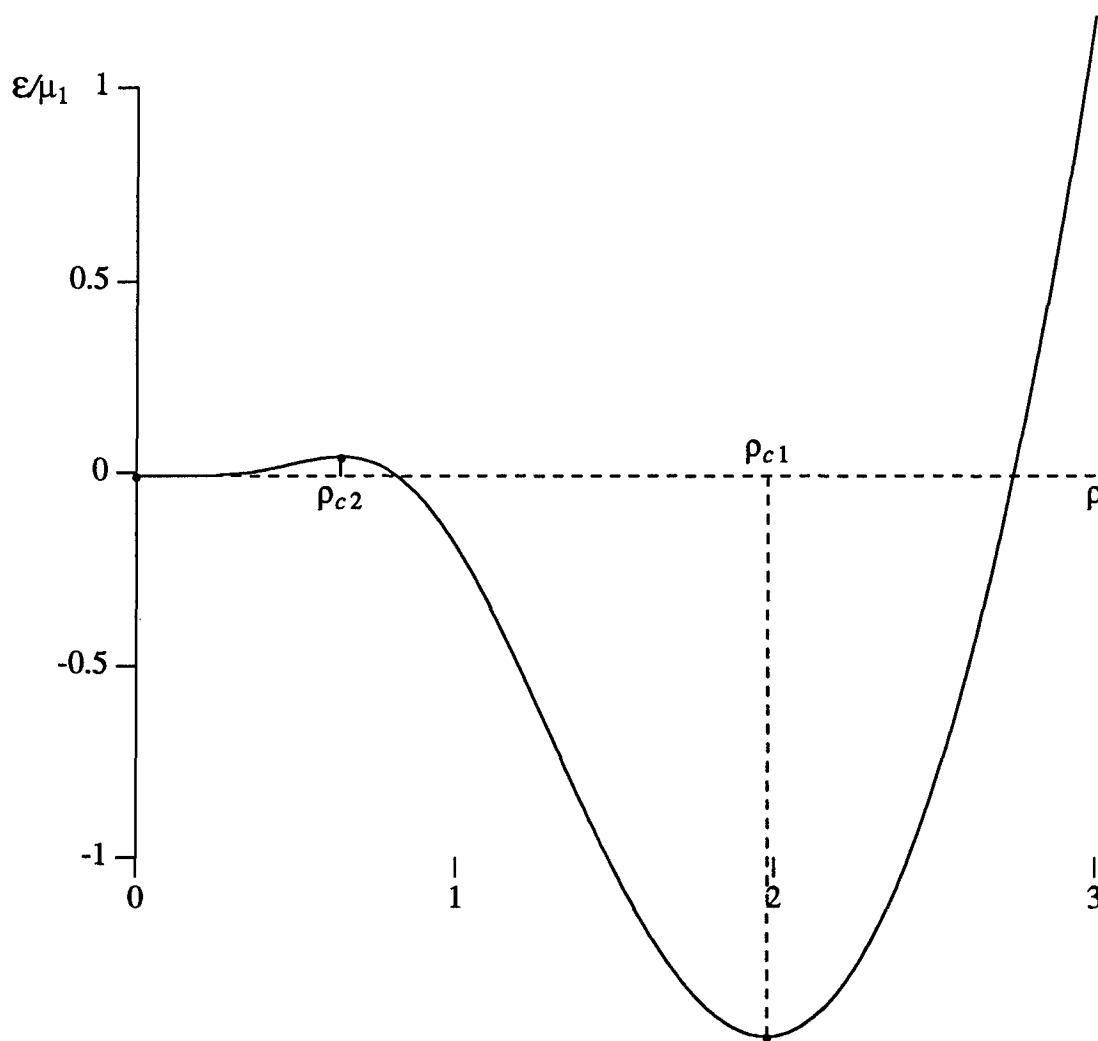


Figure 4.6(d). Energy $\frac{\epsilon(\rho)}{\mu_1} = \frac{\Phi(\rho)}{\mu_1} + \frac{p_0}{\mu_1}\Psi(\rho)$, for $p_0 = p_{cr}$ fixed, corresponding to the case of Figure 4.6(a).

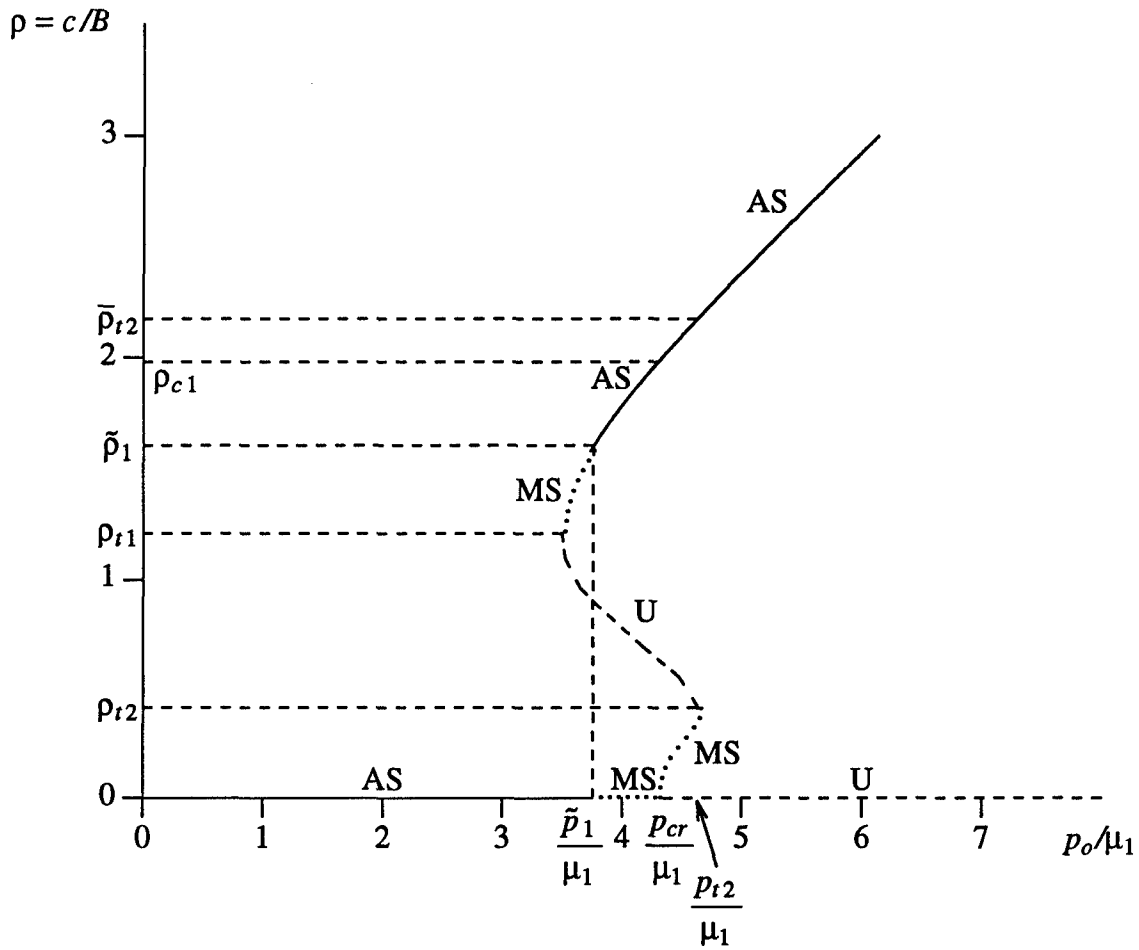


Figure 4.6(e). Stability zones corresponding to bifurcation diagrams of the type displayed in Figure 4.6(a).

Here $a_1 = 2.5$, $a_2 = 3.7$, $\beta = \frac{\mu_2}{\mu_1} = 1.0$, $f = \frac{A^3}{B^3} = \alpha^{-3} = 0.1$, $\omega = \frac{\mu_2(3+4a_2)}{\mu_1(3+4a_1)} = 1.37$.

Also $(\tilde{p}_1/\mu_1, \tilde{\rho}_1) = (3.76, 1.60)$, $(\tilde{p}_2/\mu_1, \tilde{\rho}_2) = (4.58, 0.49)$, $\bar{\rho}_{t2} = 2.18$, $\tilde{\rho}_2'' = 2.15$, $\rho_{c1} = 1.98$, $\tilde{\rho}_1 = 1.60$, $\rho_{c2} = 0.64$, $p_{t2}/\mu_1 = 4.63$.

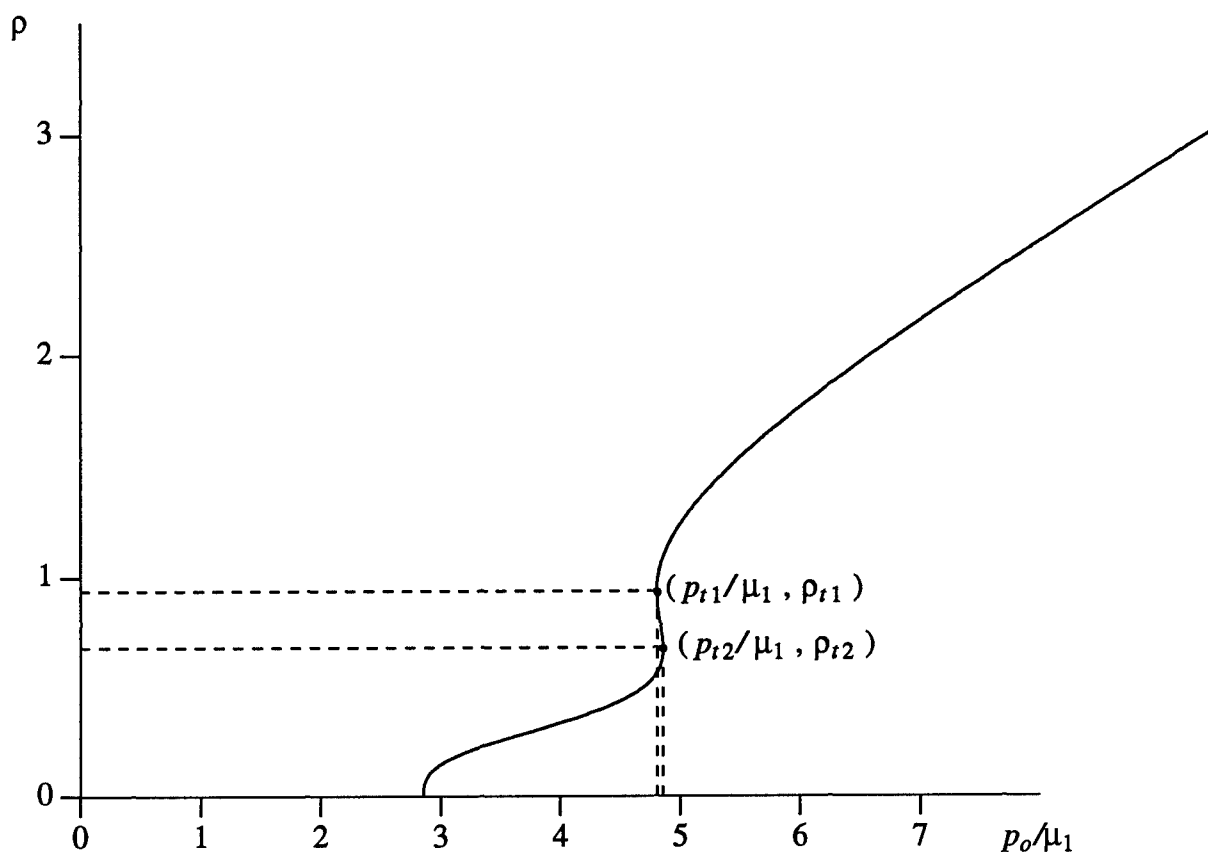


Figure 4.7. Variation of the deformed cavity radius $\rho = c/B$ with applied dead-load traction p_o/μ_1 for the anisotropic composite sphere described by (4.6.1).

Here $a_1 = 0.5$, $a_2 = 1.475$, $\beta = \frac{\mu_2}{\mu_1} = 2.0$, $f = \frac{A^3}{B^3} = \alpha^{-3} = 0.1$, $\omega = \frac{\mu_2(3+4a_2)}{\mu_1(3+4a_1)} = 3.56$.

Also $p_{cr}/\mu_1 = 2.86$, $(p_{t1}/\mu_1, \rho_{t1}) = (4.81, 0.94)$, $(p_{t2}/\mu_1, \rho_{t2}) = (4.86, 0.68)$.

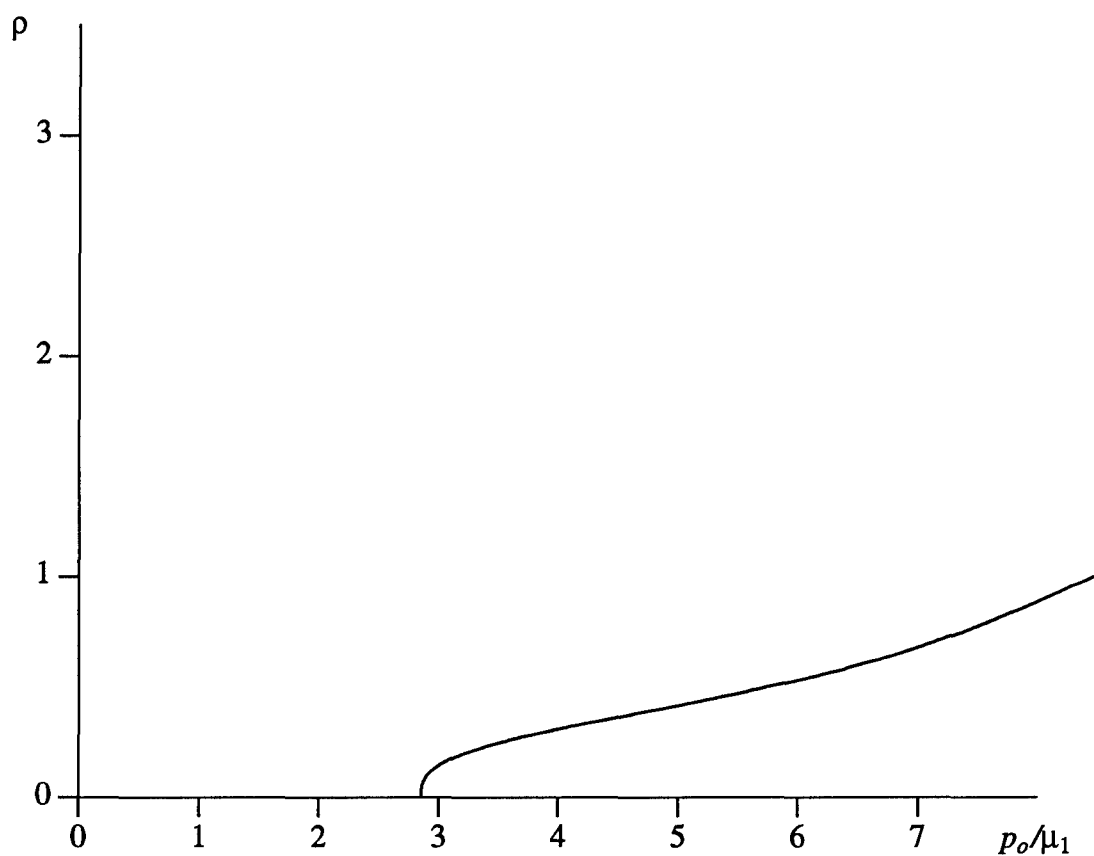


Figure 4.8. Variation of the deformed cavity radius $\rho = c/B$ with applied dead-load traction p_o/μ_1 for the anisotropic composite sphere described by (4.6.1).

Here $a_1 = 0.5$, $a_2 = 0.14$, $\beta = \frac{\mu_2}{\mu_1} = 5.0$, $f = \frac{A^3}{B^3} = \alpha^{-3} = 0.1$, $\omega = \frac{\mu_2(3+4a_2)}{\mu_1(3+4a_1)} = 3.56$.

Also $p_{cr}/\mu_1 = 2.86$.

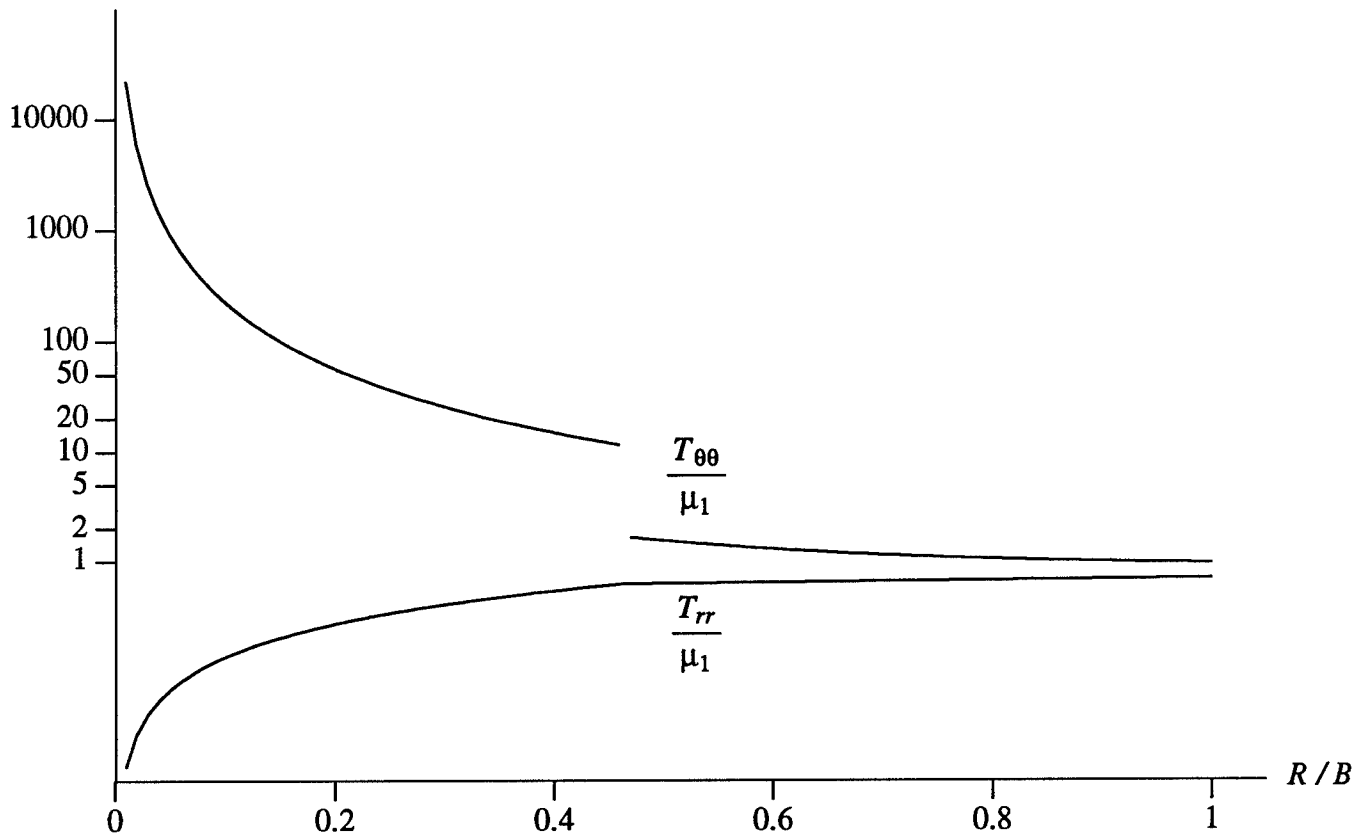


Figure 4.9. Variation of the stresses $T_{rr}(R)$, $T_{\theta\theta}(R) = T_{\phi\phi}(R)$ with undeformed radius R subsequent to cavitation for the anisotropic composite sphere described by (4.6.1). The parameters are those corresponding to Fig. 4.4, i.e., $a_1 = 1.475$, $a_2 = 3.7$, $\beta = 0.1$, $\omega = 0.2$, $f = 0.1$. Also $p_0/\mu_1 = 1.85$, $p_{cr}/\mu_1 = 3.56$. At the material interface, the hoop stresses are discontinuous, and the radial stress is discontinuous in slope.

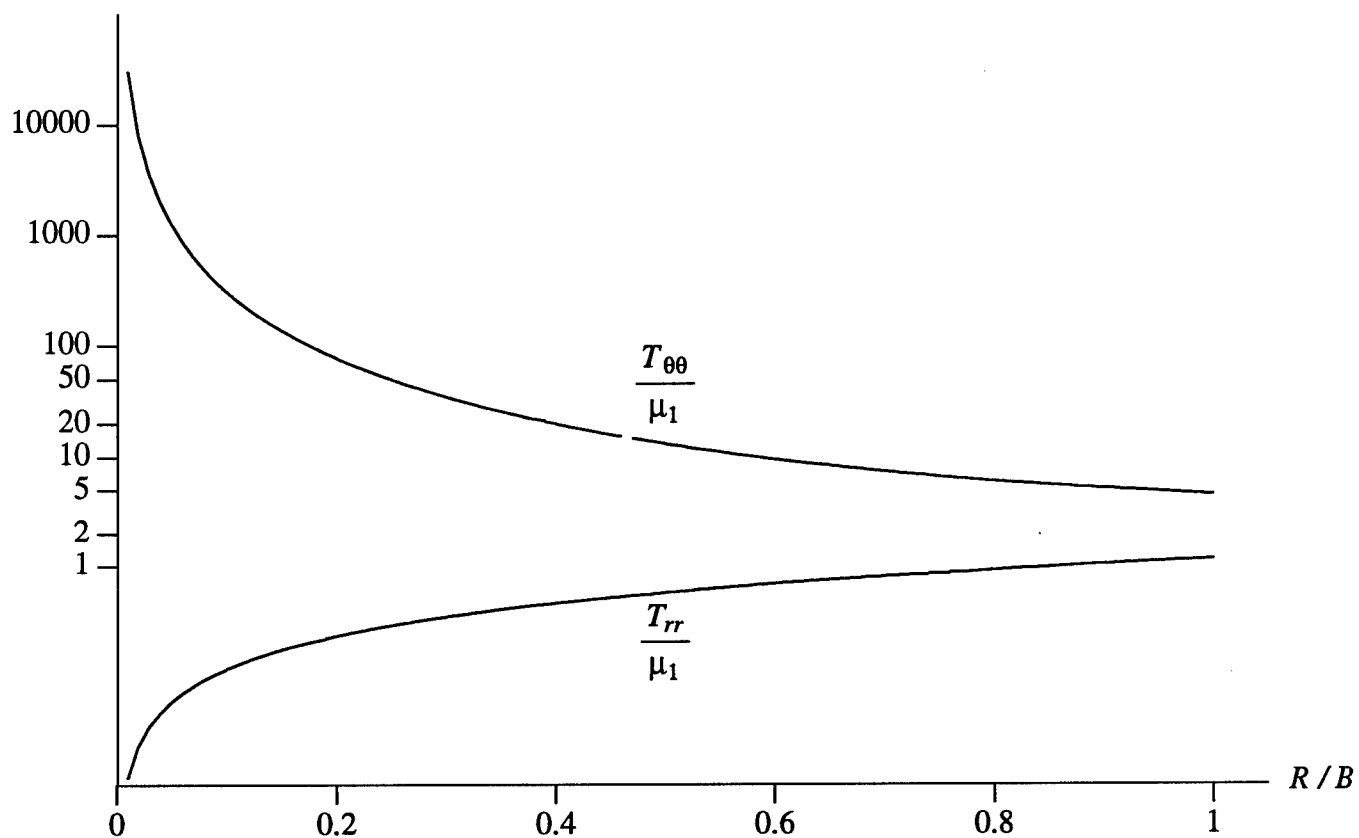


Figure 4.10. Variation of the stresses $T_{rr}(R)$, $T_{\theta\theta}(R) = T_{\phi\phi}(R)$ with undeformed radius R subsequent to cavitation for the anisotropic composite sphere described by (4.6.1). The parameters are those corresponding to Fig. 4.6, i.e., $a_1 = 2.5$, $a_2 = 3.7$, $\beta = 1.0$, $\omega = 1.37$, $f = 0.1$. Also $p_0/\mu_1 = 3.95$, $p_{cr}/\mu_1 = 4.30$.

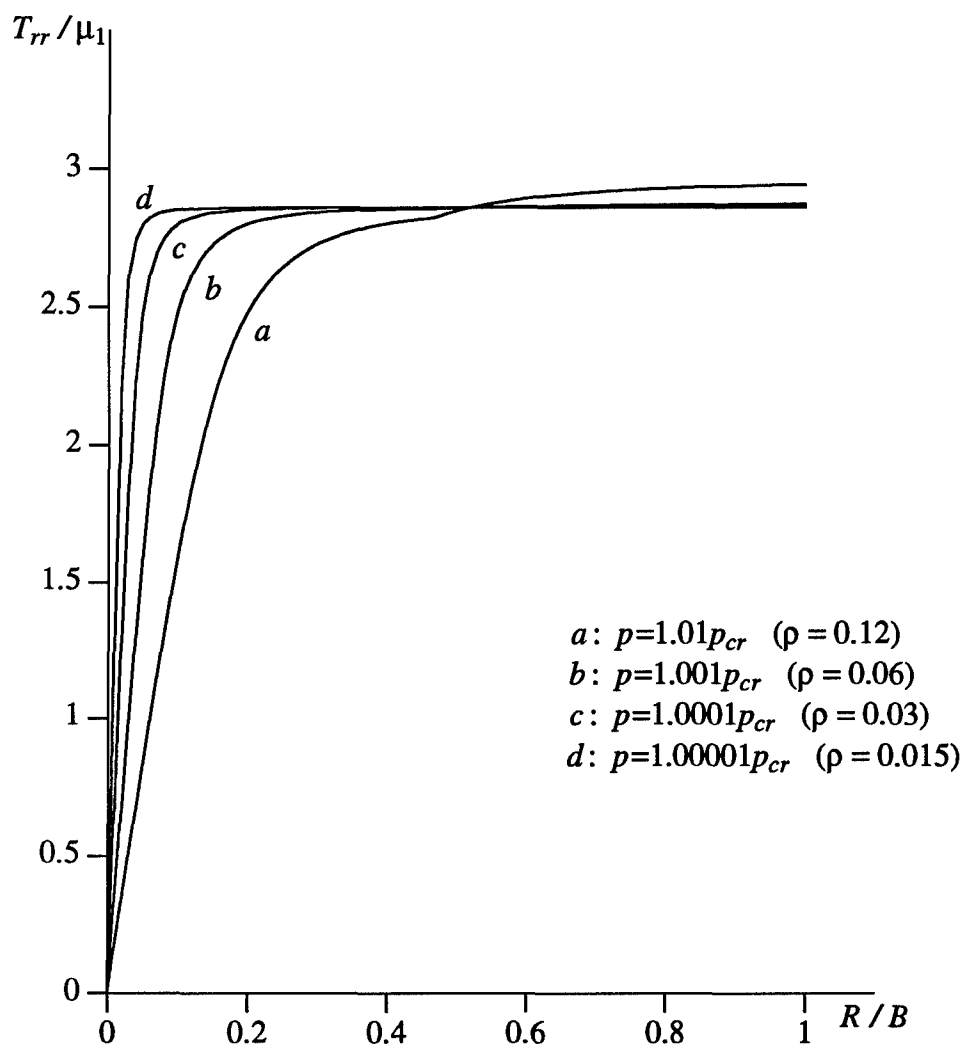


Figure 4.11. Variation of the radial stress $T_{rr}(R)$ with undeformed radius R subsequent to cavitation for the anisotropic composite sphere described by (4.6.1). The parameters are those corresponding to Fig. 4.5, i.e., $a_1 = 0.5$, $a_2 = 3.7$, $\beta = 1.0$, $\omega = 3.56$, $f = 0.1$. Here $p_{cr}/\mu_1 = 2.86$. The radial stress is discontinuous in slope at the material interface.

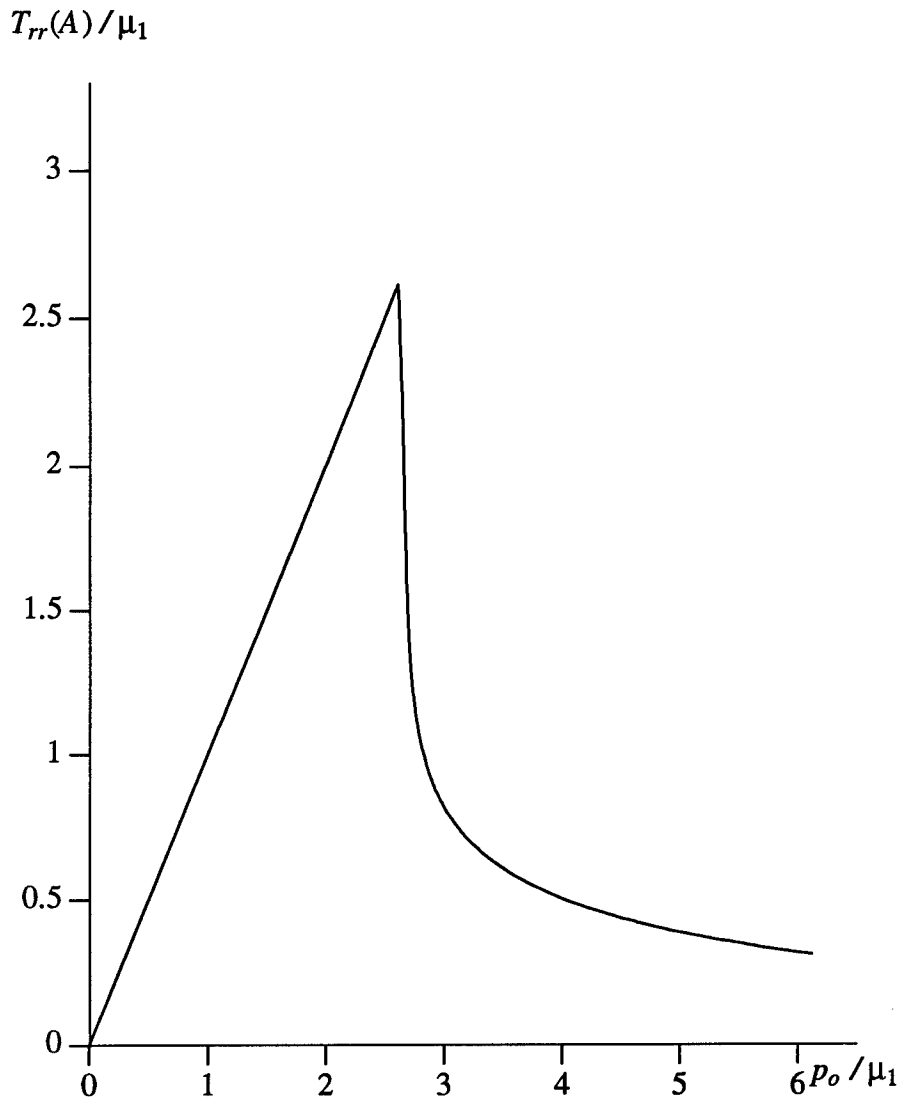


Figure 4.12. Variation of the radial stress at the interface $T_{rr}(A)$ with applied dead load traction p_o/μ_1 for the anisotropic composite sphere described by (4.6.1) with parameters corresponding to Fig. 4.3, i.e., $a_1 = 0.157$, $a_2 = 0.2477$, $\beta = \mu_2/\mu_1 = 1.0$, $\omega = 1.1$, $f = 0.1$. Here $p_{cr}/\mu_1 = 2.61$.

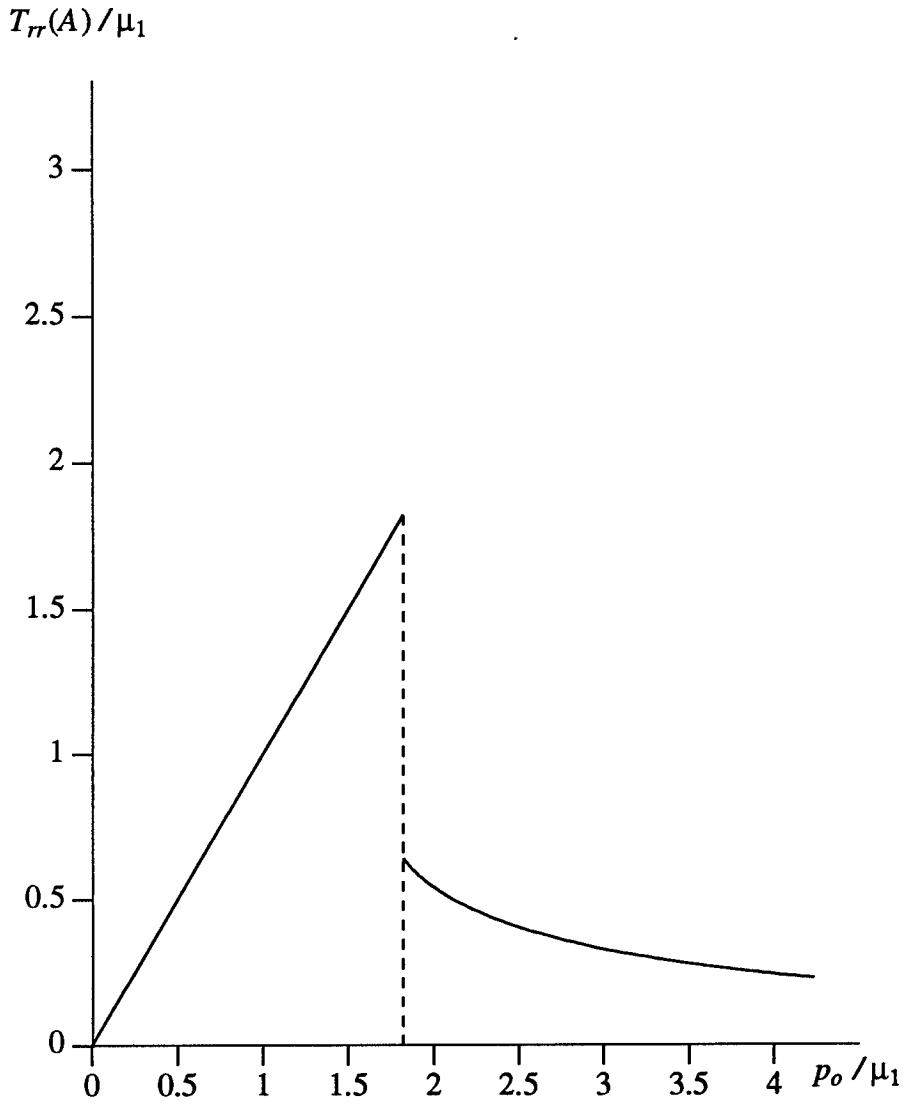


Figure 4.13. Variation of the radial stress at the interface $T_{rr}(A)$ with applied dead load traction p_o/μ_1 for the anisotropic composite sphere described by (4.6.1) with parameters corresponding to Fig.4.4, i.e., $a_1 = 1.475$, $a_2 = 3.7$, $\beta = \mu_2/\mu_1 = 0.1$, $\omega = 0.2$, $f = 0.1$. A jump discontinuity exists at $\frac{\tilde{p}}{\mu_1} = 1.82$. Here $\frac{p_t}{\mu_1} = 1.68$, $\frac{p_{cr}}{\mu_1} = 3.560$.

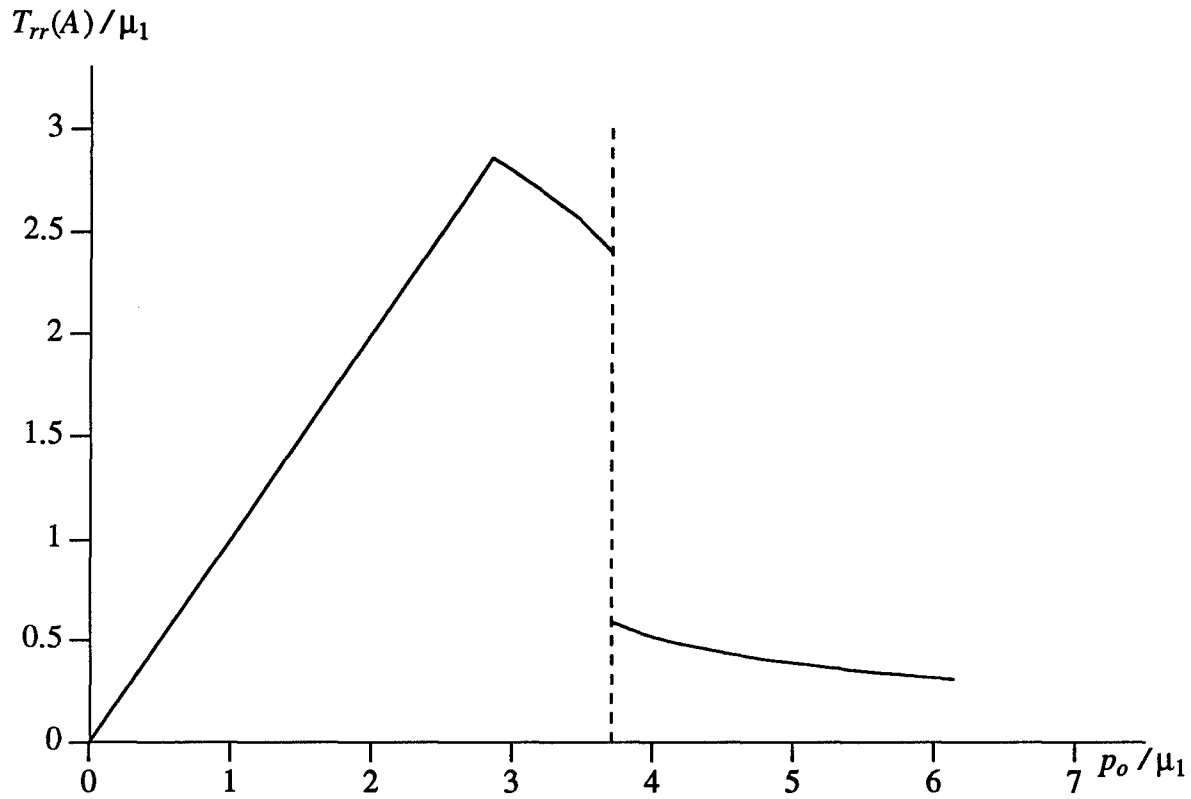


Figure 4.14. Variation of the radial stress at the interface $T_{rr}(A)$ with applied dead load traction p_o / μ_1 for the anisotropic composite sphere described by (4.6.1) with parameters corresponding to Fig. 4.5, i.e., $a_1 = 0.5$, $a_2 = 3.7$, $\beta = 1.0$, $\omega = 3.56$, $f = 0.1$. A jump discontinuity exists at $\frac{p_{tr}}{\mu_1} = 3.71$. Here $\frac{p_{t1}}{\mu_1} = 3.49$, $\frac{p_{t2}}{\mu_1} = 4.35$, $\frac{p_{cr}}{\mu_1} = 2.86$.

Chapter 5

CONCLUSIONS

We now wish to summarize some of the important and interesting results of this dissertation. The type of anisotropy considered here not only gives rise to novel types of behavior for the cavitation problem, but has also proved a worthwhile topic for investigation in its own right. As mentioned earlier, a comprehensive study of constitutive inequalities is carried out in [41] for *compressible* isotropic materials as well as for compressible materials of arbitrary symmetry (see pp. 153-171 of [41]). As no comparable fundamental studies of inequalities have been carried out for *incompressible* materials, the results of Section 2.5 are especially useful in several ways. First, we have determined the relationships between the infinitesimal elastic moduli and the nonlinear stored-energy function, and thereby determined restrictions on the nonlinear incompressible transversely isotropic strain energy density, $W(I_1, I_2, I_3, I_4, I_5)$, consistent with the classical inequalities of the associated linear theory. In addition, the methods of Section 2.5 employed to obtain these results seem to be readily extendable to materials with various symmetries. That is, the techniques of this section ought to be applicable to any material with assumed symmetries for which there correspond linearly elastic moduli with known restrictions, and thus lead to useful physically motivated inequalities on the nonlinear strain energy density. Finally in Section 2.5.3, we propose a nonlinearly elastic transversely isotropic material model and subsequently give all of the restrictions for physically reasonable response which follow from the known constitutive inequalities of the linear theory. As analytic models based on experimental results are limited even in *isotropic* finite elasticity, the need for counterparts based instead on

mathematical considerations is unavoidable, especially for illustrative purposes. In view of this, the class of materials proposed in Section 2.5.3 at least goes beyond a purely mathematical construction to include conditions for physically reasonable response, and thus should be a useful material model in other problems of incompressible transversely isotropic finite hyperelasticity.

Chapters 3 and 4 concentrate on the cavitation problem for incompressible nonlinearly elastic transversely isotropic spheres. As stated in Chapter 1, this work was motivated by two previous investigations ([4], [20]) which found the dramatic material instability of snap cavitation to occur in *compressible homogeneous transversely isotropic* spheres and *incompressible composite isotropic* spheres respectively. In Chapter 3 we were successful in obtaining more explicit results on the effects of *anisotropy* on cavitation, and in particular, on the *snap cavitation* phenomena which we found (as expected) to occur for an *incompressible homogeneous transversely isotropic* sphere. It would be interesting to investigate further the connection between the problem of Chapter 3 and that of [20, 21] as suggested by the concept of homogenization in composite material mechanics.

In Chapter 4, we obtained many interesting results on cavitation instabilities for an incompressible *composite* transversely isotropic sphere. We summarize some of these in what follows:

- (i) If the core material alone would undergo a bifurcation to the $\left\{ \begin{smallmatrix} \text{right} \\ \text{left} \end{smallmatrix} \right\}$, then the composite sphere will also bifurcate to the $\left\{ \begin{smallmatrix} \text{right} \\ \text{left} \end{smallmatrix} \right\}$ provided the surrounding shell is $\left\{ \begin{smallmatrix} \text{stiffer} \\ \text{more compliant} \end{smallmatrix} \right\}$ in tension in the radial direction than the core material.

(ii) If the core material alone would undergo a bifurcation to the $\begin{Bmatrix} \text{right} \\ \text{left} \\ \text{left} \end{Bmatrix}$, then the composite sphere will bifurcate to the $\begin{Bmatrix} \text{left} \\ \text{right} \\ \text{left} \end{Bmatrix}$ provided there is a sufficiently $\begin{Bmatrix} \text{small} \\ \text{small} \\ \text{large} \end{Bmatrix}$ core surrounded by a shell which is $\begin{Bmatrix} \text{more compliant} \\ \text{stiffer} \\ \text{stiffer} \end{Bmatrix}$ in tension in the radial direction than the core material.

(iii) If the core material alone would undergo a bifurcation to the right, the composite sphere will also bifurcate to the right provided the volume fraction of the core to the total volume exceeds $1/6\hat{p}_{cr}$.

In Chapter 4, we also derived an alternative formula for the critical load at which bifurcation from the trivial solution occurs (equation (4.5.21)) involving the stored-energy function itself rather than its derivative. This formula aided in obtaining the energy and stability results for cavitation at the end of Section 4.5 for *general* transversely isotropic composite spheres, and has the additional benefit of providing a way to calculate the critical load if, for example, the derivative of the strain energy involved in the original formula is not readily obtainable. While equation (4.5.21) results from a simple application of the integration by parts formula and the growth assumption (4.5.20), the author has been unable to find such a relationship documented in any of the previous work on cavitation given in the references. We note that (4.5.21) is clearly valid for all combinations of homogeneous or composite, isotropic or transversely isotropic incompressible materials with the appropriate interpretation for the strain energy function appearing in it.

The illustrative example of Section 4.6 provided several new descriptions of how cavitation in a composite sphere may progress in a quasi-static loading process. In particular, we found *three* possible way for the sphere to deform when a bifurcation to the right occurs, *two* of which involve material instabilities associated with a jumping phenomenon similar to the snap cavitation phenomenon originally found in [4] and [20] (recall Figures 4.5 and 4.6 and the discussions regarding them). We were also successful in determining more explicit information on how the anisotropy considered in this dissertation results in the four possible types of bifurcation found here (recall the discussion at the end of Section 4.6). Finally in Section 4.7, we were able to obtain a (general) condition on the strain energy function guaranteeing stress relaxation at the material interface after cavitation, and thus relate this to the possibility for cavitation to prevent debonding of the composite at the interface.

We wish now to comment on the effects of surface energy on cavitation, since void formation is obviously accompanied by creation of additional surface. Fracture initiation due to a hydrostatic tensile stress field was analyzed in [45] using an energy minimization approach involving *three* energy quantities: the potential energy of the external tensile stress, the strain energy, *and* the surface energy. The problem addressed in [45] was to consider the large strain and instability analysis for a small spherical cavity of initial radius a_c located in an isotropic incompressible elastic medium (a neo-Hookean sphere) and subjected to a hydrostatic tensile stress, p , at some large initial outer radius b_0 , such that $b_0 \gg a_c$. (Gent and Lindley [14] first studied the above problem by calculating the stress at infinity needed to expand a finite cavity in an infinite expanse of material indefinitely. As remarked by Ball [5], this problem is equivalent to the cavitation problem because "an infinitesimal hole in a finite piece of material behaves

like a finite hole in an infinite expanse of material." The underlying reason for this is that the equilibrium equation and boundary condition are invariant under the transformation $(\mathbf{X}, \mathbf{x}) \rightarrow (c\mathbf{X}, c\mathbf{x})^1$. It is then shown in [45] (see eqn. (31)) that

$$\frac{p_c}{E} = \frac{5}{6} \left[1 - \sqrt{\frac{16E}{75\sigma_\theta}} \right], \quad (5.1)$$

where p_c is the critical load needed to expand the cavity indefinitely, E is Young's modulus, and σ_θ is the hoop stress corresponding to the neo-Hookean sphere. As is well known in cavitation problems however, the hoop stress at the cavity wall becomes infinite (see e.g. [21], or see Sections 3.7, 4.7 and Figures 3.6, 4.10 of this dissertation). (Note that infinite stresses do not present a difficulty within the framework of nonlinear elasticity.) We therefore recover the formula for the critical load for the neo-Hookean material from (5.1) on letting $\sigma_\theta \rightarrow \infty$, i.e.,

$$p_c = \frac{5}{6} E. \quad (5.2)$$

Thus the critical load (5.2) is exactly that found from an analysis which does not incorporate surface energy effects. That is, since $E = 3\mu$ for incompressible materials, the critical load (5.2) for the neo-Hookean material can also be represented as $p_c = \frac{5}{2} \mu$, which agrees with equation (3.5.21) when $a \equiv 0$. As reported by Gent in [13], it is also interesting to note that experiments on rubbery solids seem to indicate good correlation between the predicted (5.2) and the observed critical load for the types of materials tested.

¹[5, p.607]

In conclusion, we indicate some additional areas of future research related to the considerations of this thesis. Most studies of cavitation within elasticity theory, including this one, have examined this problem in the context of spherically symmetric solutions. Recently however, several authors have obtained interesting results concerning cavitation in isotropic elasticity when the type of material instability is not restricted to radially symmetric void formation (see e.g. [3], [26]). It would therefore be of great interest to further pursue the goals of Chapters 3 and 4 of this dissertation to determine the effects of anisotropy on cavitation by relaxing the assumption of radially symmetric solutions. Another worthwhile generalization would involve the further study of cavitation in compressible anisotropic nonlinear elasticity following the early work of [4]. Finally, the considerations of Chapter 2 and the consequences found for the cavitation problem arising from anisotropy, suggest that investigations of the effects of anisotropy for other problems of nonlinear elasticity may yield many novel phenomena and exciting new results in the field of finite hyperelasticity.

Appendix A: Verification of (3.3.15)

To establish (3.3.15), we rewrite (3.3.12) as

$$p_0 = \left[1 + \frac{c^3}{B^3} \right]^{\frac{2}{3} B} \int_0^B -4 \left[(v^{-7}(s) - v^{-1}(s)) W_1 |_s + (v^{-5}(s) - v(s)) W_2 |_s + v^{-7}(s) W_5 |_s \right] \frac{ds}{s} \quad (A1)$$

where we recall the notation (3.3.8). From (3.3.3), we have

$$v^3(s) - 1 = \frac{c^3}{s^3} \quad (A2)$$

so that

$$3v^2 \frac{dv}{ds} = \frac{-3c^3}{s^4}.$$

Then

$$v^2 dv = -\frac{c^3}{s^3} \frac{ds}{s},$$

and on using (A2) we obtain

$$\frac{ds}{s} = \frac{v^2}{1 - v^3} dv. \quad (A3)$$

Also, recalling the notation (3.3.13), (3.3.14), the chain rule gives

$$\hat{W}_1(v) = (-4v^{-5} + 4v) W_1 |_R + (4v^3 - 4v^{-3}) W_2 |_R - 4v^{-5} W_5 |_R. \quad (A4)$$

Thus, substituting (A3) into (A1) and comparing with (A4), we see that the integrand in (A1) is $\hat{W}_1(v)/(1 - v^3)$ which, on changing the limits of integration according to (A2), establishes the result (3.3.15) as desired.

Appendix B: Verification of (3.5.30)

Let

$$\rho^3 = \varepsilon^{-1}, \quad 0 < \varepsilon \ll 1, \quad (\text{B1})$$

so that $\varepsilon \rightarrow 0$ implies $\rho^3 \rightarrow \infty$, and rewrite (3.5.23) as

$$\begin{aligned} P = 2(1 + \varepsilon^{-1})^{2/3} & \left\{ (1 + \varepsilon^{-1})^{-1/3} + \frac{1}{4} (1 + \varepsilon^{-1})^{-4/3} \right. \\ & + 2a \left\{ \frac{5\pi}{6\sqrt{3}} - (1 + \varepsilon^{-1})^{-1/3} + \frac{1}{2} (1 + \varepsilon^{-1})^{-2/3} - \frac{1}{4} (1 + \varepsilon^{-1})^{-4/3} + \frac{1}{5} (1 + \varepsilon^{-1})^{-5/3} + \frac{1}{8} (1 + \varepsilon^{-1})^{-8/3} \right. \\ & \left. \left. - \frac{1}{\sqrt{3}} \left[\arctan \left[\frac{2(1 + \varepsilon^{-1})^{1/3} + 1}{\sqrt{3}} \right] + \arctan \left[\frac{\sqrt{3} (1 + \varepsilon^{-1})^{1/3}}{2 + (1 + \varepsilon^{-1})^{1/3}} \right] \right] \right\} \right\}. \quad (\text{B2}) \end{aligned}$$

Substituting

$$(1 + \varepsilon^{-1})^m = \left(\frac{\varepsilon + 1}{\varepsilon} \right)^m = \varepsilon^{-m} (1 + \varepsilon)^m = \varepsilon^{-m} (1 + m\varepsilon + O(\varepsilon^2)) \quad (\text{B3})$$

into (B2) where appropriate and taking the limit as $\varepsilon \rightarrow 0$ gives to leading order,

$$\begin{aligned} \lim_{\varepsilon \rightarrow 0} P &= \lim_{\varepsilon \rightarrow 0} 2\varepsilon^{-2/3} \left\{ \varepsilon^{1/3} + \frac{1}{4} \varepsilon^{4/3} + 2a \left[\frac{5\pi}{6\sqrt{3}} - \varepsilon^{1/3} + \frac{1}{2} \varepsilon^{2/3} - \frac{1}{4} \varepsilon^{4/3} + \frac{1}{5} \varepsilon^{5/3} + \frac{1}{8} \varepsilon^{8/3} \right. \right. \\ & \quad \left. \left. - \frac{1}{\sqrt{3}} \left[\arctan \frac{2\varepsilon^{-1/3} + 1}{\sqrt{3}} + \arctan \frac{\sqrt{3} \varepsilon^{-1/3}}{2 + \varepsilon^{-1/3}} \right] \right] \right\} \quad (\text{B4}) \\ &= \lim_{\varepsilon \rightarrow 0} 2 \left\{ \varepsilon^{-1/3} + 2a \left[\frac{5\pi}{6\sqrt{3}} \varepsilon^{-2/3} - \varepsilon^{-1/3} + \frac{1}{2} - \frac{1}{\sqrt{3}} \left[\arctan \frac{2\varepsilon^{-1/3} + 1}{\sqrt{3}} + \arctan \frac{\sqrt{3} \varepsilon^{-1/3}}{2 + \varepsilon^{-1/3}} \right] \right] \right\} \end{aligned}$$

$$= \lim_{\epsilon \rightarrow 0} \left\{ 2\epsilon^{-1/3} + 4a \left[\frac{\frac{5\pi}{6\sqrt{3}} - \epsilon^{1/3} - \frac{1}{\sqrt{3}} \left[\arctan \frac{2\epsilon^{-1/3} + 1}{\sqrt{3}} + \arctan \frac{\sqrt{3} \epsilon^{-1/3}}{2 + \epsilon^{-1/3}} \right]}{\epsilon^{2/3}} \right] \right\} + 2a. \quad (\text{B5})$$

Now let

$$\delta = \epsilon^{1/3} \text{ so that } \delta = \frac{1}{\rho}. \quad (\text{B6})$$

Then $\delta \rightarrow 0$ implies $\rho \rightarrow \infty$, and (B5) becomes

$$\begin{aligned} \lim_{\delta \rightarrow 0} P &= \lim_{\delta \rightarrow 0} 2\delta^{-1} \\ &+ \lim_{\delta \rightarrow 0} 4a \left[\frac{\frac{5\pi}{6\sqrt{3}} - \delta - \frac{1}{\sqrt{3}} \left[\arctan \frac{2\delta^{-1} + 1}{\sqrt{3}} + \arctan \frac{\sqrt{3} \delta^{-1}}{2 + \delta^{-1}} \right]}{\delta^2} \right] + 2a. \quad (\text{B7}) \end{aligned}$$

Using L'Hopital's rule, the second term on the right in (B7), after some manipulation, becomes

$$4a \lim_{\delta \rightarrow 0} \frac{1}{2} \left[\frac{\delta^{-2}}{\delta^{-2} + \delta^{-1} + 1} - 1 \right] \delta^{-1},$$

or

$$-2a \lim_{\delta \rightarrow 0} \left[\frac{\delta^{-2} + \delta^{-1}}{\delta^{-2} + \delta^{-1} + 1} \right]. \quad (\text{B8})$$

Now using (B6)₂, the above expression becomes

$$-2a \lim_{\rho \rightarrow \infty} \left[\frac{\rho^2 + \rho}{\rho^2 + \rho + 1} \right] = -2a. \quad (\text{B9})$$

Therefore, on using (B6)₂ and substituting (B9) into the second term on the right in (B7), we obtain

$$\lim_{\rho \rightarrow \infty} P(\rho) = \lim_{\rho \rightarrow \infty} 2\rho - 2a + 2a = \lim_{\rho \rightarrow \infty} 2\rho, \quad (\text{B10})$$

and thus the desired result (3.5.30), i.e.,

$$P \sim 2\rho \text{ as } \rho \rightarrow \infty. \quad (\text{B11})$$

Appendix C: Verification of (3.5.16), (3.5.19), and (3.6.6)-(3.6.8)

Here we present the details of the derivation of equations (3.5.16), (3.5.19), and (3.6.6) - (3.6.8). We consider the indefinite integrals which are needed to evaluate the definite integrals (3.5.14), (3.5.18), and (3.6.4). (Constants of integration will be ignored.)

(i) *Evaluation of (3.5.14):*

As in [6], we write

$$\begin{aligned} \int \frac{v - v^{-5}}{v^3 - 1} dv &= \int \frac{v^6 - 1}{v^5(v^3 - 1)} dv \\ &= \int \frac{v^3 + 1}{v^5} dv = \int (v^{-2} + v^{-5}) dv \\ &= -v^{-1} - \frac{1}{4} v^{-4}. \end{aligned} \quad (C1)$$

On using (C1), the definite integral in (3.5.14) is immediately evaluated to yield the desired expression (3.5.16).

(ii) *Evaluation of (3.5.18):*

First, we record here the indefinite integrals (2.128, 1.) from the integral tables of Gradshteyn and Ryzhik, 1990:

$$\int \frac{dv}{v^n z_3^m} = -\frac{1}{(n-1)a v^{n-1} z_3^{m-1}} - \frac{b(3m+n-4)}{a(n-1)} \int \frac{dv}{v^{n-3} z_3^m}, \quad (C2)$$

where $z_3 = a + bv^3$, $a \neq 0$, $n \neq 1$, $b, m > 0$ are constants. Now the integral of concern in (3.5.18) can be written as

$$I \equiv \int \frac{v^{-5} - v^{-9}}{v^3 - 1} dv = \int \frac{dv}{v^5 (v^3 - 1)} - \int \frac{dv}{v^9 (v^3 - 1)} = I_1 - I_2. \quad (C3)$$

To evaluate I_2 , we use (C2) with $n = 9$, $m = 1$, $b = 1$, $a = -1$ to get

$$I_2 = \frac{1}{8v^8} + \int \frac{dv}{v^6 (v^3 - 1)}. \quad (C4)$$

The integral in (C4) is evaluated as in [5] by using (C2) with $n = 6$, $m = 1$, $b = 1$, $a = -1$ to get

$$\int \frac{dv}{v^6 (v^3 - 1)} = \frac{1}{5v^5} + \int \frac{dv}{v^3 (v^3 - 1)}. \quad (C5)$$

Reapplying (C2) with $n = 3$, $m = 1$, $b = 1$, $a = -1$ to the integral in (C5), we obtain

$$\int \frac{dv}{v^3 (v^3 - 1)} = \frac{1}{2v^2} + \int \frac{dv}{v^3 - 1}, \quad (C6)$$

and this last integral can be evaluated using standard integral tables. For example, from (2.126, 1.) of Gradshteyn and Ryzhik we obtain

$$\int \frac{dv}{v^3 - 1} = -\frac{1}{3} \ln \frac{(1 + v + v^2)^{1/2}}{v - 1} - \frac{1}{\sqrt{3}} \arctan \frac{\sqrt{3} v}{2 + v}. \quad (C7)$$

Then on using (C4), (C5), (C6), (C7), we have

$$I_2 = \frac{1}{8v^8} + \frac{1}{5v^5} + \frac{1}{2v^2} - \frac{1}{6} \ln \frac{(1 + v + v^2)}{(v - 1)^2} - \frac{1}{\sqrt{3}} \arctan \frac{\sqrt{3} v}{2 + v}. \quad (C8)$$

To evaluate I_1 , we use (C2) with $n = 5$, $m = 1$, $b = 1$, $a = -1$ to get

$$I_1 = \frac{1}{4v^4} + \int \frac{dv}{v^2 (v^3 - 1)}, \quad (C9)$$

and reapply (C2) with $n = 2$, $m = 1$, $b = 1$, $a = -1$ to the integral in (C9) to obtain

$$\int \frac{dv}{v^2(v^3-1)} = \frac{1}{v} + \int \frac{v dv}{v^3-1}. \quad (C10)$$

This last integral is given by (2.126, 2.) of Gradshteyn and Ryzhik to be

$$\int \frac{v dv}{v^3-1} = \frac{1}{6} \ln \frac{(v-1)^2}{v^2+v+1} + \frac{1}{\sqrt{3}} \arctan \frac{2v+1}{\sqrt{3}}. \quad (C11)$$

Then on using (C9), (C10), (C11), we have

$$I_1 = \frac{1}{4v^4} + \frac{1}{v} + \frac{1}{6} \ln \frac{(v-1)^2}{v^2+v+1} - \frac{1}{\sqrt{3}} \arctan \frac{2v+1}{\sqrt{3}}. \quad (C12)$$

Substituting (C12), (C8) into (C3) and noting that $\ln \frac{(v-1)^2}{v^2+v+1} = -\ln \frac{(v^2+v+1)}{(v-1)^2}$, we obtain

$$I = \frac{1}{4v^4} + \frac{1}{v} + \frac{1}{\sqrt{3}} \arctan \frac{2v+1}{\sqrt{3}} - \frac{1}{8v^8} - \frac{1}{5v^5} - \frac{1}{2v^2} + \frac{1}{\sqrt{3}} \arctan \frac{\sqrt{3}v}{2+v}. \quad (C13)$$

On using (C13) and l'Hopital's rule where appropriate, the definite integral in (3.5.18) is immediately evaluated to yield the desired expression (3.5.19).

(iii) *Evaluation of (3.6.4):*

We consider the integral in (3.6.4) as

$$I_3 \equiv \int \frac{v^{-2} + 2v^4 - 3v^2}{(v^3-1)^2} dv + a \int \frac{v^{-6} - 2v^{-2} + v^2}{(v^3-1)^2} dv = I_4 + a I_5. \quad (C14)$$

Then

$$I_4 = \int \frac{v^{-2} + 2v^4 - 3v^2}{(v^3-1)^2} dv = \frac{2v^3 - v - 1}{(1-v^3)v}, \quad (C15)$$

as given by equation (3.3) of [20]. To evaluate I_5 , we consider

$$I_5 = \int \frac{dv}{v^6(v^3-1)^2} - 2 \int \frac{dv}{v^2(v^3-1)^2} + \int \frac{v^2 dv}{(v^3-1)^2} = I_6 - 2I_7 + I_8. \quad (C16)$$

Then I_8 can be directly integrated to yield

$$I_8 = \frac{-1}{3(v^3-1)}, \quad (C17)$$

and I_7 is given by (2.131, 2.) of Gradshteyn and Ryzhik as

$$I_7 = \int \frac{dv}{v^2(v^3-1)^2} = \left[\frac{1}{v} - \frac{4}{3} v^2 \right] \frac{1}{v^3-1} - \frac{4}{3} \int \frac{v dv}{v^3-1}, \quad (C18)$$

where this last integral in (C18) was evaluated earlier in (C11). Finally, (2.128, 2.) of Gradshteyn and Ryzhik gives I_6 as

$$I_6 = \int \frac{dv}{v^6(v^3-1)^2} = \frac{-1}{3v^5(v^3-1)} - \frac{8}{3} \int \frac{dv}{v^6(v^3-1)}, \quad (C19)$$

where this last integral in (C19) was evaluated earlier by (C5) - (C7). Combining (C14) - (C19), (C11), and (C5) - (C7), we obtain

$$\begin{aligned} I_3 = \frac{2v^3 - v - 1}{(1-v^3)v} + a \left\{ \frac{-1}{3v^5(v^3-1)} - \frac{8}{3} \left[\frac{1}{5v^5} + \frac{1}{2v^2} \right. \right. \\ \left. \left. - \frac{1}{3} \ln \frac{(1+v+v^2)^{1/2}}{v-1} - \frac{1}{\sqrt{3}} \arctan \frac{\sqrt{3}v}{2+v} \right] - \frac{2}{v^3-1} \left[\frac{1}{v} - \frac{4}{3} v^2 \right] \right. \\ \left. + \frac{8}{3} \left[\frac{1}{6} \ln \frac{(v-1)^2}{v^2+v+1} + \frac{1}{\sqrt{3}} \arctan \frac{2v+1}{\sqrt{3}} \right] - \frac{1}{3(v^3-1)} \right\}. \end{aligned} \quad (C20)$$

On observing that the logarithm terms in (C20) cancel identically, and on using (C20) and l'Hopital's rule where appropriate, the definite integral in (3.6.4) is immediately evaluated. The desired expressions (3.6.6) - (3.6.8) can then be obtained by utilizing the definitions (3.5.22) and (3.6.5).

Appendix D: Verification of (4.5.9)

Here we present the details of the derivation of (4.5.9). Recall from (4.5.6) and (4.4.11)₄ that

$$\Sigma(\rho) = \frac{\Phi(\rho)}{d^2 \hat{W}^1(1) / dv^2} + \hat{p} \Psi(\rho) \quad , \quad \rho \geq 0 \quad , \quad (D1)$$

where $\Phi(\rho)$, $\Psi(\rho)$ are given by (4.5.7), (4.5.8), respectively. From (4.5.8), it is easily seen on taking derivatives that

$$\dot{\Psi}(0+) = \ddot{\Psi}(0+) = 0 \quad , \quad \ddot{\Psi}(0+) = -6 \quad . \quad (D2)$$

We thus confine attention to the evaluation of $\dot{\Phi}$, $\ddot{\Phi}$, $\ddot{\ddot{\Phi}}$ as $\rho \rightarrow 0+$ to establish the desired results.

(i) *Verification of $\dot{\Sigma}(0+) = 0$:*

By the chain-rule, we have $\dot{\Phi}(\rho) = 3\rho^2 d\Phi/d\rho^3$, where $d\Phi/d\rho^3$ is given by (4.5.17), so that

$$\dot{\Phi}(0+) = \lim_{\rho \rightarrow 0+} 3\rho^2 d\Phi/d\rho^3 = 0 \quad , \quad (D3)$$

where we have used (4.5.22) in the final step in (D3). From (D1) we have

$$\dot{\Sigma}(\rho) = \frac{\dot{\Phi}(\rho)}{d^2 \hat{W}^1(1) / dv^2} + \hat{p} \dot{\Psi}(\rho) \quad , \quad (D4)$$

so that upon evaluation of (D4) as $\rho \rightarrow 0+$ and substitution from (D2)₁, (D3), we have the desired result (4.5.9)₁, i.e.,

$$\dot{\Sigma}(0+) = 0 \quad . \quad (D5)$$

(ii) *Verification of $\ddot{\Sigma}(0+) = 0$:*

By the chain-rule, we have

$$\ddot{\Phi}(\rho) = 6\rho \frac{d\Phi}{d\rho^3} + 9\rho^4 \frac{d^2\Phi}{d(\rho^3)^2}, \quad (D6)$$

where again the first derivative on the right is given by (4.5.17), and the second by (4.5.23). Substituting (4.5.23) into (D6) and taking the limit as $\rho \rightarrow 0+$ gives

$$\begin{aligned} \ddot{\Phi}(0+) &= \lim_{\rho \rightarrow 0+} 6\rho \frac{d\Phi}{d\rho^3} \\ &+ \lim_{\rho \rightarrow 0+} 3\rho \left[\frac{\hat{W}_1^2((1 + \alpha^3 \rho^3)^{1/3}) - \hat{W}_1^1((1 + \alpha^3 \rho^3)^{1/3})}{(1 + \alpha^3 \rho^3)^{2/3}} - \frac{\hat{W}_1^2((1 + \rho^3)^{1/3})}{(1 + \rho^3)^{2/3}} \right], \end{aligned} \quad (D7)$$

where we note from an argument analogous to that used in (D3) that the first term on the right in (D7) is zero, while (3.4.2)₁, i.e., $\hat{W}_1^i(1) = 0$, ($i = 1, 2$), gives that the second term in (D7) is also zero. Thus,

$$\ddot{\Phi}(0+) = 0. \quad (D8)$$

From (D4) we have

$$\ddot{\Sigma}(\rho) = \frac{\ddot{\Phi}(\rho)}{d^2 \hat{W}_1^1(1) / dv^2} + \hat{p} \ddot{\Psi}(\rho), \quad (D9)$$

so that upon evaluation of (D9) as $\rho \rightarrow 0+$ and substitution from (D2)₂, (D8), we have the desired result (4.5.9)₂, i.e.,

$$\ddot{\Sigma}(0+) = 0. \quad (D10)$$

(iii) *Verification of $\ddot{\Sigma}(0+) = 6(\hat{p}_{cr} - \hat{p})$:*

By the chain-rule, it can be shown that

$$\ddot{\Phi}(\rho) = 6 \frac{d\Phi}{d\rho^3} + 54\rho^3 \frac{d^2\Phi}{d(\rho^3)^2} + 27\rho^6 \frac{d^3\Phi}{d(\rho^3)^3}. \quad (D11)$$

From (4.5.22), we know that the limit as $\rho \rightarrow 0+$ of the first term on the right in (D11) is $6p_{cr}$, so that the desired result will follow from showing that the last two terms in (D11) are zero as $\rho \rightarrow 0+$. We first address the second term on the right in (D11). It is easily seen that, on substitution from (4.5.23) and on using (3.4.2)₁, we have

$$\lim_{\rho \rightarrow 0+} 54\rho^3 \frac{d^2\Phi}{d(\rho^3)^2} = 0. \quad (D12)$$

To address the last term in (D11), we first differentiate (4.5.23) to obtain

$$\begin{aligned} \frac{d^3\Phi}{d(\rho^3)^3}(\rho) = \frac{1}{3} & \left\{ \frac{\frac{1}{3}\alpha^3\rho^3 [d^2\hat{W}^2/dv^2 - d^2\hat{W}^1/dv^2] ((1 + \alpha^3\rho^3)^{1/3})}{\rho^6(1 + \alpha^3\rho^3)^{\frac{4}{3}}} \right. \\ & - \frac{\left[\frac{2}{3}\alpha^3\rho^3(1 + \alpha^3\rho^3)^{-1/3} + (1 + \alpha^3\rho^3)^{2/3} \right] [\hat{W}_1^2 - \hat{W}_1^1] ((1 + \alpha^3\rho^3)^{1/3})}{\rho^6(1 + \alpha^3\rho^3)^{\frac{4}{3}}} \quad (D13) \\ & \left. - \frac{\frac{1}{3}\rho^3 \frac{d^2\hat{W}^2}{dv^2} ((1 + \rho^3)^{1/3}) + \left[\frac{2}{3}\rho^3(1 + \rho^3)^{-1/3} + (1 + \rho^3)^{2/3} \right] \hat{W}_1^2 ((1 + \rho^3)^{1/3})}{\rho^6(1 + \rho^3)^{\frac{4}{3}}} \right\}, \end{aligned}$$

where, in (D13) we have introduced the notation

$$[f - g](x) \equiv f(x) - g(x). \quad (D14)$$

Since the quantities $d^2\hat{W}^i(1)/dv^2$, ($i = 1, 2$), are finite from (3.4.2)₂ and $\hat{W}_1^i(1) = 0$ from (3.4.2)₁, substitution from (D13) into the last term in (D11) and taking the limit as $\rho \rightarrow 0+$ results in

$$\lim_{\rho \rightarrow 0+} 27\rho^6 \frac{d^3 \Phi}{d(\rho^3)^3} = 0. \quad (D15)$$

Thus, we have shown that the last two terms on the right in (D11) vanish as $\rho \rightarrow 0+$ and so

$$\ddot{\Phi}(0+) = 6p_{cr}. \quad (D16)$$

From (D9) we have

$$\ddot{\Sigma}(\rho) = \frac{\ddot{\Phi}(\rho)}{d^2 \hat{W}^1(1)/dv^2} + \hat{p} \ddot{\Psi}(\rho), \quad (D17)$$

so that upon evaluation of (D17) as $\rho \rightarrow 0+$ and substitution from (D2)₃, (D16), we have (recalling (4.4.11)₃) the desired result (4.5.9)₃, i.e.,

$$\ddot{\Sigma}(0+) = 6(\hat{p}_{cr} - \hat{p}). \quad (D18)$$

REFERENCES

- [1] Abeyaratne, R. and Hou, H.-s. (1989). Growth of an infinitesimal cavity in a rate-dependent solid. *J. Appl. Mech.*, **56**, 40-46.
- [2] Abeyaratne, R. and Hou, H.-s. (1991a). Void collapse in an elastic solid. *J. Elasticity*, **26**, 23-42.
- [3] Abeyaratne, R. and Hou, H.-s. (1991b). On the occurrence of the cavitation instability relative to the asymmetric instability under symmetric dead-load conditions. *Q. J. Mech. Appl. Math.*, **44**, 429-449.
- [4] Antman, S. S. and Negrón-Marrero, P. V. (1987). The remarkable nature of radially symmetric equilibrium states of aeolotropic nonlinearly elastic bodies. *J. Elasticity*, **18**, 131-164.
- [5] Ball, J. M. (1982). Discontinuous equilibrium solutions and cavitation in nonlinear elasticity. *Phil. Trans. R. Soc. Lond., A* **306**, 557-610.
- [6] Chou-Wang, M.-S. and Horgan, C. O. (1989a). Void nucleation and growth for a class of incompressible nonlinearly elastic materials. *Int. J. Solids and Structures*, **25**, 1239-1254.
- [7] Chou-Wang, M.-S. and Horgan, C. O. (1989b). Cavitation in nonlinear elastodynamics for neo-Hookean materials. *Int. J. Engineering Science*, **27**, 967-973.
- [8] Chung, D.-T., Horgan, C. O. and Abeyaratne, R. (1986). The finite deformation of internally pressurized hollow cylinders and spheres for a class of compressible elastic materials. *Int. J. Solids and Structures*, **22**, 1557-1570.
- [9] Chung, D. -T., Horgan, C. O. and Abeyaratne, R. (1987). A note on a bifurcation problem in finite plasticity related to void nucleation. *Int. J. Solids and Structures*, **23**, 983-988.
- [10] Ertan, N. (1988). Influence of compressibility and hardening on cavitation. *ASCE J. of Engineering Mechanics*, **114**, 1231-1244.
- [11] Ericksen, J. L., and Rivlin, R. S. (1957) Large elastic deformations of homogeneous anisotropic materials. *J. Rational Mech. Anal.*, **3**, 281-301.
- [12] Eubanks, R. A. and Sternberg, E. (1954) On the axisymmetric problem of elasticity theory for a medium with transverse isotropy. *J. Rational Mech. Anal.*, **3**, 89-101.

- [13] Gent, A. N. (1990). Cavitation in rubber: a cautionary tale. *Rubber Chem. Technol.* **63**, G49-G53.
- [14] Gent, A. N. and Lindley, P. B. (1958). Internal rupture of bonded rubber cylinders in tension. *Proc. R. Soc. Lond., A* **249**, 195-205.
- [15] Gurtin, M. E. (1981). *An Introduction to Continuum Mechanics*. Academic Press, San Diego.
- [16] Haughton, D. M. (1986). On non-existence of cavitation in incompressible elastic membranes. *Q. J. Mech. Appl. Math.*, **39**, 289-296.
- [17] Haughton, D. M. (1990). Cavitation in compressible elastic membranes. *Int. J. of Engineering Science*, **28**, 163-168.
- [18] Horgan, C. O. (1992). Void nucleation and growth for compressible nonlinearly elastic materials: an example. *Int. J. Solids and Structures*, **29**, 279-291.
- [19] Horgan, C. O. and Abeyaratne, R. (1986). A bifurcation problem for a compressible nonlinearly elastic medium: growth of a micro-void. *J. Elasticity*, **16**, 189-200.
- [20] Horgan, C. O. and Pence, T. J. (1989a). Void nucleation in tensile dead-loading of a composite incompressible nonlinearly elastic sphere. *J. Elasticity*, **21**, 61-82.
- [21] Horgan, C. O. and Pence, T. J. (1989b). Cavity formation at the center of a composite incompressible nonlinearly elastic sphere. *J. Appl. Mech.*, **56**, 302-308.
- [22] Horgan, C. O. and Pence, T. J. (1989c). Void nucleation due to large deformations in nonlinearly elastic composites. *Proceedings of the 4th Japan-US Conference on Composite Materials*, Washington, D.C., June 1988 (ed. by Vinson, J. R.) pp. 232-241. Technomic Publishing Co., Lancaster, PA.
- [23] Hou, H.-s and Abeyaratne, R. (1992). Cavitation in elastic and elastic-plastic solids. *J. Mech. Phys. Solids*, **40**, 571-592.
- [24] Hou, H.-s and Zhang, Y. (1990). The effect of axial stretch on cavitation in an elastic cylinder. *Int. J. Nonlinear Mechanics* **25**, 715-722.
- [25] Huang, Y., Hutchinson, J. W. and Tvergaard, V. (1991). Cavitation instabilities in elastic-plastic solids. *J. Mech. Phys. Solids* **39**, 223-242.
- [26] James, R. D. and Spector, S. J. (1989). The formation of filamentary voids in solids. *J. Mech. Phys. Solids* **39**, 783-814.
- [27] Jaunzemis, W. (1967). *Continuum Mechanics*. McMillan, New York.
- [28] Meynard, F. (1992). Existence and nonexistence results on the radially symmetric

cavitation problem. *Quart. Appl. Math.* **50**, 201-226.

[29] Ogden, R. W. (1984). *Non-Linear Elastic Deformations*. Ellis Horwood Limited, England.

[30] Pericak-Spector, K. A. and Spector, S. J. (1988). Nonuniqueness for a hyperbolic system: cavitation in nonlinear elastodynamics. *Arch. Rat. Mech. Anal.*, **101**, 293-317.

[31] Podio-Guidugli, P., Vergara Caffarelli, G. and Virga, E. G. (1986). Discontinuous energy minimizers in nonlinear elastostatics: an example of J. Ball revisited. *J. Elasticity*, **16**, 75-96.

[32] Sivaloganathan, J. (1986a). Uniqueness of regular and singular equilibria for spherically symmetric problems of nonlinear elasticity. *Arch. Ration. Mech. Analysis*, **96**, 97-136.

[33] Sivaloganathan J. (1986b). A field theory approach to stability of radial equilibria in nonlinear elasticity. *Math. Proc. Camb. Phil. Soc.*, **99**, 589-604.

[34] Sivaloganathan, J. (1991). Cavitation, the incompressible limit, and material inhomogeneity. *Quart. Appl. Math.* **49**, 521-541.

[35] Spencer, A. J. M. (1972). *Deformations of Fibre-reinforced Materials*. Oxford University Press, Oxford.

[36] Spencer, A. J. M. (1982). The formulation of constitutive equations for anisotropic solids. In *Mechanical Behavior of Anisotropic Solids* (Proceedings of Euromech Colloquium 115, ed. by J.-P. Boehler) pp. 3-26. Martinus Nijhoff, The Hague.

[37] Steigmann, D. J. (1992). Cavitation in elastic membranes — an example. *J. Elasticity* **28**, 277-287.

[38] Stuart, C. A. (1985). Radially symmetric cavitation for hyperelastic materials. *Ann. Inst. Henri Poincaré-Analyse non lineaire*, **2**, 33-66.

[39] Stuart, C. A. (1993). Estimating the critical radius for radially symmetric cavitation. *Quart. Appl. Math.* **51** (in press).

[40] Tian-hu, H. (1990). A theory of the appearance and growth of the micro-spherical void. *Int. J. of Fracture*, **43**, R51-R55.

[41] Truesdell, C. and Noll, W. (1965). *The Non-Linear Field Theories of Mechanics*. Handbuch Der Physik, **III/3**. Springer-Verlag, New York.

[42] Tvergaard, V. (1990). Material failure by void growth to coalescence. In *Advances in Applied Mechanics* (ed by J. Hutchinson and T. Wu), vol. 27, pp. 83-151. Academic Press, San Diego.

- [43] Tvergaard, V., Huang, Y. and Hutchinson, J.W. (1992). Cavitation instabilities in a power hardening elastic-plastic solid. *European J. of Mechanics A (Solids)* 11 , 215-232.
- [44] Walker, J. L. (1956). Structure of ingots and castings. In *Liquid Metals and Solidification*, pp. 319-336. American Society for Metals, Cleveland.
- [45] Williams, M. L. and Schapery, R. A. (1965). Spherical flaw instability in hydrostatic tension. *Int. J. Fracture Mechanics*, 1 , 64-71.